Università
degli Studi
di Padova

Dipartimento
di Ingegneria
dell'Informazione

Nonlinear Mixed-Effects Intravenous and Oral Minimal Models to Assess Insulin Secretion and Action

School Director
Prof. Matteo Bertocco
Advisor
Prof. Claudio Cobelli
Bioengineering Coordinator
Prof. Giovanni Sparacino

Ph.D. candidate
Anna Largajolli

Ph.D. School
in Information Engineering
(Bioengineering)
2013 XXV ciclo

Considerate la vostra semenza:
fatti non foste a viver come bruti,
ma per seguir virtute e canoscenza.
Inferno, Canto XXVI, vv. 118-120

Summary

Diabetes is a serious metabolic disorder that according to the International Diabetes Federation (IDF) [1] 2012 report affects about 371 million of people worldwide. This number is likely to increase in the next years especially due to the contribution of the emerging countries where health care is less effective. That is the reason why in these years scientific research has been carried out intensely facing diabetes with different field expertise from cellular biology to pharmacology to engineering and so on. Various scientific questions were answered but still many others are to come. For instance, different tests were developed to study the glucose-insulin system in vivo whose data were analyzed with model based approaches to extrapolate some knowledge of the underlying phenomena of the glycemic control. The research presented here aims to analyze data coming from different test by exploiting the nonlinear mixed-effects approach modeling population method (NLMEM) in order to study the glucose-insulin system. This statistical approach is largely employed in pharmacokinetics and pharmacodynamics (PKPD) studies during drug development but is not that much widespread in metabolic studies. This technique is really appealing because is able to quantify not only the individual and population parameters but also is able to identify the biological sources of inter-individual and intra-individual variability. Moreover the nonlinear mixed-effects approach is particularly recommended in "sparse dataset", the typical epidemiological study condition, where the standard individual techniques have difficulties in getting the physiological information from the data. In this case a complete statistical description is obtainable by borrowing the lack of information from the entire population thus potentially reducing the need for blood samples and invasive trials. Because of its potential, the nonlinear mixed-effects approach offers a valuable modeling tool to be investigated and validated on data coming from metabolic studies as those regarding the glucose-insulin system. The rationale of this work was first to optimize the metabolic minimal models that where built using the standard individual estimation approach by exploiting to the full the potentials of the nonlinear mixed-effects. Then, the second step was to choose the best algorithm to solve the likelihood maximization required by using the nonlinear mixed-effects, that due to the model parametric nonlinearity generally does not have an explicit solution. Finally, the last part was evaluating the model performances providing evidence for the quality of the results. To do this, in addition to the use of the available statistical tests for nonlinear mixed-effects, an ad hoc technique was developed to ensure a correct model performance assessment. This thesis is the natural extension and integration of Denti et al work [2, 3] where the IVGTT glucose minimal model was identified investigating different estimation methods and studying the effect of the introduction of the covariates. In this

work, the glucose, insulin and c-peptide minimal models during an intravenous glucose tolerance test (IVGTT) are revised with the final aim of implementing an integrated system. Moreover with the same technique the glucose and c-peptide minimal model during a meal tolerance test (MTT) are implemented. By moving from an intravenous to an oral test a new scientific challenge is faced in terms of increased complexity of the experiment and of the physiology since the gastro intestinal tract has to be considered. More precisely, as a first step, new different estimation methods were compared on a data rich and data poor glucose simulated dataset using the IVGTT glucose minimal model in order to understand which is the best estimator to use. The results select the First-Order Conditional Estimation as method of choice and show its robustness to poor sampling. As a second step, the IVGTT glucose minimal model was implemented using the nonlinear mixed-effects approach as a two compartment model with a delay term that is able to describe all the time dynamic of glucose in order to make the integration with the other IVGTT models possible. Afterwards, the C-peptide IVGTT minimal model was implemented and a covariate analysis was carry out. In particular after having introduced a delay term, a correlation analysis between the covariates was done and a following generalized additive models (GAM) analysis was performed between the parameters and the covariates in order to test the time consuming forward and backward covariate insertion on a small subset of possible parameter-covariate relations. Finally the IVGTT insulin model was implemented by introducing a time delay, coherently with the C-peptide model, a second compartment that is able to catch all the kinetics of the data and other modeling expedients. Once the insulin and glucose minimal models were implemented by NLMEM, an integrated model was identified that is able to describe simultaneously the glucose and insulin kinetics. As a third main step, the meal tolerance test (MTT) data were analyzed. The C-peptide minimal model was implemented using the nonlinear mixed-effects and estimated on a full and reduced dataset of healthy subjects. The same model was tested in populations with different degrees of pathology such as prediabetic and diabetic subjects. Then the meal glucose minimal model was implemented using the same technique on a simulated MTT dataset. Different models were implemented to describe the rate of appearance (Ra) and we looked for the best model that ensures the compromise between the best prediction of Ra data and the best estimation of the insulin sensitivity.

Typically in a PKPD study the performance of the models are evaluated using the visual predictive check (VPC) that is a diagnostic tool based on a comparison between the statistics obtained from the simulated data using the estimated population parameters and the true observed data. All the models presented in this thesis have at least one forcing

function that is a time varying known input function. An "ad hoc VPC" was developed to better study these types of model. In particular the standard VPC method presents some pitfalls during the simulation step because it does not take into consideration a link between the simulated parameters and the forcing function associated. In this thesis a new method is proposed to have a correct evaluation of the VPC results.
To conclude, in this thesis we proved the advantages of using the population approach with respect to the standard individual technique: it prevents the use of Bayesian a priori information, it can handle sparse dataset and so future studies for protocol reduction are now possible, it permits the introduction of new modeling parts and covariate analysis can be carried out.

Sommario

Il diabete è una grave malattia metabolica che secondo l' International Diabetes Federation (IDF) [1] colpisce circa 371 milioni di persone in tutto il mondo. Questo numero è destinato a crescere nei prossimi anni grazie al contributo dei paesi dove la sanitá e la prevenzione sono meno efficaci. Questo è il motivo per cui in questi anni la ricerca scientifica è stata portata avanti intensamente studiando il diabete da diversi punti di vista: dalla biologia cellulare alla farmacologia alla ingegneria e via dicendo. Molti quesiti scientifici sono stati risolti ma molti altri sono ancora aperti. Recentemente sono stati sviluppati diversi test per studiare il sistema glucosio insulina in vivo i cui dati sono stati analizzati con approcci basati su modelli matematici che servono a estrapolare della conoscenza sui fenomeni sottostanti del controllo glicemico.
La ricerca qui presentata si propone di analizzare i dati provenienti da test differenti sfruttando l' approccio di popolazione nonlineare a effetti misti (NLMEM) per studiare il sistema glucosio-insulina. Questo approccio statistico è largamente impiegato in studi di farmacocinetica e farmacodinamica (PKPD) durante lo sviluppo di farmaci, ma non è molto diffuso negli studi metabolici. Questa tecnica è molto interessante perché non solo è in grado di quantificare i parametri dell' individuo e della popolazione, ma è in grado di identificare le fonti biologiche della variabilitá inter-individuale e intra-individuale. Inoltre l' approccio non lineare a effetti misti è particolarmente indicato in "dataset sparsi", la condizione tipica degli studi epidemiologici in cui le tecniche standard individuali hanno difficoltá ad ottenere le informazioni dai dati. In questo caso una descrizione completa statistica è ottenibile recuperando la mancanza di informazioni dalla popolazione riducendo cosí potenzialmente la necessitá di campioni di sangue e di prove invasive. Grazie al suo potenziale, l' approccio non lineare a effetti misti offre un valido strumento di modellazione da utilizzare e convalidare su dati provenienti da studi metabolici, come quelli che riguardano il sistema glucosio-insulina.
Il razionale di questo lavoro è stato innanzitutto ottimizzare i modelli metabolici che sono stati costruiti utilizzando l' approccio standard di stima individuale sfruttando al massimo le potenzialitá del metodo ad effetti misti non lineari. Poi, il secondo passo è stato quello di scegliere il miglior algoritmo per risolvere la massimizzazione della likelihood richiesta nei modelli implemtentati con tecnica non lineare a effetti misti, che a causa delle non linearitá presenti nei modelli spesso non ha una soluzione esplicita. Infine, l' ultima parte è stata la valutazione delle prestazioni dei modelli che fornisce la prova della qualitá dei risultati. Per fare questo, in aggiunta all' uso di test statistici giá disponibili e adatti al metodo NLMEM, una tecnica ad hoc è stato sviluppata per garantire una corretta valutazione delle prestazioni di alcuni modelli.

Questa tesi è l' estensione naturale e l' integrazione del lavoro di Denti et al [2, 3, 4] dove il modello minimo del glucosio IVGTT è stato identificato indagando diversi metodi di stima e su cui sono state introdotte le covariate. In questo lavoro, i modelli minimi del glucosio, insulina e C-peptide minimo durante un test di tolleranza al glucosio per via endovenosa (IVGTT) sono stati rivisti, con l' obiettivo finale di implementare un sistema integrato. Inoltre si sono implementati con la stessa tecnica il modello minimo del glucosio e del C-peptide durante un test di tolleranza al glucosio orale (MTT). Passando da un carico di glucosio endovenoso ad uno orale una nuova sfida scientifica viene affrontata in termini di maggiore complessitá degli esperimenti e della fisiologia in quanto il tratto gastrointestinale deve essere considerato.
Piú precisamente, in una prima fase, diversi metodi di stima sono stati confrontati su un dataset simulato usando il modello minimo del glucosio IVGTT con campionameto ricco e ridotto, al fine di capire quale è il miglior stimatore da utilizzare. I risultati hanno selezionato il metodo First order Conditional (FOCE) e hanno dimostrato la sua robustezza nel campionamento ridotto. In una seconda fase, il modello del glucosio IVGTT minimo è stato implementato utilizzando l' approccio non lineare a effetti misti come un modello a due compartimenti con un tempo di ritardo che è in grado di descrivere la dinamica del glucosio per tutta la durata dell' esperimento, al fine di rendere l' integrazione con gli altri modelli IVGTT possibile. Successivamente, il modello minimo del C-peptide IVGTT è stato implementato ed è stata svolta uâ analisi delle covariate. In particolare dopo aver introdotto un ritardo, sono state effettuate un analisi di correlazione fra le covariate e una successiva analisi, usando i generalized additive models (GAM), tra i parametri e le covariate al fine di ottenere un sottoinsieme piccolo di possibili combinazioni tra parametri e covariate su cui svolgere la time consuming forward and backward analysis in NONMEM. Infine, il modello dell' insulina IVGTT è stato implementato introducendo un ritardo, coerentemente con il modello del C-peptide, un secondo compartimento in grado di catturare la cinetica dei dati ed ulteriori espedienti modellistici. Una volta che i modelli minimi dell' insulina e del glucosio sono stati implementati usando le tecniche NLMEM, è stato costruito un modello integrato che è in grado di descrivere contemporaneamente la cinetica dell' insulina e del glucosio. Come terzo passo sono stati analizzati i dati del test di tolleranza al glucosio orale (MTT). Il modello minimo del C-peptide è stato implementato utilizzando le tecniche NLMEM ed è stato stimato su un dataset di soggetti sani con campionamento ricco e ridotto. Lo stesso modello è stato testato in popolazioni con differenti livelli di patologia come i soggetti prediabetici e diabetici. Poi con la stessa tecnica è stato realizzato il modello minimo del glucosio orale su un datset simulato MTT. Diversi modelli sono stati implementati

per descrivere la velocitá di comparsa del glucosio nel sangue (Ra) ed è stato scelto il modello che è in grado di garantire il compromesso tra la migliore predizione di dati di Ra e la migliore stima della sensibilitá all' insulina.
In genere in uno studio PKPD le prestazioni dei modelli sono valutate con la tecnica del visual predictive check (VPC). Questo è uno strumento diagnostico basato su un confronto tra le statistiche ottenute dai dati simulati utilizzando i parametri della popolazione stimati e i dati veri osservati. Tutti i modelli presentati in questa tesi hanno almeno una funzione forzante che è una funzione di ingresso tempo variante nota ed un VPC "ad hoc" è stato sviluppato per studiare proprio questo tipo di modelli. In particolare il metodo VPC standard ha presentato alcuni problemi durante la fase di simulazione perché non prende in considerazione il legame tra i parametri simulati e la funzione forzante associata. In questa tesi è stato quindi proposto un nuovo metodo che permette di avere una corretta valutazione dei risultati del VPC.
Per concludere, in questa tesi abbiamo dimostrato i vantaggi dell' utilizzare un approccio di popolazione rispetto alla tecnica standard individuale: evita l' uso di informazioni bayesiane a priori, puó gestire dataset sparsi e cosí futuri studi per la riduzione del protocollo sono ora possibili, permette l' introduzione di nuove parti di modellazione e l' analisi delle covariate puó essere ora effettuata.

Contents

Introduction

This thesis is the natural extension of Denti et al work [4] where are clearly shown the advantages of using the population approach with respect to the traditional individual weighted least square (WLS) approach. This approach in fact unlike the traditional approach is particularly effective during the model estimation when the sampling scheme is reduced or data are largely variable. In these situations the population approach is able to compensate the lack of information by borrowing the knowledge spread on the population and include it during the estimation step. Moreover the population approach is able to investigate and possibly identify the sources of variability in the population which makes the technique more appealing then the individual approach. In pharmacokinetic and pharmacodynamic (PKPD) studies this approach is largely employed as it allows a possible cost reduction of the trials and less invasive experiments whereas in metabolic studies this technique is less widespread but due to its potentials it is worthy to investigate its effects also in this field.
In this thesis is carried on the investigation of the glucose-insulin system started by Denti et al [4] not only after an intravenous but also after an oral glucose perturbation. In particular by exploiting the potentials of the population approach some of the minimal models that were developed so far with the traditional individual approach are revised. New modeling parts are added, Bayesian a priori information is avoided when possible, covariates information is added (i.e. subject physiological characteristic such as weight,

height ...) and possible protocol reductions are studied.
In the following chapters we explored the population approach advantages to study the glucose-insulin system in many ways. In particular in chapter 3 different population estimation methods on a simulated dataset are tested using the IVGTT glucose minimal model and their behavior on various discarded sampling schemes are explored. In chapter 4 a two compartment glucose minimal model during an intravenous glucose tolerance test (IVGTT) is implemented and its performance is compared with the one compartment glucose minimal model described by Denti et al [2]. In chapter 5 the IVGTT C-peptide minimal model is implemented and a covariate analysis is carried out. In chapter 6 the IVGTT glucose two compartment minimal model is integrated with a revised IVGTT insulin minimal model. In chapter 7 and 8 the glucose insulin system is studied after an oral glucose perturbation test (OGTT) by doing so we move into a more complex and variable context as the GI tract is involved during the experiment. In particular in chapter 7 four different models to describe the glucose rate of appearance are proposed and matched with the oral glucose minimal model. In chapter 8 the oral C-peptide minimal model is explored on a rich, a reduced and furtherly reduced datasets and its performance is studied to identify different pathophysiolgical groups. Finally in chapter 9 a revision of the evaluating model technique, the Visual Predictive Check, is proposed to study the models, like the minimal models, that present forcing functions.

Background

2.1 The glucose insulin system

Glucose is a simple sugar that represents a primary font of energy for the whole body. Even if all the cells metabolize sugar the body tissues can be classified differently according to their glucose uptake. In particular the brain nervous tissue and the red blood cells are *glucose dependent tissue or insulin independent* because a continuous sugar intake must be present to guarantee their metabolic activity. This fix and continuous intake of the nerve cells amounts to about 100 mg/min (150 g/24 h) in a normal individual [5, 6]. The muscular and the adipose tissues are *insulin dependent tissues* because in their cells are present the glucose transporters GLUT-4 that are responsible for the insulin regulated glucose transport and storage in the cell. The liver, the pancreas and the hypothalamus are the *glucose sensors* organs in the sense that they are able to detect the glucose concentrations and start an appropriate action. Finally the intestine and the kidney are *glucose eater* organs in the sense that they deal with the glucose income and return. At steady state, that means that there is no ingestion of food and no physical activity, the glucose blood concentration is kept greater than 65 mg/dl. This is achieved through the liver that provides glucose in blood and through the pancreas that controls that the glucose is used by the insulin dependent tissues and that is not released in big amounts by the liver. The pancreas is able to perform these actions through the

β-cells that secrete the insulin hormone that reaches the system circulation after liver degradation, and is peripherally cleared primarily by the kidneys. The hypothalamus prevent the brain and the glucose-dependent organs in general from hypoglycemia by increasing the glucose hepatic production and limiting the glucose uptake by the insulin dependent tissues. During a meal ingestion the intestine provides in the blood circulation some glucose that through the insulin action is stored in the muscular and the adipose tissues. At the same time insulin inhibits the hepatic glucose production. Moreover the glucose load itself stimulates the glucose uptake in the insulin dependent organs and in the liver and limits the glucose hepatic production. Although this is a very synthetic analysis of the glucose homeostasis, the processes and the organs that have just been described are a good approximation of the glucose-insulin system and its glycemic control mechanism Fig. 2.1. These control interactions are usually referred to as *insulin sensitivity* and *β-cell responsivity*. In other words insulin sensitivity is the capacity of insulin to regularize the level of glucose in plasma whereas the β-cell responsivity is the ability of the pancreas to secrete insulin in an efficient fashion. Any deregulations of the processes just described can provoke hypoglycemia or hyperglycemia that are the cause of dangerous situations for the body such as ketoacidosis, dehydration and coma. When the human body is not able to compensate these deregulations, begins the chronic disease called *diabetes mellitus*. Diabetes mellitus is a metabolic alteration due to a reduce activity of the insulin hormone or an occlusion of its secretion or both. The main characteristic of this chronic disease is a status of hyperglycemia that in long term is combined with other peculiar severe complications such as retinopathy that leads to blindness, nephropathy that leads to kidney failure, neuropathy that leads to ulcer and macro angiopathy that leads to premature arteriosclerosis. According to the international diabetes federation (IDF) [1] in 2012 there were about 371 millions diabetic patients around the world (Fig. 2.2). This number is likely to increase especially thanks to the contribution of the developing countries [1, 7]. In fact according to the World Health Organization [7] the 80% of the diabetic patients around the world come from low and middle income countries. According to the American Diabetes Association (ADA) guidelines [8] a patient can be diagnosed of diabetes mellitus if its glycemic levels in venous blood at fasting are equal or greater than 126 mg/dl or if its glycemic levels after two hours from a glucose meal eaten during a glucose tolerance test (OGTT) are greater or equal than 200 mg/dl (Tab. 2.1) Moreover two other categories were defined to describe altered glucose tolerance conditions that are placed halfway between the healthy state and the diabetic state. In particular was defined the Impaired glucose tolerance (IGT) category as patients with glycemic levels between 140-200 mg/dl after two hours

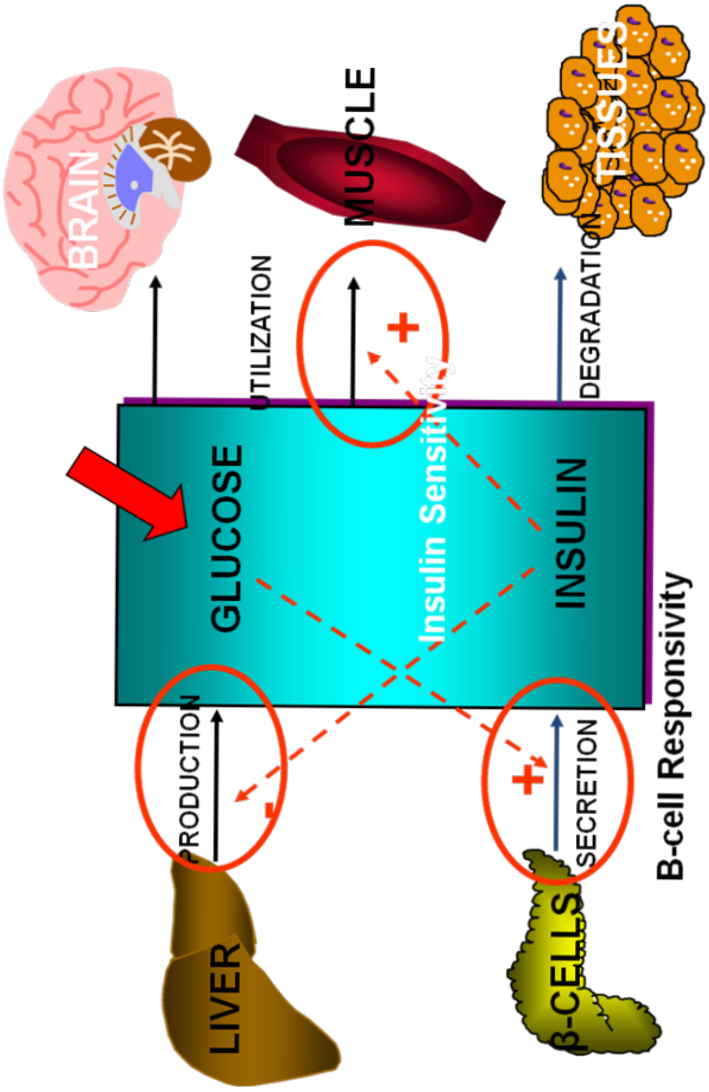

Figure 2.1: The glucose-insulin system scheme: glucose is produced (mainly by the liver), distributed, and utilized in both insulin-independent (e.g., central nervous system and red blood cells) and insulin-dependent (muscle and adipose tissues) tissues. Insulin is secreted by pancreatic beta cells, reaches the system circulation after liver degradation, and is peripherally cleared primarily by the kidneys. The glucose and insulin systems interact by feedback control signals, e.g., if a glucose perturbation occurs (after a meal), beta-cells secrete more insulin in response to the increased plasma glucose concentration and in turn insulin signaling promotes glucose utilization and inhibits glucose production so as to bring rapidly and effectively plasma glucose to the physiological level.

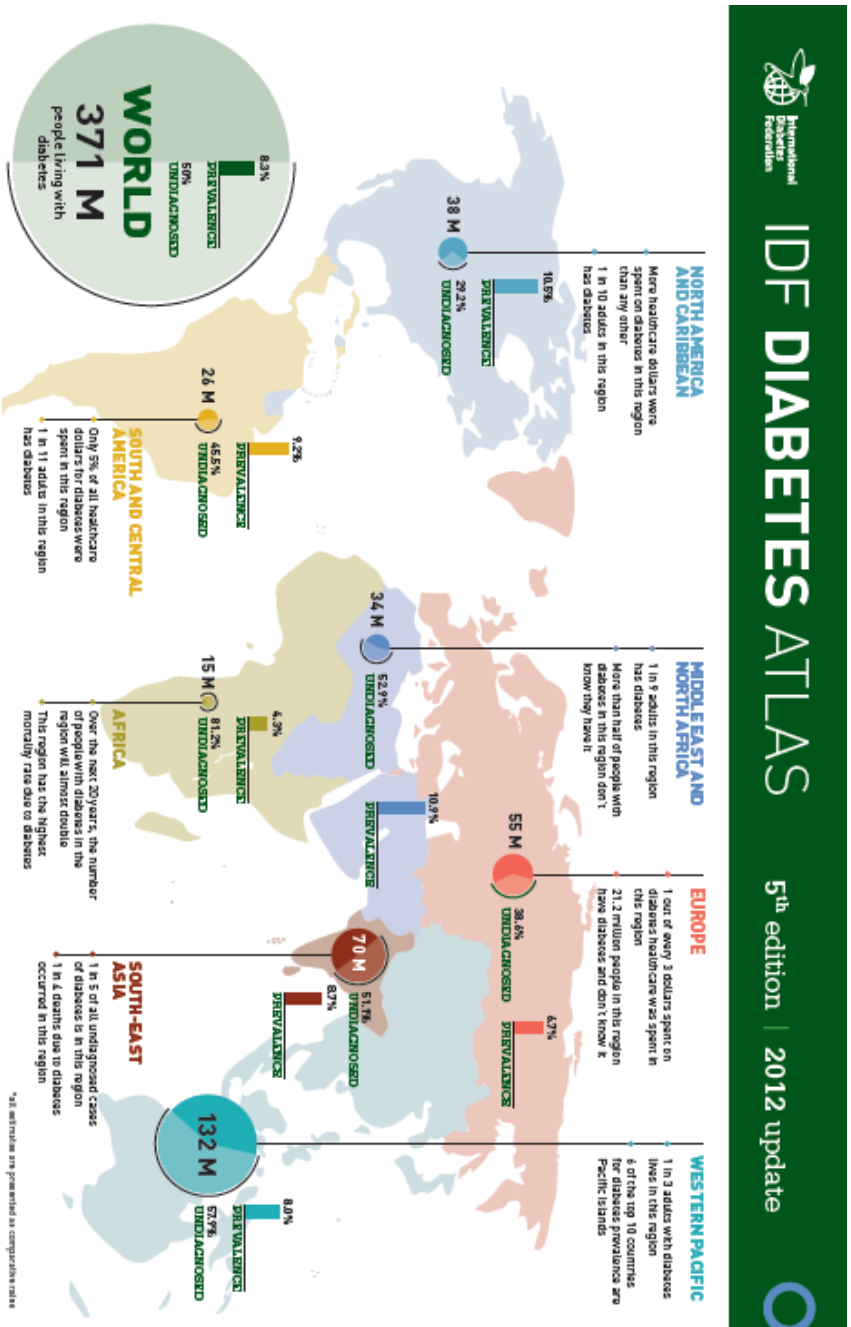

Figure 2.2: 2012 IDF diabetes statistics [1]

from a glucose meal and the Impaired fasting glucose (IFG) that were defined as patients with glycemic levels at fasting between 100-126. Diabetes was classified by ADA in 1997 and approved by the world health organization (OMS) in different categories according to etiopathogenesis criteria. The main two are described in the following subchapters.

state	*FPG glucose level (mg/dl)*	*2-h plasma glucose in OGTT (mg/dl)*
healthy	≤ 99	≤ 139
IFG	100- 125	≤ 139
IGT	≤ 99	140-199
diabetic	≥ 126	≥ 200

Table 2.1: ADA diabetes classification using glucose levels at time 0 and at 2 h after an OGTT

Type 1 diabetes

Type 1 diabetes mellitus is usually diagnosed in children and young adults and affects an estimated 5% of all the diabetes cases [8]. It is caused by an autoimmune destruction of the β-cell of the pancreas that in other terms means no insulin secretion. The recognized origins nowadays are both genetic and environmental. The lack of insulin creates hyperglycemia in the glucose blood and to fix this is necessary to use a daily insulin therapy that maintains blood sugar levels within the physiological range. The therapy consists on injecting insulin analogs that mimics the missing endogenous insulin profiles. Likewise a pancreas transplantation is necessary or recently also islet cell transplantations are explored. Transplantation is still in an experimental phase.

Type 2 diabetes

Type 2 diabetes is the most common form of diabetes (about the 90% of diabetes cases [8]).Traditionally is considered as the adult diabetes, it is increasing also in children. It is related to an insulin secretion deficiency and to an insulin resistance. Insulin resistance is the inability of the insulin dependent tissues to respond adequately to normal levels of insulin. For example liver would inappropriately release glucose into the blood despite the insulin presence that should promote the inhibition of the mechanism. The type 2 diabetes causes are a combination of lifestyle and genetic factors. For example obesity, diet, sedentary lifestyle, increasing aging and race (African Americans, native Americans, Latinos etc) are some of the risk factors for the disease development. Insulin administration normally is not necessary with this kind of diabetes, usually increasing physical exercise and dietary modification are initially sufficient to lower down the glucose

levels into physiological ranges. In case these two are not enough then medication or insulin is needed.

2.2 Methods and protocols to study the glucose and insulin system

In these years research has been carried out intensely to study the mechanism of regulation of the glucose insulin system. Many approaches have been proposed to grasp information from the system and study its efficiency starting from simple indices like HOMA and QUIKI [9] to more sophisticated technique such as the Euglycemic/Hyperglycemic Clamp [10]. The first two indices are poor indicator of the system efficiency since they are based only on the fasting values of glucose and insulin and do not take into account the dynamic of the system in their formulation. The Clamp technique is a more sophisticated method that aims to measure insulin secretion (β-cell responsivity) and insulin resistance (insulin sensitivity). In particular the first is obtained through the hyperglycemic clamp where the plasma glucose is firstly raised by a priming infusion and then the desired glucose concentration is kept constant. Under these conditions the insulin is biphasic and provides then a measure of the β-cell response. The insulin resistance instead is measured through the euglycemic or hyperinsulinemic clamp where the insulin levels are acutely raised and maintained high by a prime continuous infusion of insulin whereas plasma glucose is kept constant at basal levels by a variable glucose infusion that corresponds to the glucose uptake by all the body tissues. These two protocols are invasive, expensive and requires prepared technicians to carry out the experiment successfully that means that they cannot be applied in epidemiology studies where the number of patients and experiments to carry out is big. Moreover since they force the system at a different steady state from the basal they lose the description of the system dynamic and they focus on a measurement to derive the insulin secretion and the insulin resistance. The approach that has so far the best results in describing the glucose and insulin system is the model based approach. This method rely on a description of the system under analysis through a mathematical model that enables to quantify mechanisms in the inaccessible pools from the measures of the accessible pool [11]. In our case the system under study is the glucose-insulin system and through the mathematical modeling approach for example we are able to quantify not directly accessible information such as the insulin secretion through the simple measurement of the blood levels of glucose and C-peptide, an insulin co secreted substance. There are two protocols to study the glucose and insulin system through a mathematical model approach, the difference between them is that they perturb the

system in a different way at the beginning of the experiment. The intravenous glucose tolerance test (IVGTT) gives the glucose dose intravenously in plasma whereas the oral glucose tolerance test (OGTT or MTT) administers the glucose dose orally. Moving from the intravenous to the oral administration means increasing the modeling challenges because the variable GI tract, through which the glucose appears in plasma, has to be described 2.3. Once the experimental data are collected following the selected protocol, some statistical assumptions on the measurement error are made and the mathematical model can be applied on the experimental data. Its parameters reflect a description of the system response and of its inaccessible pool. The most widely used mathematical models to study the glucose and insulin system are the *minimal models* that are at the same time parsimonious and describe the key components of the system functionality [12]. The two protocols are described hereafter.

Intravenous glucose tolerance test (IVGTT)

The Intravenous glucose tolerance test consists on an injection in one arm of glucose usually about 0.3 g/kg total body weight and on the other arm there is a withdrawal of blood for the following four hours. A following modification of the protocol was proposed that consists on an injection of glucose at time 0 min followed by an infusion of insulin (0.02 units/kg total body weight, begun at 20 min) given as a square wave over 5 min. Blood is sampled over the next four hours. This modified protocol is called the insulin modified IVGTT and helps to have more informative data to determine afterwards the insulin kinetics. The minimal models proposed to interpret this kind of data are described in the following paragraph.

Oral glucose / Meal tolerance test (OGTT/MTT)

The oral glucose and the meal tolerance tests consist both on an oral glucose dose consumption that in case of an OGTT is a standard oral dose of glucose ($\sim$ 75 g) ingested in 5 minutes whereas in case of an MTT is a mixed meal (10 kcal/kg body weight, 45% carbohydrate, 15% protein, 40% fat) usually consisting of three scrambled eggs, Canadian bacon, and glucose Jell-O (containing 1.2 g/kg body weight of dextrose) and consumed within 15 min. Following the oral dose blood samples are withdrawal for the following 7 hours. The minimal models proposed to interpret this kind of data are described in the following paragraph.

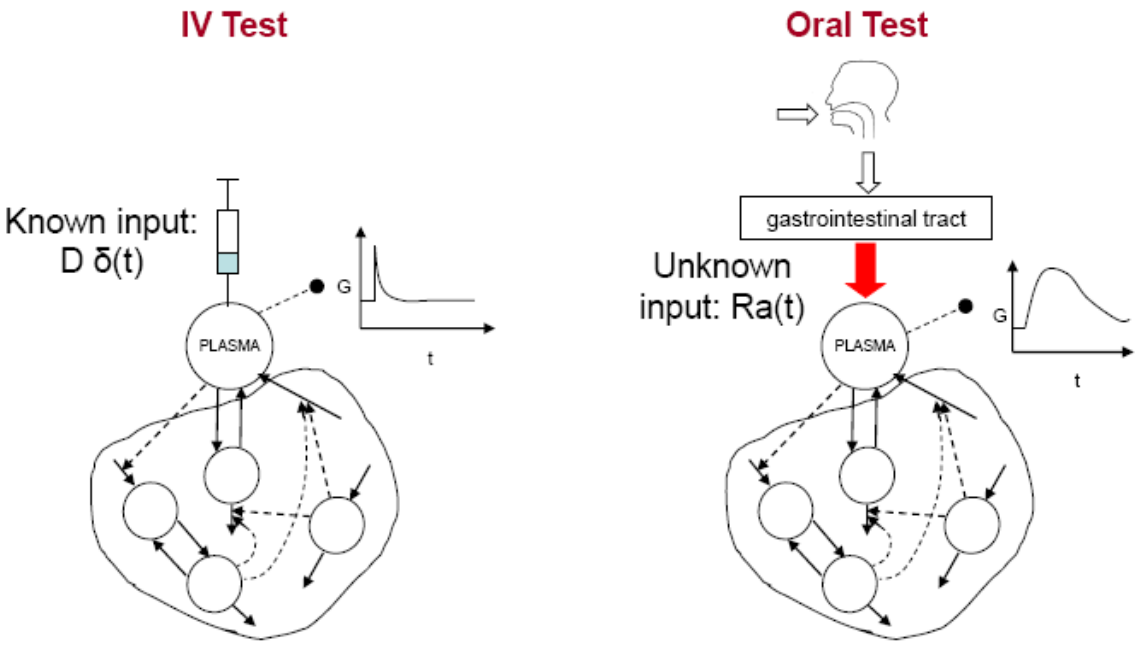

Figure 2.3: Intravenous and oral glucose tolerance test scheme.

2.3 Models for IVGTT data and models for MTT data

In the following section are described the models developed to study the glucose and insulin system during an intravenous or an oral glucose load. These models were designed using the traditional individual approach weighted nonlinear least square (WNLS) that was applied on the experimental data of each single subject. Remeber that this individual approach is feasible only on data rich situation such as the two protocols IVGTT and MTT where are present 21 samples for each subject. In case of sparse or noisy dataset or in case of locally identifiable models Bayesian analysis has shown to be effective [13, 14, 15, 16] but this kind of analysis has the main drawback of knowing a priori statistical information that might be not easy to have.

IVGTT minimal models

Glucose minimal model

The IVGTT glucose minimal model is a compartmental model allowing the quantitative description of glucose metabolism and insulin control. In figure there is a schematic rappresentation of it (Fig. 2.4). Glucose is presented in a single compartment, the plasma,

and the fluxes in and out of this compartment represent the tissue uptake and the Net Hepatic Glucose Balance (NHGB), both controlled by remote insulin that is insulin present in the interstitial fluid. For model identifiability reason a riparametrization was

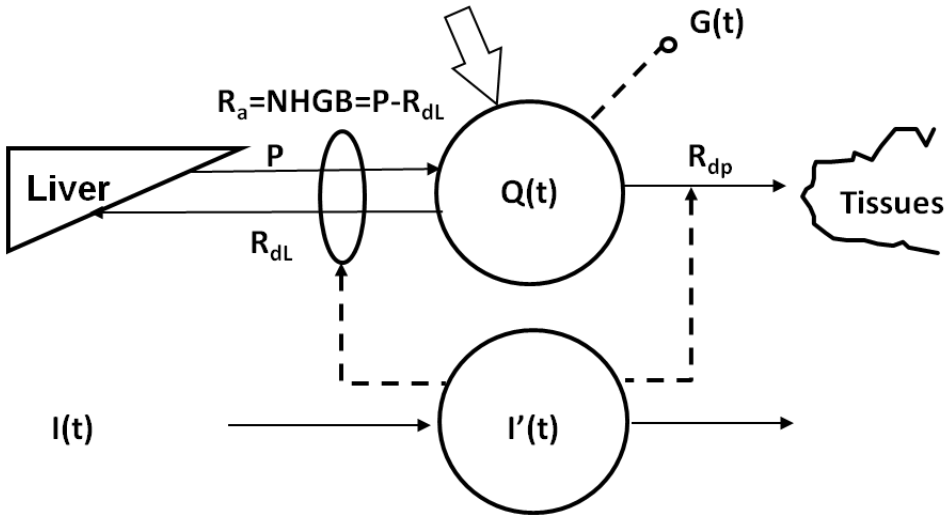

Figure 2.4: IVGTT glucose minimal model schematic representation

done [17] that leads to the following equations:

$$\begin{aligned} Q'(t) &= -(S_G + X(t)) \cdot Q(t) + S_G \cdot Q_b \qquad Q(0) = D + G_b \cdot V \\ X'(t) &= -p2 \cdot X(t) + p2 \cdot S_I \cdot (I(t) - I_b) \qquad X(0) = 0 \end{aligned} \tag{2.1}$$

where D (mg/kg) denotes the glucose dose per unit of body mass, Q(t) (mg/kg) is glucose mass in plasma and Q_b its basal value, G(t) (mg/dl) is plasma glucose concentration and G_b its basal value, I(t) (pmol/l) is insulin concentration and I_b its basal value, and X(t) is insulin action ($min - 1^{-1}$). The uniquely identifiable model parameters are: S_G (min^{-1}) glucose effectiveness, S_I ($min^{-1}pmol^{-1}l$) insulin sensitivity, p2 (min^{-1}) the insulin action parameter, and V (dl/kg) the apparent glucose distribution volume per unit of body mass. S_G and S_I in particular are well known metabolic indexes that are able to distinguish among different pathophisiological states in the glucose and insulin system. S_G measures the ability of glucose per se, at basal insulin, to stimulate glucose disappearance and to inhibit endogenous glucose production whereas S_I measures the ability of insulin to enhance the glucose per se stimulation of its disappearance and the glucose per se inhibition of endogenous production. The model considers data from min 8 of the experiment because the one compartment formulation cannot take into account for the quickest kinetics. To remedy this and an S_G overestimation and an S_I

underestimation a two compartment glucose minimal model was proposed by Cobelli et al [18]. The two compartment model expression is the following:

$$\begin{aligned} Q_1'(t) &= -(S_G + X(t)) \cdot Q_1(t) + S_G \cdot Q_{1b} - k_{21} \cdot Q_1(t) + k_{12} \cdot Q_2(t) \qquad Q_1(0) = D + G_b \cdot V \\ Q_2'(t) &= k_{21} \cdot Q_1(t) - k_{12} \cdot Q_2(t) \qquad Q_2(0) = \frac{k_{21} \cdot Q_{1b}}{k_{12}} \\ X'(t) &= -p2 \cdot X(t) + p2 \cdot S_I \cdot (I(t) - I_b) \qquad X(0) = 0 \end{aligned} \tag{2.2}$$

Due to identifiability problem a bayesian analysis was used to make the model uniquely identifiable that fixed the rates between the two compartments of glucose (i.e. k_{12} and k_{21}) to a priori knowledge.

C-peptide minimal model

The C-peptide minimal model [19] is a widely used tool to assess pancreatic β-cell function. It can assess the insulin secretion since C-peptide is secreted equimolarly with insulin, and its extraction by the liver is negligible.In Fig. 2.5 is presented a schematic representation of the model. The model equations are presented in Eq. 5.1.

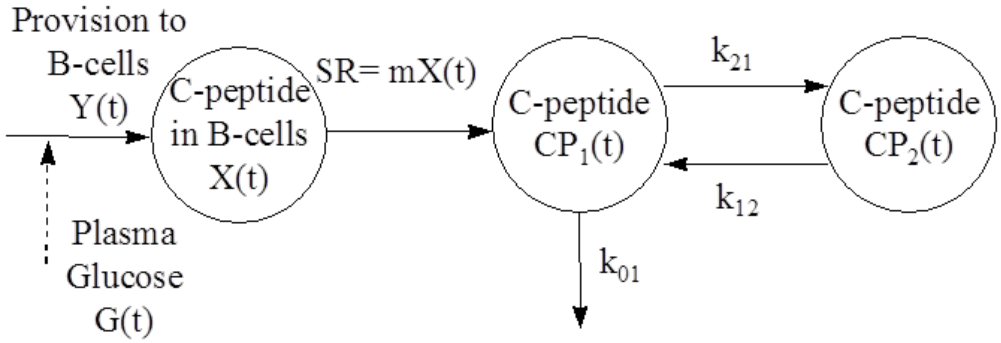

Figure 2.5: IVGTT C-peptide minimal model schematic representation.

$$
\begin{aligned}
CP_1'(t) &= -(k_{01}+k_{21})\cdot CP_1(t) + k_{12}\cdot CP_2(t) + m\cdot X(t) \qquad CP_1(0) = CP_b \\
CP_2'(t) &= -k_{12}\cdot CP_2(t) + k_{21}\cdot CP_1(t) \qquad CP_2(0) = CP_b\cdot k_{21}/k_{12} \\
X'(t) &= -m\cdot X(t) + Y(t) \qquad X(0) = X_0 + (k_{01}\cdot CP_b)/m \\
Y'(t) &= \begin{cases} -\alpha\cdot(Y(t) - \beta\cdot(G(t)-G_b) - k_{01}\cdot CP_b) & \\ Y(0) = (k_{01}\cdot CP_b), & \text{if } \beta\cdot(G(t)-G_b) - k_{01}\cdot CP_b \geq 0 \\ -\alpha\cdot(Y(t)) & \\ Y(0) = (k_{01}\cdot CP_b), & \text{if } \beta\cdot(G(t)-G_b) - k_{01}\cdot CP_b < 0 \end{cases}
\end{aligned}
\tag{2.3}
$$

where CP_1 and CP_2 are the C-peptide concentration in the accessible and peripheral compartments respectively (pmol/l) and CP_b is its basal value, X (pmol/l) is the C-peptide amount in the β-cell and Y is the C-peptide provision in the β-cell (pmol l^{-1} min^{-1}). The transfer rate between CP_1 and CP_2 k_{12}, k_{21} and k_{01} (min^{-1}) are fixed kinetics determined through the Van Cauter formulas [20]. G is the glucose concentration (mg/dl) and G_b is its basal value. The uniquely identifiable parameters are: the secretion rate constant m (measured in min^{-1}), the provision rate constant α (measured in min^{-1}), the second-phase sensitivity to glucose β (measured in dl mg^{-1} pmol l^{-1} min^{-1}) and the incremental amount of C-peptide secreted during the first phase X_0 (measured in pmol/l). This model is widely used because it provides indexes of β-cell sensitivity to glucose during the first and the second phase of insulin secretion. In particular the derived β-cell responsivity indexes are:

- the first phase β-cell responsivity to glucose $\phi_1 = \frac{X_0}{\Delta G}$ where ΔG is the maximal excursion of glucose above basal;
- the second phase β-cell responsivity to glucose $\phi_2 = \beta$;
- the total β-cell responsivity to glucose $\phi_t = \phi_2 + \frac{\phi_1\cdot\Delta G}{\int_0^\infty (G(t)-G_b)\,dt}$ representing the average increase above basal of pancreatic secretion over the average glucose stimulus.

Insulin minimal model

The insulin minimal model was proposed by Toffolo et al [21] to describe the insulin kinetics and secretion in order to assess the hepatic extraction in a second moment through the combined use of insulin and C-peptide minimal models results. Note that to identify the insulin model was used the IM-IVGTT that through more informative insulin

data facilitates a reliable estimation of insulin kinetics in each individual, a prerequisite to avoid errors in modeling secretion. The model has the following expression.

$$
\begin{aligned}
I'(t) &= -n \cdot I(t) + m \cdot X(t) + U(t) && I(0) = I_b \\
X'(t) &= -m \cdot X(t) + Y(t) && X(0) = X_0 + (n \cdot I_b)/m \\
Y'(t) &= \begin{cases}
-\alpha \cdot (Y(t) - \beta \cdot (G(t) - G_b) - n \cdot I_b) & \\
Y(0) = (n \cdot I_b), & \text{if } \beta \cdot (G(t) - G_b) - n \cdot I_b \geq 0 \\
-\alpha \cdot (Y(t)) & \\
Y(0) = (n \cdot I_b), & \text{if } \beta \cdot (G(t) - G_b) - n \cdot I_b < 0
\end{cases}
\end{aligned}
\tag{2.4}
$$

where I is the insulin concentration in plasma (pmol/l) and I_b its basal value, X (pmol/l) is the insulin amount in the β-cell and Y is the insulin provision in the β-cell (pmol l^{-1} min^{-1}). G is the glucose concentration in plasma (mg/dl) and G_b is its basal value and U is the exogenous insulin input (pmol l^{-1} min^{-1}) different from zero in the 20/25 min interval. The uniquely identifiable parameters are: the rate constant of insulin disappearance n (1/min), the secretion rate constant m (measured in min^{-1}), provision rate constant α (measured in min^{-1}), the second-phase sensitivity to glucose β (measured in dl mg^{-1} pmol l^{-1} min^{-1}) and the incremental amount of insulin secreted during the first phase X_0 (measured in pmol/l).

MTT minimal models

Glucose minimal model

The oral glucose minimal model was proposed by Dalla man et al [22, 23] and its schematic representation id presented in Fig. 2.6. The model has the following expression:

$$
\begin{aligned}
Q'(t) &= -(S_G + X(t)) \cdot Q(t) + S_G \cdot Q_b + Ra_{meal}(\mathbf{p}, t) && Q(0) = G_b \cdot V \\
X'(t) &= -p2 \cdot X(t) + p2 \cdot S_I \cdot (I(t) - I_b) && X(0) = 0
\end{aligned}
\tag{2.5}
$$

where Q (mg/kg) is the glucose mass in plasma and Q_b (mg/kg) its basal value, G_b (mg/dl) is the basal glucose concentration in plasma, I (μU/ml) is insulin plasma concentration and I_b (μU/ml) its basal value, X (min^{-1}) is insulin action, Ra (mg kg^{-1} min^{-1}) is the glucose unknown rate of appearance in plasma, V (dl/kg) is the volume distribution, S_G (min^{-1}) is glucose effectiveness, SI (min^{-1} μU^{-1} ml) is insulin sensitivity and p2 (min^{-1}) is an insulin action parameter. Note that Ra_meal is a parametric function expressed as dependent of a vector of unknown parameters $\mathbf{p}$. In particular Ra_{meal} is described by a

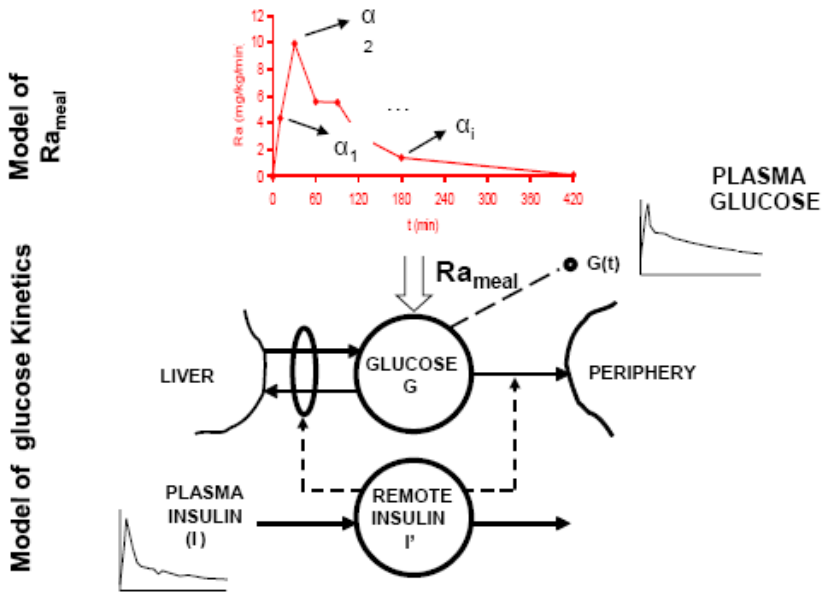

Figure 2.6: MTT glucose minimal model schematic representation.

piecewise-linear function with a given number of breakpoints that are more concentrated at the first part of the experiment where the signal varies more rapidly and more sparsely afterwards. The rate of appearance can be described by the following equation:

$$Ra_{meal}(\mathbf{p},t) = \begin{cases} \alpha_{i-1} + \frac{\alpha_i - \alpha_{i-1}}{t_i - t_{i-1}} \cdot (t - t_{i-1}), & \text{if } t_{i-1} \le t \le t_i, \qquad i = 1, ..., 8 \\ 0, & \text{otherwise} \end{cases} \tag{2.6}$$

where α_i are the unknown parameters and t_i are the breakpoints. Note that α_2 was not estimated but derived using the following constraint on the area under the curve of Ra_{meal}:

$$\int_0^\infty Ra_{meal}(\mathbf{p},t)\,dt = \frac{D \cdot f}{BW} \tag{2.7}$$

where D is the dose (mg), f is the fraction of the ingested dose (fixed to 0.9) and BW (kg) is the subject weight. For identifiability reason the model parameter S_G, V were fixed to population values respectively 0.025 (min^{-1}) and 1.45 (dl/kg) and a gaussian bayesian prior was considered for p2 (min^{-1}) with $\ln(\text{p2}) \in N(-4.414, 0.4414)$.

C-peptide minimal model

The C-peptide oral minimal model was proposed by Breda et al [24, 25] and is described by the following equations:

$$
\begin{aligned}
CP_1'(t) &= -(k_{01}+k_{21})\cdot CP_1(t) + k_{12}\cdot CP_2(t) + SR_n & CP_1(0) &= CP_b \\
CP_2'(t) &= -k_{12}\cdot CP_2(t) + k_{21}\cdot CP_1(t) & CP_2(0) &= \frac{CP_b\cdot k_{21}}{k_{12}} \\
Y'(t) &= \begin{cases} -\alpha\cdot(Y(t)-\beta\cdot(G(t)-G_b)+k_{01}\cdot CP_{1b}) & \\ Y(0) = k_{01}\cdot CP_{1b}, & \text{if } \beta\cdot(G(t)-G_b)+k_{01}\cdot CP_{1b}\geq 0 \\ -\alpha\cdot(Y(t)) & \\ Y(0) = k_{01}\cdot CP_{1b}, & \text{if } \beta\cdot(G(t)-G_b)+k_{01}\cdot CP_{1b}< 0 \end{cases}
\end{aligned}
\tag{2.8}
$$

where CP_1 and CP_2 are the C-peptide concentration in the accessible and peripheral compartments respectively (pmol/l), SR_n is the secretion rate (pmol l^{-1} min^{-1}), Y is the releasable C-peptide provision (pmol/l min), G is the glucose concentration (mg/dl) and G_b its basal value. The transfer rate between CP_1 and CP_2 k_{12}, k_{21} and k_{01} (min^{-1}) are fixed kinetics determined through the Van Cauter formulas [20]. The model also assumes that SR_n is made up of a static (SR_s) and a dynamic (SR_d) component as it is described in Eq. 2.9. The static secretion is proportional to the insulin provision controlled with some delay ($1/\alpha$ where α is measured as (min^{-1})) by glucose concentration above a threshold level G_b, through the parameter β (measured in dl mg^{-1} pmol l^{-1} min^{-1}). Whereas the dynamic secretion represents the secretion of insulin from the promptly releasable pool and is proportional to the rate of increase of glucose through a constant parameter k (min^{-1}).

$$
\begin{aligned}
SR_n(t) &= SR_s(t) + SR_d(t) \\
SR_s(t) &= Y(t) \\
SR_d(t) &= \begin{cases} k\cdot\frac{dG}{dt}, & \text{if } \frac{dG}{dt}\geq 0 \\ 0 & \text{if } \frac{dG}{dt}< 0 \end{cases}
\end{aligned}
\tag{2.9}
$$

As the IVGTT C-peptide minimal model also the oral has some derived indexes that describe the *beta*-cell responsivity. In particular the derived indexes:

- the static β-cell responsivity (Φ_s) is defined as:

$$\Phi_s = \beta \tag{2.10}$$

- the dynamic β-cell responsivity (Φ_d) is defined as:

$$\Phi_d = k \tag{2.11}$$

- Overall or total β-cell responsivity (Φ_t) can be derived from the previous calculated index as:

$$\Phi_t = \Phi_s + \frac{\Phi_d \cdot \Delta G}{\int_0^\infty (G(t) - G_b)\, dt} \tag{2.12}$$

  where ΔG is the maximal excursion of glucose above basal.

2.4 Nonlinear mixed-effects models

Very often in epidemiological studies, when experimental data are available for a large number of subjects, it is of interest to determine not only the individual characteristics but also the description of the parameters distribution across the population. Many approaches have been developed to determine both the features from the easiest that is a straightforward statistic (mean and variance) on the individual parameter estimates set (i.e. standard two stage (STS) [26]) to more sophisticated iterative methods that alternates at each iteration until convergence an individual and a population optimization phase such as the iterative two stage (ITS)[27] or the global two stage (GTS) [27]. Finally a more sophisticated technique is the Nonliner mixed effects models (NLMEM) approach. With this technique each individual data is described by the following individual level model:

$$y_{ij} = f(\mathbf{p_i}, x_{ij}) + \epsilon_{ij} \qquad 1 \leq i \leq m \qquad 1 \leq j \leq n_i \tag{2.13}$$

where y_{ij} is the j-th observation of the i-th subject at some known time instant x_{ij} and ϵ_{ij} is the measurement error of the i-th subject in the j-th sample.
The NLMEM assumes a two stage hierarchy of variability through different probability distribution that allows the investigator to have more flexibility in the study design. The first stage describes the intra individual variability (measurement error and unforeseen error sources) whereas the second stage describes the inter individual variability (physiological variability). The intra individual variability, the so called *Residual Unknown Variability* (RUV), is assumed to be normally distributed with zero mean and variance that might be dependent on the model prediction or the measured data. For example the RUV of the i-th subject at the j-th observation with variance dependent on the model

prediction would be expressed like in the following equation:

$$\epsilon_{ij} \sim N(0, (\sigma f(\mathbf{p_i}, x_{ij}))^2) \tag{2.14}$$

where σ is the proportional error variance. The second stage of variability is explainable due to the fact that the individual parameters are seen as realizations of a certain distribution that is characterized by a mean vector that represents the so called *fixed effects* $\boldsymbol{\theta}$, the features that do not vary among the population, and by a variance matrix ($\boldsymbol{\Omega}$) that is the population variability or the Between subject variability (BSV). In other words the vector of parameters of the i-th subject can be described through the so called population level model as:

$$\mathbf{p}_i = g(\boldsymbol{\theta}, \boldsymbol{\eta}_i, \mathbf{a}_i) \tag{2.15}$$

where $\boldsymbol{\eta}_i$ are the *random effects* of the subject i that are assumed normally distributed, with zero mean and variance $\boldsymbol{\Omega}$. The flexibility of the technique is guaranteed by the definition of the probability density function g which can also incorporate other factors such as physiological information about the subject $\mathbf{a}_i$ (e.g. body height and weight). This makes the NLMEMs very appealing as it allows easy incorporation of *covariates* in the model. Note that Eq. 2.15 characterizes how $\mathbf{p}_i$ vary among individuals due to systematic association with the individual characteristic ($\mathbf{a}_i$) or due to unexplained variation in the population like biological variation. The $\boldsymbol{\Omega}$ matrix determines the magnitude of the unexplained variation.

The NLMEM rely on a Maximum likelihood estimator that was expanded with respect to the original single subject formulation to take into account the inter subject variability of the parameters and the within-individual error [28]. The population likelihood 2.16 is defined as the sum of all the i-th individual contribution that are twice the negative logarithm of the joint marginal density of the data $\mathbf{y}_i$ for subject i. In formulae the total objective function (L) is:

$$L = -2log(p(\mathbf{y}|\boldsymbol{\theta}, \boldsymbol{\Omega}, \boldsymbol{\sigma})) = \sum_{i=1}^{m} L_i = -2 \sum_{i=1}^{m} log(\int_{-\infty}^{\infty} l(\mathbf{y}_i|\mathbf{p}, \boldsymbol{\sigma}) h(\mathbf{p}|\boldsymbol{\theta}, \boldsymbol{\Omega})\, d\mathbf{p}) \tag{2.16}$$

where l($\mathbf{y_i}$ | $\mathbf{p}$,$\boldsymbol{\sigma}$) is the individual observed data likelihood for subject i and h($\mathbf{p}$ | $\boldsymbol{\theta}, \boldsymbol{\Omega}$) is the probability density of the vector of parameters $\mathbf{p}$ given the fixed effects $\boldsymbol{\theta}$ and the variability of the random effects $\boldsymbol{\Omega}$ and $\boldsymbol{\sigma}$ is the RUV. Usually in PKPD the probability density of the individual vector of parameters $\mathbf{p}$ is assumed to be Gaussian or the transformation is Gaussian (lognormal distribution) and in formulae not including

a constant term this can be written as:

$$h(\mathbf{p}|\boldsymbol{\theta}, \boldsymbol{\Omega}) = \frac{1}{\sqrt{|\boldsymbol{\Omega}|}} exp[-\frac{1}{2}(\mathbf{p}-\boldsymbol{\theta})'\boldsymbol{\Omega}^{-1}(\mathbf{p}-\boldsymbol{\theta})] \tag{2.17}$$

To find the values of $\boldsymbol{\theta}$, $\boldsymbol{\Omega}$ and $\boldsymbol{\sigma}$ that best fit all the subject data the joint marginal density has to be maximized that means minimize the 2.16. Due to nonlinear parameter relations the m k-dimensional integrals usually do not have a close form. The computational burden of the iterative algorithm like Newton Raphson that maximize the problem increase significantly at each internal iteration step since for each subject a k-dimensional integral have to be evaluated through numerical techniques. Many approximations to the integrals have been proposed to make them more tractable. Here we introduce the NLMEM methods implemented in the NONMEM software [29] that are used in the thesis and we divide them in two different groups that represent two ways to treat the integral approximation problem: methods that linearize the likelihood (e.g. first order conditional-FOCE) and methods based on the Expectation-Maximization (EM) algorithm and that approximate in different ways the E-step (e.g. iterative two stage-ITS, Monte Carlo with importance Sampling IMP, importance sampling with mode a posteriori IMPMAP and Stochastic approximation EM-SAEM). These two groups are called the 2-stage hierarchical maximum likelihood methods where the first stage of the hierarchy is represented by the individual likelihood of the data $\mathbf{y}_i$ $l(\mathbf{y}_i|\mathbf{p}, \boldsymbol{\sigma})$ and the second stage is the likelihood of the set of parameters $\mathbf{p}$ given some knowledge on the parameter distribution (h($\mathbf{p} \mid \boldsymbol{\theta}, \boldsymbol{\Omega}$)). In this thesis was analyzed also a method that adds a further third hierarchical stage to the individual and population step that takes into account the uncertainty of the knowledge of the parameters $\boldsymbol{\theta}$, $\boldsymbol{\Omega}$ and $\boldsymbol{\sigma}$. This method is the Bayesian method (BAYES).

Likelihood linearization methods

The FOCE method linearize the model [29](2.13) with a Taylor first order approximation around a properly individualized parameter estimate. The alternative objective function that is minimized is the following:

$$L_N = -2log(p(\mathbf{y}|\boldsymbol{\theta}, \boldsymbol{\Omega}, \boldsymbol{\sigma})) = \sum_{i=1}^{m} L_{iN} \tag{2.18}$$

where the approximate individual likelihood contribution is given by:

$$L_{iN} = -2log(p(\mathbf{y}_i, \hat{\mathbf{p}}_i|\boldsymbol{\theta}, \boldsymbol{\Omega}, \boldsymbol{\sigma})) - log|\hat{\mathbf{B}}_i| \tag{2.19}$$

where the first term is the approximate joint probability density of the i-th subject around the mode or of the distribution ($\hat{\mathbf{p}}_i$) and the second term is the Taylor first order approximation to the conditional variance matrix of the parameters. The resolution of the algorithm is done through a 2-step process: first each individual data are fitted with $\boldsymbol{\theta}$, $\boldsymbol{\Omega}$ and $\boldsymbol{\sigma}$ set. The modes of the distribution $\hat{\mathbf{p}}_i$ and $\hat{\mathbf{B}}_i$ are found and the L_N function is constructed as the sum of each individual contribution. Then with a quasi-Newton Rhapson routine the optimal values of $\boldsymbol{\theta}$, $\boldsymbol{\Omega}$ and $\boldsymbol{\sigma}$ are found. Potential pitfalls of this method is when the number of samples for each subject is small (the more samples the more the approximation is accurate) and when the assumptions of normality are infringed.

EM based methods

The Expectation Maximization (EM) algorithm aim is to maximize the exact likelihood when the observations can be seen as incomplete. Note that in the NLMEM the missing data or non observed data are the individual random effects. Each iteration of the algorithm consists of two steps: the E-step where the expectation of the log-likelihood given current population estimates is calculated and the M-step where new population estimates are calculated maximizing the function obtained in the former step. If the population density $\mathrm{h}(\mathbf{p} \mid \boldsymbol{\theta}, \boldsymbol{\Omega})$ of a given $\mathbf{p}$ is a multivariate normal distribution (or the transformation of $\mathbf{p}$ is normal) it can be shown that at the minimum of the objective function the following relationships are true:

$$\begin{aligned} \boldsymbol{\theta} &= \frac{1}{m}\sum_{i=1}^{m} \bar{\mathbf{p}}_i \\ \boldsymbol{\Omega} &= \frac{1}{m}\sum_{i=1}^{m} \bar{\boldsymbol{\Omega}}_i \end{aligned} \tag{2.20}$$

This relations correspond to the M-step that is evaluated at each iteration after having calculated the E-step that is described by the following equations:

$$\begin{aligned} \bar{\mathbf{p}}_i &= \int_{-\infty}^{\infty} \mathbf{p} z(\mathbf{p}|\mathbf{y}_i, \boldsymbol{\theta}, \boldsymbol{\Omega}, \boldsymbol{\sigma})\, d\mathbf{p} \\ \boldsymbol{\Omega}_i &= (\bar{\mathbf{p}}_i - \boldsymbol{\theta})(\bar{\mathbf{p}}_i - \theta)' + \int_{-\infty}^{\infty} (\mathbf{p} - \bar{\mathbf{p}}_i)(\mathbf{p} - \bar{\mathbf{p}}_i)' z(\mathbf{p}|\mathbf{y}_i, \boldsymbol{\theta}, \boldsymbol{\Omega}, \boldsymbol{\sigma})\, d\mathbf{p} \end{aligned} \tag{2.21}$$

Where the first equation is the conditional mean vector of $\mathbf{p}$ for subject i and the second equation is the contribution to the population variance from each subject i and the integral term is conditional variance matrix of $\mathbf{p}$ for subject i. $z(\mathbf{p}|\mathbf{y}_i, \boldsymbol{\theta}, \boldsymbol{\Omega}, \boldsymbol{\sigma})$ is the

conditional density of $\mathbf{p}$ given data $\mathbf{y}_i$ and population parameters $\boldsymbol{\theta}$, $\boldsymbol{\Omega}$ and $\boldsymbol{\sigma}$ and is described in the following equation:

$$z(\mathbf{p}|\mathbf{y}_i, \boldsymbol{\theta}, \boldsymbol{\Omega}, \boldsymbol{\sigma}) = \frac{l(\mathbf{y}_i|\mathbf{p}, \boldsymbol{\sigma})h(\mathbf{p}|\boldsymbol{\theta}, \boldsymbol{\Omega})}{\int_{-\infty}^{\infty} l(\mathbf{y}_i|\mathbf{p}, \boldsymbol{\sigma})\mathbf{h}(\mathbf{p}|\boldsymbol{\theta}, \boldsymbol{\Omega})\, \mathbf{dp}} \tag{2.22}$$

At each iteration given fixed values for $\boldsymbol{\theta}$ and $\boldsymbol{\Omega}$ these two equations 2.21 are calculated, the so called E-step. The E-step can be calculated in close form under specific conditions that is the f is linear in $\mathbf{p}$ and RUV does not depend on the random effects. In the remaining situations there is no analytical solution to the E-step and so many approaches were proposed to approximate it. In particular different Monte Carlo sampling methods were used to calculate the integration step present in both the conditional mean and variance matrix (Eq. 2.21) by randomly sample over the entire space of $\mathbf{p}$ and evaluate the integrals by summation. Note that by substituting Eq. 2.22 in both Eq. 2.21 it is evident the presence of the same integral of the population likelihood in the denominator and of a similar integral in the numerator that due to parameter nonlinearity does not have a close form (see Eq. 2.23).

$$\begin{aligned} \bar{\mathbf{p}}_i &= \frac{\int_{-\infty}^{\infty} \mathbf{p} p(\mathbf{y}_i, \mathbf{p}|\boldsymbol{\theta}, \boldsymbol{\Omega}, \boldsymbol{\sigma})\, d\mathbf{p}}{\int_{-\infty}^{\infty} p(\mathbf{y}_i, \mathbf{p}|\boldsymbol{\theta}, \boldsymbol{\Omega}, \boldsymbol{\sigma})\, d\mathbf{p}} \\ \boldsymbol{\Omega}_i &= (\bar{\mathbf{p}}_i - \theta)(\bar{\boldsymbol{p}}_i - \theta)' + \frac{\int_{-\infty}^{\infty} (\mathbf{p} - \bar{\mathbf{p}}_i)(\mathbf{p} - \bar{\mathbf{p}}_i) p(\mathbf{y}_i, \mathbf{p}|\boldsymbol{\theta}, \boldsymbol{\Omega}, \boldsymbol{\sigma})\, d\mathbf{p}}{\int_{-\infty}^{\infty} p(\mathbf{y}_i, \mathbf{p}|\boldsymbol{\theta}, \boldsymbol{\Omega}, \boldsymbol{\sigma})\, d\mathbf{p}} \end{aligned} \tag{2.23}$$

Several Monte Carlo methods were developed to evaluate the conditional mean and variance matrix among them the importance sampling that is implemented in NONMEM software [29] in the estimation method IMP [30] and in the estimation method IMPMAP [29] and the stochastic approximation method that is implemented in NONMEM software in the estimation method (SAEM) [31]. These methods can be made as accurate as possible with the disadvantage of having a big computation time load. Here we briefly describe the different way to treat the E-step using the EM based algorithm implemented in the NONMEM software [29]:

Iterative two stage (ITS)

The ITS algorithm first suggested by Steimer et al [27], implements the E-step through the same linearized approximation that is done in FOCE. In particular each individual fit is carried out to obtain the individual mode $\hat{\mathbf{p}}_i$ and $\hat{\mathbf{B}}_i$ that are then used in the M-step

that is simply their average value in the population:

$$\begin{aligned} \boldsymbol{\theta} &= \frac{1}{m}\sum_{i=1}^{m}\hat{\mathbf{p}}_i \\ \boldsymbol{\Omega} &= \frac{1}{m}\sum_{i=1}^{m}\hat{\boldsymbol{\Omega}}_i \end{aligned} \tag{2.24}$$

Importance sampling (IMP) / Importance sampling supported by mode a posteriori (IMPMAP)

The IMP method [30] implements the E-step by approximating the integral using a Monte Carlo sampling method that draw the samples in more informative positions with respect to the direct sampling that requires the integration in all the parameter space. In this way the variance of the Monte Carlo estimator is reduced. The population likelihood is weighted adjusted with an importance sampling function $b(\mathbf{p})$ that approximate the joint density $l(\mathbf{y}_i|\mathbf{p},\boldsymbol{\sigma})h(\mathbf{p}|\boldsymbol{\theta},\boldsymbol{\Omega})$:

$$L = -2\sum_{i=1}^{m} log(\int_{-\infty}^{\infty} l(\mathbf{y}_i|\mathbf{p},\boldsymbol{\sigma})\frac{h(\mathbf{p}|\boldsymbol{\theta},\boldsymbol{\Omega})}{b(\mathbf{p})}b(\mathbf{p})\,d\mathbf{p}) \tag{2.25}$$

In the IMP estimation method in the first iteration the normal distribution proposal (sampling) density from which Monte Carlo samples are drawn comes from an FOCE analysis. In the IMPMAP estimation step instead the FOCE linearization method is present at each step to build the normal distribution proposal sampling density from which Monte Carlo samples are drawn.

Stochastic approximation expectation maximization (SAEM)

The SAEM method [31] is a stochastic approximation of the traditional EM method. In particular it consists in replacing the usual E-step with a stochastic procedure composed of two steps: a simulation step and a stochastic approximation step. For the k-th iteration of the algorithm the iter in the E-step would be this:

- *SIMULATION STEP*: draw m_k individual parameters $\mathbf{p}_k(i)$ (with i=1,:. , m_k) from the posterior density $h(\mathbf{p}|\boldsymbol{\theta}_k,\boldsymbol{\Omega}_k)$
- *STOCHASTIC APPROXIMATION*: update $Q_k(\boldsymbol{\delta})$ where $\boldsymbol{\delta} = [\boldsymbol{\theta},\boldsymbol{\Omega},\boldsymbol{\sigma}]$:

$$\hat{Q}_k(\boldsymbol{\delta}) = \hat{Q}_{k-1}(\boldsymbol{\delta}) + \gamma_k(\frac{1}{m_k}\sum_{i=1}^{m_k} logp(\mathbf{y}_i,\mathbf{p}_k(i)|\boldsymbol{\theta},\boldsymbol{\Omega},\boldsymbol{\sigma}) - \hat{Q}_{k-1}(\boldsymbol{\delta})) \tag{2.26}$$

Note that for all k ∈ N $\gamma_k \in [0,1]$, $\sum_{k=1}^{\infty} \gamma_k = \infty$, $\sum_{k=1}^{\infty} \gamma_k^2 = \infty$

where γ_k is a sequence of positive step sizes decreasing to 0. The maximization step consist in maximizing $\hat{Q}_k(\boldsymbol{\delta})$ and finding the new $\boldsymbol{\theta}_{k+1}, \boldsymbol{\Omega}_{k+1}$ If the simulation step cannot be performed directly the algorithm was combined with the MCMC procedure where the sequence $\mathbf{p}_k$ is a Markov Chain with transition kernels ($\prod \delta k$). The new simulation step will draw $\mathbf{p}_k$ from the transition probability $\prod \delta k(\mathbf{p}_{k-1})$. Note that for any $\delta \in \Gamma$, the transition kernel $\prod \delta$ generates a uniformly ergodic chain which invariant probability is $h(\mathbf{p}|\boldsymbol{\theta}, \boldsymbol{\Omega})$. Note that there is also an implementation of SAEM using simulated annealing to prevent the algorithm from local minima and to ensure then the global minima achievement. In this way the algorithm is faster and robust to initial estimates.

Bayesian method

The Bayesian method (BAYES) [32] does not maximize the likelihood but give back a complete distribution profile of the population parameters $\boldsymbol{\theta}$, $\boldsymbol{\Omega}$ and $\boldsymbol{\sigma}$ ($\mathbf{p}(\boldsymbol{\theta}, \boldsymbol{\Omega}, \boldsymbol{\sigma}|\mathbf{y}, \mathbf{q}, \mathbf{H}, \mathbf{w}, \boldsymbol{\tau})$) and the maximum likelihood estimates can be identified by choosing the set with the highest frequency. In particular the complete distribution can be calculated through the following equation:

$$\begin{aligned} p(\boldsymbol{\theta}, \boldsymbol{\Omega}, \boldsymbol{\sigma}|\mathbf{y}, \mathbf{q}, \mathbf{H}, \mathbf{w}, \boldsymbol{\tau}) &= \frac{p(\mathbf{y}, \boldsymbol{\theta}, \boldsymbol{\Omega}, \boldsymbol{\sigma}|\mathbf{q}, \mathbf{H}, \mathbf{w}, \boldsymbol{\tau})}{p(\mathbf{y}|\mathbf{q}, \mathbf{H}, \mathbf{w}, \boldsymbol{\tau})} \\ &= \frac{p(\mathbf{y}|\boldsymbol{\theta}, \boldsymbol{\Omega}, \boldsymbol{\sigma})\pi(\boldsymbol{\theta}, \boldsymbol{\Omega}, \boldsymbol{\sigma}|\mathbf{q}, \mathbf{H}, \mathbf{w}, \boldsymbol{\tau})}{\int_{-\infty}^{\infty} p(\boldsymbol{y}, \boldsymbol{\theta}, \boldsymbol{\Omega}, \boldsymbol{\sigma}|\mathbf{q}, \mathbf{H}, \mathbf{w}, \boldsymbol{\tau}) d\boldsymbol{\theta} d\boldsymbol{\Omega} d\boldsymbol{\sigma}} \\ &= \frac{\prod_{i=1}^{m} [\int_{-\infty}^{\infty} l(\mathbf{y}_i|\mathbf{p}, \boldsymbol{\sigma}) h(\mathbf{p}|\boldsymbol{\theta}, \boldsymbol{\Omega})\, d\mathbf{p}] \pi(\boldsymbol{\theta}, \boldsymbol{\Omega}, \boldsymbol{\sigma}|\mathbf{q}, \mathbf{H}, \mathbf{w}, \boldsymbol{\tau})}{\int_{-\infty}^{\infty} \prod_{i=1}^{m} [\int_{-\infty}^{\infty} l(\mathbf{y}_i|\mathbf{p}, \boldsymbol{\sigma}) h(\mathbf{p}|\boldsymbol{\theta}, \boldsymbol{\Omega})\, d\mathbf{p}] \pi(\boldsymbol{\theta}, \boldsymbol{\Omega}, \boldsymbol{\sigma}|\mathbf{q}, \mathbf{H}, \mathbf{w}, \boldsymbol{\tau})\, d\boldsymbol{\theta} d\boldsymbol{\Omega} d\boldsymbol{\sigma}} \end{aligned} \tag{2.27}$$

where $\pi(\boldsymbol{\theta}, \boldsymbol{\Omega}, \boldsymbol{\sigma}|\mathbf{q}, \mathbf{H}, \mathbf{w}, \boldsymbol{\tau})$ is the probability of the population parameters based on prior knowledge. In particular $\boldsymbol{\theta}$ is modeled as a normal distribution $\mathbf{N}(\mathbf{q}, \mathbf{H})$, $\boldsymbol{\Omega}$ is a Whishart distribution $\mathbf{W}(\mathbf{w})$ and $\boldsymbol{\sigma}$ is modeled as a gamma distribution with parameter $\boldsymbol{\tau}$. If there is no prior knowledge on the experiment $\mathbf{H}$ should be large and $\boldsymbol{\tau}$ should be small: these are the so called uninformative prior that mean that there is a great search region for the parameters $\boldsymbol{\theta}$, $\boldsymbol{\Omega}$ and $\boldsymbol{\sigma}$ with a consequent computational expensive load. The process to evaluate Eq. 2.27 would be with Monte Carlo to randomly select from their prior distribution the population parameter $\boldsymbol{\theta}$, $\boldsymbol{\Omega}$ and $\boldsymbol{\sigma}$ from which randomly select the $\mathbf{p}$ and then evaluate the likelihood. In conclusion the result is a collection of

the population parameters $\boldsymbol{\theta}$, $\boldsymbol{\Omega}$ and $\boldsymbol{\sigma}$ with their frequency and by choosing the highest frequency are identified the maximum likelihood estimates. To increase the efficiency of the Monte Carlo method the Markov Chain Monte Carlo (MCMC) has been used implemented through algorithms like the Metropolis-Hastings or the Gibbs sampling.

Stochastic nonlinear mixed effects methods to quantify IVGTT data

3.1 Overview

The nonlinear mixed effects models (NLMEM) are widespread modeling techniques in PKPD analysis and epidemiological studies because they can produce a description of not only the individual but also of the population features. Moreover, they are able to deal with individual data sparseness by borrowing the lack of information from the entire population. In this way, the NLMEM do not fail where instead other techniques, such as the traditional individual weighted least squares (WLS), sometimes do. The NLME approach relies on the maximization of a likelihood function that due to model parametric nonlinearity not always has an explicit solution. Various techniques have been proposed to solve this problem including the first order (FO) and the first order conditional (FOCE) estimation methods that approximate the likelihood function through a linearization; the expectation maximization algorithm (EM) that maximize the exact likelihood; the Bayesian estimation method where a third stage of variability, the distribution of the population parameters, is taken into account [28]. Recently, new estimation methods that rely on the EM algorithm have been implemented in the last release of the population software NONMEM [29]. These methods are: the iterative two stage (ITS), Monte Carlo

importance sampling EM (IMP), Monte Carlo importance sampling EM assisted by Mode a Posteriori estimation (IMPMAP) and the Stochastic Approximation EM (SAEM). Moreover, another new method is available, the Markov Chain Monte Carlo Bayesian Analysis (BAYES), next to the more known FO and FOCE. With this article we want to complete the Denti et al [2] simulation study by evaluating the newest population methods applied on the IVGTT glucose minimal model.

3.2 Introduction

The IVGTT glucose minimal model (MM) is a well known tool to study the glucose-insulin system in different pathophysiological states after an intravenous glucose perturbation. Indeed, its parameter SI, the insulin sensitivity, that is the overall effect of insulin to stimulate glucose uptake and inhibit glucose production, represents an important metabolic index in clinical and epidemiological trials. By now the model has been identified using both individual and population approaches. At the beginning the weighted least square (WLS) single subject technique was used and applied on the data of each individual. The WLS, though, in typical epidemiological conditions such as sparse and noisy data per individual does not produce satisfactory estimations. In order to improve this aspect, the population approaches were then introduced to identify the MM by exploiting the not used information spread on the subject collection. Vicini et al [33] identified the MM by the iterative two stage (ITS), a population technique. This method is made up of two steps: first each subject's data is separately fitted and then the population parameter estimates are obtained. This procedure is repeated until convergence. Afterwards, Agbaje et al [34] used a different population approach to identify the same model: the Bayesian hierarchical method [32]. This method adds a third stage of knowledge to the individual and population step that is the prior distribution of the population parameters. More recently [2], the MM was quantified using both iterative methods, like the Global two stage (GTS) and ITS and other techniques like the first order (FO) and the first order conditional (FOCE). These last two methods are approximated solutions of the nonlinear mixed effects models (NLMEM) approach that aims to characterize the individual and population description by maximizing a likelihood function. Due to nonlinear parametric dependencies it is almost impossible to have an explicit solution of this optimization problem. FO and FOCE methods fix this by approximating the likelihood through a linearization. This work is the natural follow up of Denti et al [2] where different population estimation methods, implemented in the software SPK [35], were tested in a simulation study. In particular the study aims are mainly two. The first is to complete

the population analysis done so far in the MM with the latest methods implemented in the software NONMEM [29]. Three new optimization techniques have never been applied so far to quantify the MM parameters: the Monte Carlo importance sampling EM (IMP) [30], the Monte Carlo importance sampling EM assisted by Mode a Posteriori estimation (IMPMAP) [2] and the Stochastic Approximation EM (SAEM) [31]. These three, together with the ITS method, are implemented in NONMEM by exploiting the characteristic two steps of the Expectation-Maximization algorithm (EM). In the first step (the expectation step) the expectation of the log-likelihood given current estimates of the population parameters is calculated and, in the second step (the maximization step), new population parameters that maximize the expectation are computed. This procedure is repeated until there are no visible changes in the objective function. Note that the four different implementations of the EM algorithm are different approximations of the expectation step for which no analytical solution is available. The second aim of this work is to test the robustness of the different methods in a data poor context by comparing their performances on two randomly generated datasets obtained by removing respectively 50% and 75% of the original samples respectively. All our analysis is carried out using the software NONMEM VII [29].

3.3 Material and Methods

1. *Synthetic Data*
   As already mentioned this work is the Denti et al [2] natural follow up but carried out with different software and estimation methods. The dataset used is the same. The dataset (dataset A1) consists of 58 simulated insulin modified IVGTT profiles (dose 330 mg/kg glucose at time 0, 0.02 units/kg of insulin at time 20). This dataset was obtained through two steps. Firstly, the MM was identified using the individual estimation method WLS, implemented in the software SAAM II [36], in 58 nondiabetic young subjects (mean age 23±3 and mean BMI 24.5 ± 2.9 kg/m^2) that underwent an IVGTT in the Clinical Research Center at the Mayo Clinic, Rochester, MN. Blood samples were collected at -120, -30, -20, -10, 0, 2, 4, 6, 8, 10, 15, 20, 22, 25, 26, 28, 31, 35, 45, 60, 75, 90, 120, 180 and 240 min for measurement of glucose and insulin concentrations. Secondly, the profiles were simulated using the individual estimates obtained at the first step and a measurement noise equal to the 2% of the simulated profile was added. In order to exploit the potentials of the population technique and to test the robustness of the estimates we evaluate the different methods performance in a data poor context. In particular the simulated

dataset was reduced by randomly removing the original samples. The first time 50% of the original samples were randomly removed (dataset A2), while the second time instead 75% of the original samples were removed (dataset A3). In this way the typical condition of the epidemiological studies, that is few and noisy data per individual, was recreated. Note that only the glucose data were reduced whereas the insulin data that acts as a forcing function in the model was not. This choice was made because the work aim is to test different estimation methods and not really simulate a real experiment data sparseness situation.

2. *Glucose minimal model*
   The IVGTT MM is described by:

$$\begin{aligned} Q'(t) &= -(S_G + X(t)) \cdot Q(t) + S_G \cdot Q_b \qquad Q(0) = D + G_b \cdot V \\ X'(t) &= -p2 \cdot X(t) + p2 \cdot S_I \cdot (I(t) - I_b) \qquad X(0) = 0 \end{aligned} \tag{3.1}$$

   where Q is the glucose mass in plasma (mg/kg) and Qb its basal value, Gb is the basal glucose concentration in plasma (mg/dL), I is insulin plasma concentration (pmol/L) and Ib its basal value, X is insulin action ($min^{-}1$). The uniquely identifiable parameters are: glucose effectiveness SG ($min^{-}1$), insulin sensitivity SI ($min^{-}1\ pmol^{-}1$ L), insulin action parameter p2 ($min^{-}1$) and volume V (dL/kg). The model is not designed to take into account the first 8 minutes of glucose so the corresponding measurements were excluded from the modeling analysis.

3. *Population assumptions*
   In the population analysis done using the NLME approach data are described by the model:

$$y_{ij} = f(\mathbf{p_i}, x_{ij}) + \epsilon_{ij} \qquad 1 \leq i < m \qquad 1 \leq j < n_i \tag{3.2}$$

   where y_{ij} is the jth observation of the ith subject at some known time instant x_{ij}. Here, m is the number of individuals and n_i is the number of observations of the individual i. Pi is the vector of model parameters for the ith individual. The model parameters across the population are assumed to be lognormal distributed. In particular they can be described by:

$$\begin{aligned} p_{ki} &= \theta_k e^{\eta_{ki}} \\ \boldsymbol{\eta}_i &= N(0, \boldsymbol{\Omega}) \end{aligned} \tag{3.3}$$

   where p_{ki} is the kth model parameter of the ith subject, $\boldsymbol{\theta}_k$ is the typical value of

the kth parameter common to the entire population and η_{ki} is the random effect of the kth model parameter of the ith subject. $_{ki}$ is assumed to be independently distributed with zero mean and Gaussian with $\mathbf{\Omega}$ being a positive definite covariance matrix Eq. 3.3. The $\mathbf{\Omega}$ values define the Between-Subject Variability (BSV). The omega set up matrix was chosen coherently with Denti et al [3] including just the correlations term between the S_I-P2 and S_G-V. The variability due to measurement and model errors, known as the residual unknown variability (RUV), instead is described by ϵ_{ij} which is assumed to be independently distributed with zero mean and Gaussian with standard deviation described by σ (proportional error variance) being an additional parameter to estimate:

$$\epsilon_{ij} = N(0, (\sigma y_{ij})^2) \tag{3.4}$$

4. *Nonlinear mixed effects methods*
   The reference estimates (REF) were obtained by the WLS approach implemented in SAAM II [36] applied on the original data. Then the other methods were applied on the simulated dataset. At first we investigated the standard two-stage (STS) performance which is another individual WLS that we implemented in NONMEM. Then we applied the population approach NLME that provides different estimation methods due to computational non feasibility of the exact solution of the likelihood maximization. Firstly, we applied the FOCE algorithm that is a linearization of the likelihood function. Then, we used the EM algorithm based estimation methods. These methods are the ITS, the IMP, the IMPMAP and the SAEM. Finally we applied the BAYES method that adds the third stage of variability due to the population parameters. The priors that were given to the population estimates were vague as in Agbaje et al [34], representing the lack of information about parameter distributions.

5. *Analysis of Results*
   In order to assess the different methods performance both the individual and the population estimates were evaluated and compared to REF estimates. As far as the population results are concerned, we evaluated the percentages of discrepancy between the estimated (fixed effects and square root of the BSVs) and the true values. The true values are the geometrical mean and standard deviation of the individual estimates REF. As far as the individual results are concerned, we evaluated the goodness of the individual estimates assessed by the square Root of the Mean

Square Error (RMSE):

$$RMSE = \sqrt{\sum_{k=1}^{m} \frac{(\mathbf{p}_i - \hat{\mathbf{p}}_i)^2}{m}} \tag{3.5}$$

where $\mathbf{p}_i$ is the true parameter value (REF) for subject i, $\hat{\mathbf{p}}_i$ its estimate, and m is the number of subjects involved in the analysis. For readability purposes, these values were indicated as percentage of the true population mean of each parameter.

3.4 Results

As already said, we exploited the population approaches to the full by analyzing both the population and the individual results in the simulated dataset (A1) and in its two reduced versions (A2-A3). Before proceeding it, is important to make a remark. All the methods were successful and no subject was excluded from the analysis. However some methods are more sensitive to initial estimates. In order to make them run smoothly we used a software feature that allows minimizing in cascade different methods; i.e. starting from the most stable whose final estimates are given as initial estimates to the subsequent less stable method. These methods were SAEM, IMP, IMPMAP and BAYES and each one was preceded in the minimization by ITS which is a more stable and at the same time fast technique in producing reliable estimates.

1. *Population results*

   For the population estimates in dataset A1, in general, all methods provide results coherent with the ones that were used for the simulation. However, not all the methods behave the same. Looking at Table 3.1, we can see that the best performing methods are ITS, FOCE and BAYES where all the fixed effects estimates discrepancy percentage do not exceed the 4% modulus and the discrepancies percentage of the BSV square root (values in brackets) do not exceed 28% modulus. The parameter that is worst estimated in these three methods in both the fixed effects and in the BSV is S_G. Whereas SAEM, IMP and IMPMAP tend to underestimate S_I (fixed effects percentage discrepancy values from -11% using SAEM or IMP to the -13% using the IMPMAP) and p2 (fixed effects percentage discrepancy values from -7% using SAEM or IMP to the -8% using IMPMAP). The parameter whose mean is estimated more precisely using all the estimation methods is V, whereas S_G, S_I and p2 are affected by a slightly larger error. The population approach, anyway, works

better than the individual approach STS. Looking at Table 3.1, one can see that STS presents the largest BSV. The overestimation of the variance of the population was expected as it is already well known in literature [26]. The population approach improvement due to the information borrowed across the population is expected to grow with the paucity of data. Looking now at the reduced dataset A2 and the furtherly reduced dataset A3, we can see that the discrepancy of the estimates, as expected, becomes larger with the samples reduction. This is true apart from some cases where instead there is the opposite effect. In particular, looking at table 3.1 we can see that if we consider the parameter S_I estimated with the SAEM method and we move from dataset A1 to dataset A3, the parameter fixed effect seems to be estimated better with less samples. This effect is a typical feature of the population approach, especially in a poor data context. In fact when there is not enough individual information (i.e. few samples per individual), a condition that is merely tolerated by the individual approach, a sort of constraint is generated between the individual estimates that tends to bring them together towards the population mean. This phenomenon is known in literature as shrinkage [37]. Also in these two reduced dataset, in general the parameter whose mean is estimated more precisely is V, whereas S_G, S_I and p2 are affected by a slightly larger error. The individual approach worsens its performance moving from dataset A2 to A3 as one can see clearly in Tab. 3.1from the increase of discrepancy percentage of the BSV square root.

2. *Individual results*

As far as the individual results are concerned, all the different population estimation methods perform comparable apart from the STS. In Fig. 3.1.the RMSE percentage of the individual estimates are presented. Looking at dataset A1, all the methods estimate well V and S_I, whereas S_G and p2 have a RMSE percentage larger than 13%. Also in this case, analyzing the individual results, the population approaches behave better than the individual approach represented by STS. Moreover, moving the attention to the reduced datasets, the same trend that was previously observed in the population results, is present here: RMSE percentage increases as expected with the lack of samples. V and S_I, as in A1 dataset individual results, are the parameters that are estimated more precisely. Regarding the comparison between the individual and the population approach, the population technique improvement due to the borrowed information across the subjects is larger in the two reduced datasets. In particular, the difference between the %RMSE values of

		ΔS_G	ΔVOL	ΔS_I	$\Delta p2$
dataset A1	STS	-2	0	0	0
		(74)	(173)	(41)	(47)
	ITS	4	0	-2	1
		(-25)	(-1)	(4)	(-8)
	FOCE	4	0	-2	1
		(-28)	(-2)	(4)	(-10)
	SAEM	0	1	-11	-7
		(-30)	(1)	(6)	(-9)
	BAYES	2	-1	0	2
		(-17)	(21)	(8)	(-2)
	IMP	3	-1	-11	-7
		(-25)	(0)	(7)	(7)
	IMPMAP	5	-1	-13	-8
		(-26)	(-1)	(10)	(-5)
dataset A2	STS	1	-1	1	-13
		(93)	(184)	(46)	(65)
	ITS	10	-1	-1	-9
		(-27)	(0)	(2)	(7)
	FOCE	10	-1	-1	-8
		(-29)	(-2)	(3)	(-10)
	SAEM	7	0	-9	-17
		(-32)	(-2)	(6)	(-5)
	BAYES	8	-1	-1	-6
		(-17)	(21)	(8)	(-1)
	IMP	7	-1	-6	-12
		(-28)	(1)	(4)	(-7)
	IMPMAP	7	-1	-10	-14
		(-29)	(-2)	(9)	(-4)
dataset A3	STS	-11	-3	-13	-4
		(122)	(257)	(94)	(107)
	ITS	13	-1	-1	-3
		(-40)	(-18)	(-10)	(-31)
	FOCE	13	-1	-1	-4
		(-53)	(-26)	(-9)	(-24)
	SAEM	13	-1	-4	-3
		(-42)	(-20)	(-6)	(-39)
	BAYES	10	-1	-1	-1
		(-44)	(-18)	(-4)	(-19)
	IMP	12	-1	-5	-6
		(-53)	(-25)	(-7)	(-20)
	IMPMAP	15	-2	-6	-9
		(-53)	(-25)	(-6)	(-19)

Table 3.1: The distance of the estimated values for both the fixed effects and the square root of the BSV (in brackets) from the true values are reported as percentage differences normalized to the true values for the three datasets

the STS method and the other corresponding values of the different population techniques increases moving from dataset A2 to dataset A3. In other words, the population approach features can be better appreciated in severely reduced datasets.

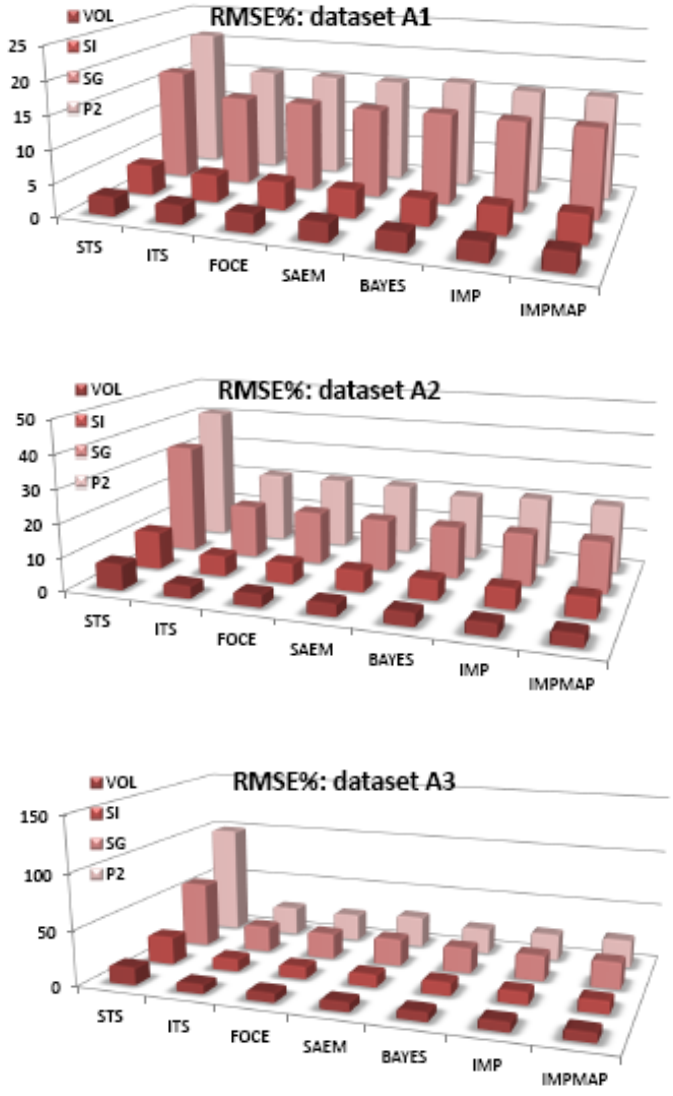

Figure 3.1: RMSE of the individual parameters expresses as percentage of the true population mean for the three datasets.

3. *Residual Unknown variability*

In the population approach the residual unknown variability (RUV) represents the variability due to model error and measurement error. RUV is estimated with the parameter σ that was not fixed to 2% of the data (the error structure that was used to individually generate the data) but was left free to be optimized by the algorithm.

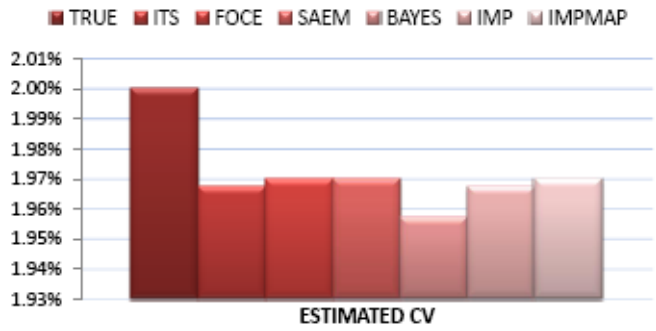

Figure 3.2: Estimated CV with the different methods in dataset A1

In Fig. 3.2 the estimated σ in the dataset A1 for the different population methods are compared with the true value (2%). Note that STS σ is not present because it is the worst performing method with 1.69% estimated CV. The measurement error was on average well estimated by all the methods apart from STS. BAYES, IMP and ITS seem to slightly underperform as we can see from Fig. 3.2. In table 3.2 are presented the estimated CV in the three datasets with all the different methods. The size of the measurement error is evaluated quite well in all the methods as the sample size decreases apart from STS method that clearly underestimates the RUV. This underestimation can be explained knowing that STS does not use population information during the estimation process. When the data points are very few for each individual as in dataset A2 and A3, it is easy to accommodate the parameter values to fit the experimental data since there are no constraints like in the population approach (e.g. the population parameters) that bind the parameters to remain close to plausible values. Note that the RUV for the other methods tends to become slightly bigger with the discarding of the dataset meaning

that with fewer information spread in the population there are more error sources.

	estimated CV		
	dataset A1	dataset A2	dataset A3
TRUE	2.00%	2.00%	2.00%
STS	1.69%	1.32%	0.65%
ITS	1.97%	2.01%	2.21%
FOCE	1.97%	2.01%	2.22%
SAEM	1.97%	2.00%	2.28%
BAYES	1.96%	1.98%	2.07%
IMP	1.97%	2.00%	2.21%
IMPMAP	1.97%	2.00%	2.21%

Table 3.2: Estimated CV with the different methods in the three datasets.

3.5 Disussion and Conclusions

We have confirmed that the population approach behaves better than the individual approach and that this trend is more evident with the samples reduction in the dataset. Not all the population estimation methods perform equally as well. We suggest to use ITS and FOCE since they are stable to initial estimates and at the same time they produce reliable estimates. BAYES is less stable but it produces comparable and maybe improvable estimates if more informative population priors are given. Finally, from this analysis we do not recommend to use SAEM, IMP and IMPMAP as they perform slightly worse and are less stable.

The IVGTT glucose minimal model: a two compartment model

4.1 Introduction

The glucose minimal model [17] during an intravenous glucose tolerance test (IVGTT) is a widely used tool in the metabolic field because from it are estimated very important physiological indexes such as the insulin sensitivity (S_I) and the glucose effectiveness (S_G). In particular these indexes are defined as the overall effect of stimulating glucose uptake and inhibiting glucose production in presence (S_I) or absence (S_G) of an insulin incremental effect. However it has been shown [18, 38, 39, 40] that the traditional one glucose compartment (1GMM) formulation causes under modeling of the glucose kinetics with a consequent underestimation of S_I and an overestimation of S_G. To deal with this under modeling a second compartment (2GMM) that describes the non accessible pool of the glucose system was appended to the main glucose compartment. The numerical identification of the 2GMM with the traditional weighted least squares (WLS) requires Bayesian a priori knowledge on the two transfer rates between the two glucose compartments due to model identification problems. In this article we exported the 2GMM in a population approach context and consequently we avoid the need of a priori knowledge on the glucose transfer rates by exploiting the nonlinear mixed effects models

(NLMEM) approach. The NLMEM in fact resort to the population information spread in the collection of subjects that creates a prior that facilitate the estimation process. In this way the NLMEM are able to deal with individual data sparseness by borrowing the lack of information from the entire population. In particular the individual parameter is seen as a realization of a distribution that is characterized by a typical value, the fixed effect, that is common to the entire population and by a certain variability, the between subject variability (BSV), that explains the spread of the parameter individual values among the population. Moreover we implemented in the model a delay term through a transit model [41] that aims to describe the dose infusion of two minutes, the distribution of the glucose dose in the body and possible technical problems during each individual experiment (different beginning of the experiment, longer infusion) before glucose appears in plasma. By introducing this delay we add more flexibility in the model to describe the first part of the data that enables to catch the glucose dynamics from minute 0 of the experiment to the end. This 2GMM was compared with the previously published 1GMM that was also implemented using the NLMEM. This comparison was done to confirm in a population context the overestimation of S_G and the underestimation of S_I that was previously detected using the classical individual estimation method (WNLS). Finally we integrate on the model a typical PKPD analysis the so called allometric scaling [42] that consists on describing the model parameters like clearances and volumes with empirically derived size relations. This analysis helps to explain in a deterministic way part of the BSV of these parameters through the use of different weight information and consequently to reduce the estimated BSV.

4.2 Material and methods

1. *Data*

   The data, provided by the Clinical Research Center at the Mayo Clinic, Rochester, MN, USA, originates from an insulin modified IVGTT protocol performed on 204 nondiabetic subjects (118 M /86 F, mean age 55.53±21.66 mean BMI 26.62±3.39 kg/m2). Blood samples were collected at -120, -30, -20, -10, 0, 2, 4, 6, 8, 10, 15, 20, 22, 25, 26, 28, 31, 35, 45, 60, 75, 90, 120, 180 and 240 min for measurement of glucose, insulin and C-peptide concentrations. Different weight information were collected to improve the parameter estimation process by adding some individual information the so called covariates. In table 4.1 are summed up the weight descriptors characteristic.

Covariate	Name	Units	Mean	Min	1stQ	Median	3rdQ	Max
BW	Body weight	kg	77.95	53	68.9	79	87	129
VAF	Visceral abdominal fat	cm^2/CT slice	141.84	11.86	62.54	125.09	206.73	478.23
TAF	Total abdominal fat	cm^2/CT slice	301.76	43.94	193.28	292.32	407.66	837.5
TBF	Total body fat	grams	23413.06	4884	17364	22520	28420	46986
%TBF	percentage of total body fat	%	32.41	7.3	25.8	31.6	39.75	56.7
LBM	Lean body mass	kg	49.53	30.1	38.5	51.84	58.68	74.58

Table 4.1: Continuous covariates for the glucose-insulin system measured in our 204 subject database. Statistics include minimum and maximum value, 1^{st} and 3^{rd} quartiles, and mean and median.

2. *The one compartment glucose minimal model (1GMM)*

The 1GMM implemented in NLMEM by Denti et al [2] is described by the following two equations:

$$\begin{aligned} Q'(t) &= -(S_G + X(t)) \cdot Q(t) + S_G \cdot Q_b \qquad Q(0) = D \cdot BW + G_b \cdot V \\ X'(t) &= -p2 \cdot X(t) + p2 \cdot S_I \cdot (I(t) - I_b) \qquad X(0) = 0 \end{aligned} \tag{4.1}$$

where Q is the glucose mass in plasma (mg), Gb is the basal glucose concentration (mg/dl), I is insulin plasma concentration (pmol/l) and Ib is its basal value, X is insulin action (min^{-1}) and D is the dose (330 mg/kg). The parameters of the model are the following: the glucose effectiveness SG (min^{-1}), the insulin sensitivity SI (min^{-1} $pmol^{-1}$ l), the insulin action p2 (min^{-1}) and the volume V (dl). The final set of unknown parameters is $\mathbf{p}$=[cl_{S_G}, S_I, V, p2] where cl_{S_G} (dl/min)is the clearance of S_G. Usually, glucose measurements prior to 8 min are excluded from the parameter estimation, because the one-compartment model is not designed to account for the quickest phase of glucose kinetics.

3. *The two compartments glucose minimal model (2GMM)*

The 2GMM [38] was revised by adding a delay term in the appearance of glucose in plasma due to the infusion and distribution of the glucose in the body. In particular a transit model [41] was inserted in the original formulation of the model by using a cascade of first order models with a single transfer rate k_{tr}. The final

model is described by the following equations:

$$\begin{aligned} Q_1'(t) &= -(S_G + X(t)) \cdot Q_1(t) + S_G \cdot Q_{1b} - k_{21} \cdot Q_1(t) + k_{12} \cdot Q_2(t) \\ &\quad + D \cdot BW \cdot \frac{(k_{tr} \cdot t)^n}{n!} \cdot e^{-k_{tr} \cdot t} \qquad Q_1(0) = G_b \cdot V \\ Q_2'(t) &= k_{21} \cdot Q_1(t) - k_{12} \cdot Q_2(t) \qquad Q_2(0) = \frac{k_{21}}{k_{12}} \cdot G_b \cdot V \\ X'(t) &= -p2 \cdot X(t) + p2 \cdot S_I \cdot (I(t) - I_b) \qquad X(0) = 0 \end{aligned} \tag{4.2}$$

where Q_1 and Q_2 is the glucose mass in plasma (mg) in the accessible and non accessible pool of the glucose system, G_b is the basal glucose concentration (mg/dl), I is insulin plasma concentration (pmol/l) and I_b is its basal value, X is insulin action (min^{-1}) and D is the dose (330 mg/kg). The parameters of the model are the following: the glucose effectiveness S_G (min-1), the insulin sensitivity S_I (min^{-1} $pmol^{-1}$ l), the insulin action p2 (min^{-1}), the volume V (dl), the glucose two compartment transfer rate k_{21} and k_{12} (min^{-1}), the transit model transfer rate k_{tr} (min^{-1}) and the number of compartments n. Note that k_{tr} can be expressed as a function of n and of the mean transit time (MTT) (min) or the time of delay of the glucose appearance in blood in the following way:

$$k_{tr} = \frac{n+1}{MTT} \tag{4.3}$$

In this article we estimate n and MTT. Note that the parameters S_G, k_{21} and k_{12} were expressed as clearances because by definition are more informative than their corresponding transfer rates. Moreover between the accessible and the non accessible compartment was supposed a diffusion process meaning that at the equilibrium state the concentration are the same so as a consequence also the clearance between those two compartments. To sum up the final set of unknown parameters are **p**=[cl_{S_G}, S_I, V, p2, cl_k, V_2, n, MTT] where cl_{S_G} (dl/min)is the clearance of S_G, cl_k (dl/min) is the clearance of the parameters that was supposed to be equal in the two compartments due to the diffusion hypothesis and V_2 (dl) is the volume of the non accessible compartment. Note that the model compartments were expressed in mass to have the parameters that do not depend implicitly on weight information and to be able to introduce this information through the allometric scaling.

4. *Population modeling assumptions*

Nonlinear mixed effects models (NLMEM) are able to quantify both the population and the individual parameters and identify by a hierarchical approach the biological sources of intra-individual and inter-individual variability. More specifically, in a first step, the data are described by:

$$y_{ij} = f(\mathbf{p_i}, x_{ij}) + \epsilon_{ij} \qquad 1 \leq i \leq m \qquad 1 \leq j \leq n_i \tag{4.4}$$

where y_{ij} are is the jth observation (in our case glucose concentration) of the ith subject at some known time instant x_{ij}. Here, n is the number of individuals and mi is the number of observation of individual i. $\mathbf{P}_i$ is the vector of model parameters of the ith individual. The variability due to measurement and model errors, better known as the residual unknown variability (RUV), is explained through ϵ_{ij} which is assumed to be independently distributed with a zero mean and Gaussian distribution:

$$\epsilon_{ij} = N(0, (\sigma_{prop} y_{ij} + \sigma_{add})^2) \tag{4.5}$$

The variance model for both 1GMM and 2GMM is described as a combination of a proportional and an additive error model where σ_{prop} and σ_{add} are additional parameters to estimate. In a second step, the model parameters are represented as function of some physiologically meaningful attributes that do not vary across the population ($\boldsymbol{\theta}$, fixed effects, i.e. values that are common to all subjects) and some others that do ($\boldsymbol{\eta}_i$, random effects, i.e. values typical of a specific subject). In our model we chose the function:

$$p_{ki} = \theta_k e^{\eta_{ki}} \tag{4.6}$$

where p_{ki} is the kth model parameter of the ith subject, θ_k is the typical value of the kth parameter common to the entire population and η_{ki} is the random effect of the kth model parameter of the ith subject. The random effect $\boldsymbol{\eta}_i$ are assumed to be independently distributed with a zero mean and Gaussian distribution:

$$\boldsymbol{\eta}_i \sim N(0, \boldsymbol{\Omega}) \tag{4.7}$$

with $\boldsymbol{\Omega}$ being a positive definite diagonal covariance matrix. With this formulation the second stage of variability, better known as Between-Subject Variability (BSV), is explained. The omega matrix set up of the 1GMM was chosen coherently with

Denti et al [3] including just the correlations term between the S_I-P2 and CL_{SG}-V. The omega set up of the 2GMM was full. Note that the parameter n is not present in the $\mathbf{\Omega}$ matrix because is assumed constant in the population. In particular n is fixed to a population value big enough but not enormous (n=100) to facilitate the computational process. The value n is the smallest that through a simulation process do not change dramatically by visual inspection the glucose profiles.

5. *Analysis of the results*

The first step of the analysis is to show the 2GMM model fit and compare it with the 1GMM fit. Both the population and the individual results were analyzed with particular attention to the mean of the weighted individual and population residuals. Then the second step is to confirm at the population level the trend that was previously detected [38] in a smaller subset of subjects using the traditional WNLS individual analysis. In this work was highlighted an overestimation S_G and an underestimation of S_I. To show this trend we compare both the population estimates and the mean of the individual estimates. Finally the last part of the analysis is to introduce the allometric scaling in the 2GMM and show its benefit in terms of drop of objective function and reduction of the BSV.

6. *Allometric scaling*

It has been widely shown the importance of the introduction of size measures in pharmacokinetic parameter estimates [42] especially in pediatric study where the population PK characteristics in terms of growth and maturation is likely to be not homogenous with a consequent more difficult characterization of the dose. This theory yields that parameters like volume and clearance are related to size information like weight through the so called allometric model that are power model formulated in this way:

$$p_i = \theta_p \cdot \left(\frac{W_i}{W_{median}}\right)^a \tag{4.8}$$

where p_i is the individual parameter, θ_p is the parameter fixed effect common to the entire population, W_i is the weight of the individual i and W_{median} is the median weight and a is the coefficient that is equal to $\frac{3}{4}$ in case of clearance parameter or 1 in case of volume parameter. To determine the most informative parameters weight predictor a linear regression between each volume parameters and the different weight predictors (body weight, lean body mass, visceral abdominal fat..) of the dataset was done due to the allometric linear relationship. For the clearance

parameters instead the predictors selected in the first step were introduced in all the different combinations and the drop of objective function was the rule of thumb to find the best combination.

7. *Algorithms*

   All the model estimation analysis were carried out using the software NONMEM 7.2.0 [29] that implements the NLMEM approach which consists in obtaining the population parameters by maximizing a likelihood function. Because of the computational infeasibility of the exact solution, different approximations were proposed. Here we applied the First Order Conditional Estimation (FOCE) approximation with INTERACTION coherently with was found previously in literature [2] and what was found in chapetr 3.

4.3 Results

All the run minimized successfully with their own covariance step and the estimated parameters observed the imposed distribution. The histograms of the logarithm of the individual estimates of the 2GMM are presented in Fig. 4.1: the gaussianity of the distributions is respected.

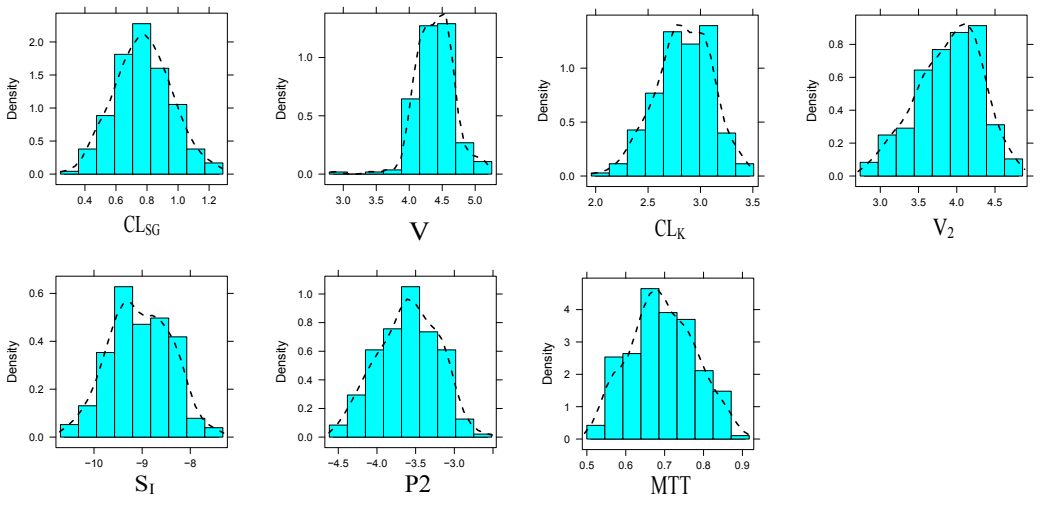

Figure 4.1: Histogram of the logarithm of the individual estimates of the 2GMM

The first step of the analysis is to show the fit of the 2GMM model and compare it with the 1GMM fit. In Fig. 4.2 are presented the mean and the standard deviation of the

individual weighted residuals (IWRES) calculated from the individual predictions in the two models 1GMM and 2GMM. There is also a zoom in the temporal window that goes from minute 0 to minute 25. The two models present a reasonably good fit in terms of amplitude and pattern: the mean individual weighted residuals did not show systematic deviations from zero and it lays within the range [-1 +1]. The new formulation of the 2GMM is able to describe the kinetics from time zero which is not possible in the 1GMM and is able to improve the description of the kinetics in the first part of the experiment (around min 10-20). This last feature is evident in Fig. 4.3 where are presented the typical subject fit and its individual weighted residuals in the temporal window of 10-26 min using the 1GMM and the 2GMM model. The 2GMM is able to describe better the data and its residuals are smaller in this particular time window.

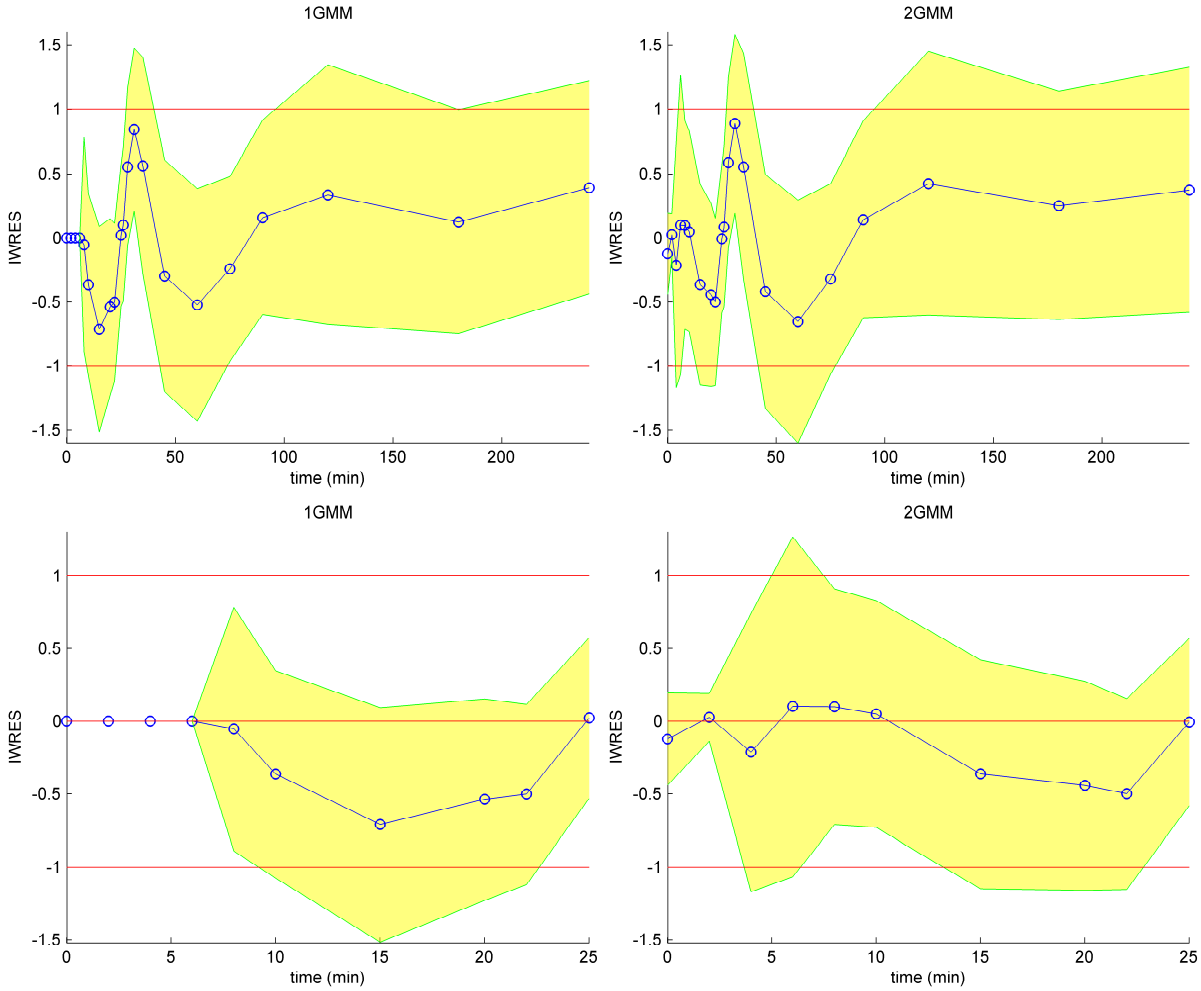

Figure 4.2: Mean ± standard deviation of individual glucose weighted residuals (IWRES)

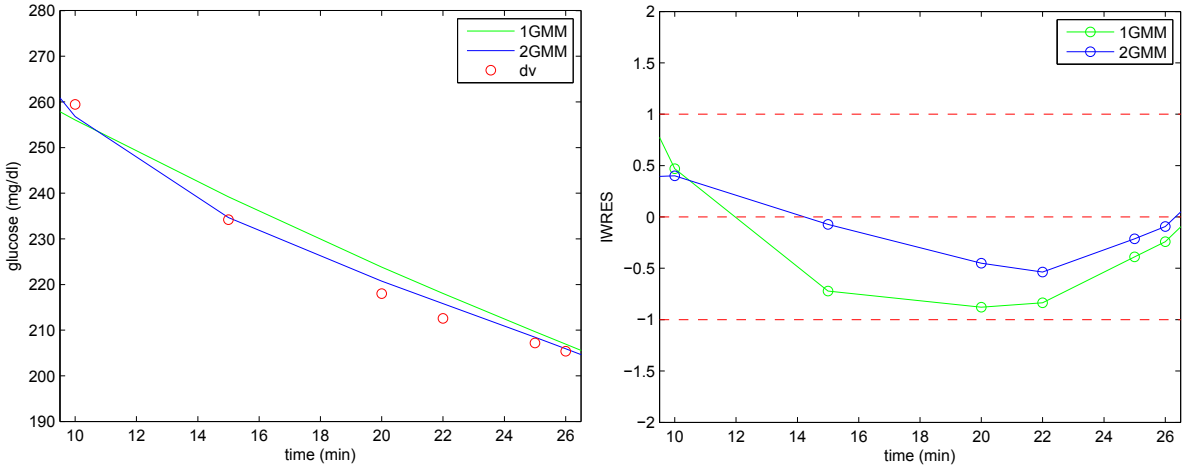

Figure 4.3: Typical subject fit (on the left) and weighted individual residual (IWRES) using the 1GMM and the 2GMM models in the temporal window that goes from 10 to 26 min.

In Fig. 4.4 are presented the average and the standard deviation of the population residuals calculated from the population predictions in the two models 1GMM and 2GMM with a particular attention to the first part of the data from minute 0 to minute 25. The two models present a reasonably good fit in terms of pattern and amplitude. As in the individual residuals the 2GMM is able to describe the initial 8 minutes of the experiment and is able to improve the description of the kinetics in the first part of the experiment (around min 10-20).

The second step of the analysis was to compare the population and individual estimates of the well known physiological indexes S_G and S_I to confirm the trend previously detected. In particular as far as the population estimates are concerned the overestimation of S_G and underestimation of S_I in the 1GMM is confirmed by the values of the population estimates as shown in the graph bar in Fig. 4.5. Precision of these indexes estimated in the 2GMM was comparable to that of the 1CMM. The same situation can be found looking at the mean of the individual estimates of the two models that have the following average values: S_I^1 7.29E-05 $\pm$ 4.67E-05 [l $pmol^{-1}$ min^{-1}] vs S_I^2 1.44E-04 $\pm$ 9.46E-05 [l $pmol^{-1}$ min^{-1}] and $CL^1_{S_G}$ 2.53 $\pm$ 0.47 [dl min^{-1}] vs $CL^2_{S_G}$ 2.21 $\pm$ 0.41 [dl min^{-1}].

The third step of our analysis is the introduction of covariates in the volume and clearances 2GMM parameters with relations described following the allometric scaling theory. Before starting with this analysis is important to underline that all the parameters of the 2GMM have shrinkage values [37] that are under the limit of alarm of 20-30%. This is important because in presence of high shrinkage the volume parameters - covariates relations detected might be false because there is not enough information in the data to

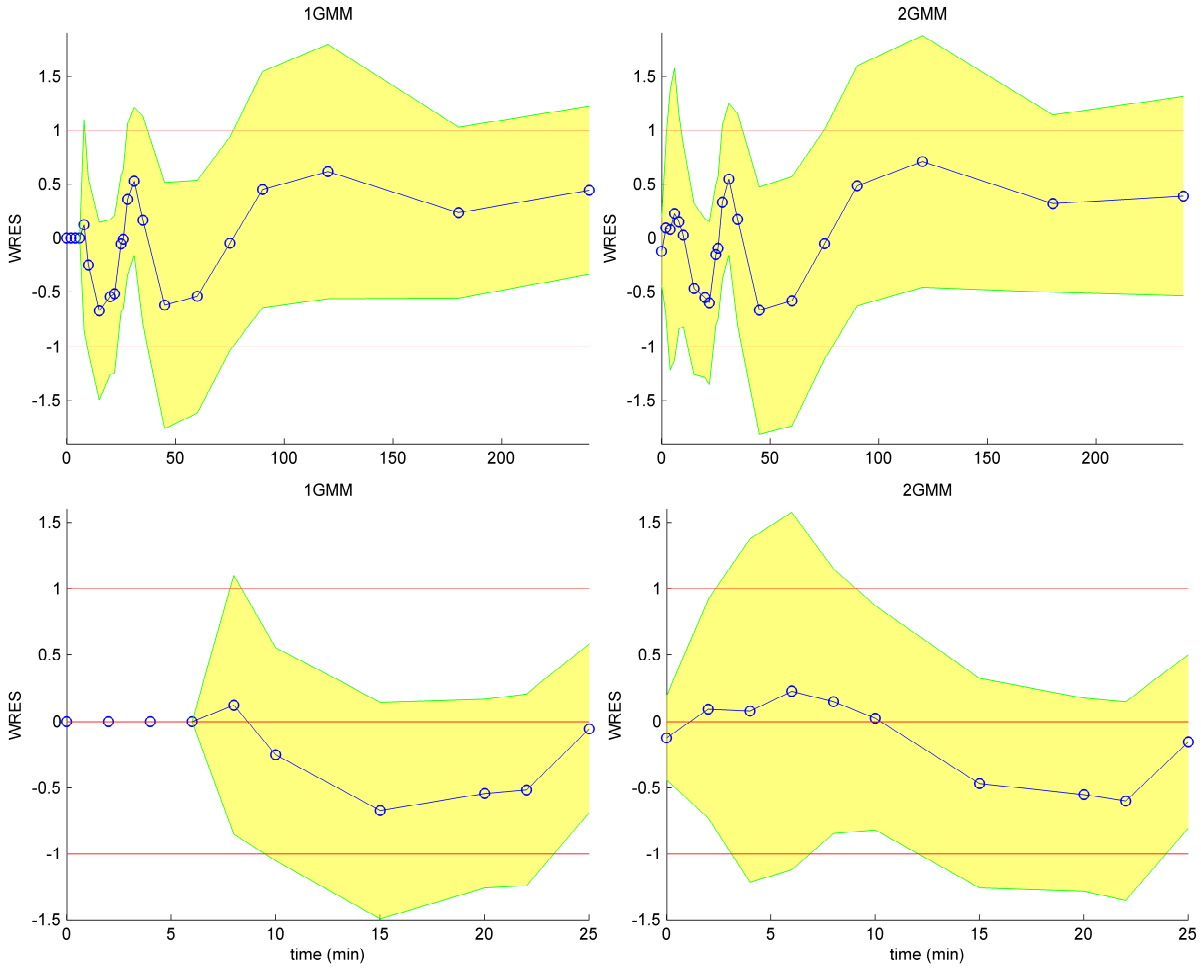

Figure 4.4: Mean ± standard deviation of population glucose weighted residuals (WRES)

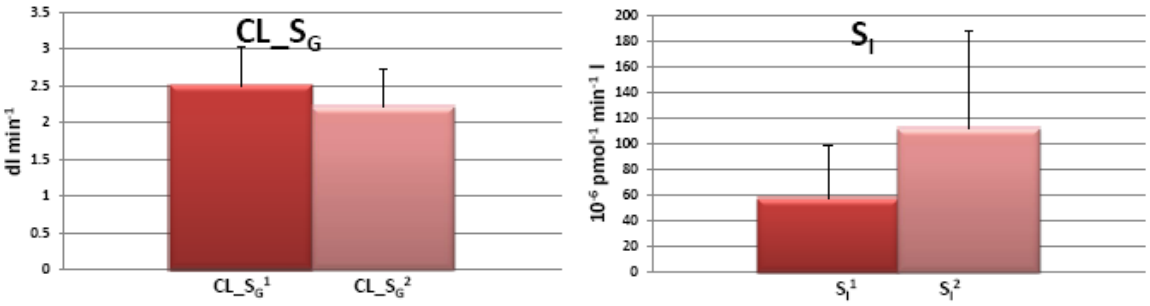

Figure 4.5: Bar graph of the population estimates of CLSG and SI in the 1GMM and 2GMM

permit reliable estimates of the BSV. In particular the shrinkage values range from a maximum of 20.5% relative to the S_G parameter to a minimum of 3.2% relative to the parameter V that is the volume of the accessible compartment of glucose. In our dataset more than one descriptor of weight is present. By exploiting the allometric scaling theory assumptions that is the volume linearly depends on weight information, we firstly fit a linear regression between the V and V_2 individual estimates and each weight predictors. The strongest relations with the two parameters were then selected to form the covariate subset that was tested for the clearance parameters in all the possible combinations in the NONMEM software [29]. The combination that present the biggest drop of function was selected as the final model. In Tab. 4.2 are presented the R^2 value of the linear model fit between the volume parameters and the weight predictors. The predictors selected are for V the BW and for V_2 the LBM.

R^2	V	V_2
BW	0.198	0.216
VAF	0.025	0.139
TAF	0.028	0.079
TBF	0.048	0.002
PTBF	$4.41 \cdot 10^{-5}$	0.092
LBM	0.109	0.304

Table 4.2: R^2 values of the linear regression between the 2GMM V and V_2 individual estimates and all the weight predictors

The biggest drop of function was obtained with the following final combination of weight predictors with clearance and volume parameters:

$$\begin{aligned} CL_{S_G i} &= \theta_{CLS_G} \cdot exp(\eta_{CLS_G i}) \cdot \left(\frac{LBM_i}{LBM_{median}}\right)^{0.75} \\ CL_{ki} &= \theta_{CLk} \cdot exp(\eta_{CLki}) \cdot \left(\frac{LBM_i}{LBM_{median}}\right)^{0.75} \\ V_i &= \theta_V \cdot exp(\eta_{Vi}) \cdot \left(\frac{BW_i}{BW_{median}}\right) \\ V_{2i} &= \theta_{V2} \cdot exp(\eta_V 2_i) \cdot \left(\frac{LBM_i}{LBM_{median}}\right) \end{aligned} \tag{4.9}$$

This is the final model parameter formulation with allometric scaling for the subject i. In Tab. 5.3 are presented the population estimates obtained in the base model and in the final model with the allometric scaling introduction. The weight information in the final model helped to reduce the parameter BSV by explaining it in a deterministic way.

In particular the CL_{S_G} BSV swift from 23% to 20.6%, the V BSV moves from 30% to 25.6%, the CL_K BSV moves from 33% to 31.5% and finally the V2 BSV moves from 45.7% to 32.4%. The drop of objective function is statistically significant and it is around 270 points.

In Fig. 4.6 are presented the population prediction in the base model and in the final model: it is clear the reduction of variability in the final model that it translates into a more compressed graph towards the bisector of the plane.

The shrinkage of the final model ranges from a minimum value of 4.4% of the parameter V to a maximum value of 25.5% of the parameter CL_K: all the values are below the limit of alert 20-30%. In Fig. 4.7 are presented the individual and the population fits of some random individuals. Finally in Fig. 4.8 is presented the visual predictive check (VPC) [43] of the final model. The graph yields that the model is able to catch the data variability as the CI of the percentiles of the simulated profiles are on the whole able to follow the percentiles of the observed data.

Model parameters	Units	base model		final modes	
		population estimates	RSE %	population estimates	RSE %
Fixed Effects					
CL_SG	dl/min	2.21	3%	2.35	2.9%
V	dl	82.1	3.30%	83	2.8%
SI	l $pmol^{-1}$ min^{-1}	112	6.80%	112	6.0%
p2	1/min	0.0273	5.40%	0.0272	4.9%
CL_k	dl/min	16.9	7.50%	19.2	6.4%
V_2	dl	47.5	5.10%	53.1	3.8%
MTT	min	1.99	0.80%	2	0.8%
n	-	100	-	100	-
Random effects					
Interindividual Variability					
ω $CLSG$		23.00%	12.6%	20.60%	12.1%
ω V		30.00%	7.2%	25.60%	8.9%
ω S_I		67.10%	8.2%	67.80%	8.1%
ω P2		42.3%	12.1%	41%	12.6%
ω CL_K		33.00%	15.1%	31.50%	17.4%
ω V_2		45.70%	12.1%	32.40%	14.2%
ω MTT		9.10%	7.7%	9.10%	7.4%
correlation CL_SG V		4.60%	326.1%	-10.50%	154.3%
correlation SI CLSG		-20.10%	66.7%	-27.90%	51.3%
correlation SI VOL		-39.30%	25.3%	-25.10%	43.4%
correlation P2 CLSG		-15.80%	101.3%	-24.00%	65.4%
correlation P2 VOL		18.80%	74.5%	28.40%	47.2%
correlation P2 SI		65.20%	14.4%	67.60%	13.5%
correlation CLK CLSG		37.90%	47.2%	11.00%	205.5%
correlation CLK VOL		18.30%	105.5%	24.00%	79.2%
correlation CLK SI		41.40%	33.1%	32.90%	43.5%
correlation CLK P2		36.20%	55.5%	45.70%	46.2%
correlation VOL2 CLSG		23.60%	62.3%	-7.80%	207.7%
correlation VOL2 VOL		-39.10%	28.1%	-72.00%	9.6%
correlation VOL2 SI		26.70%	37.3%	24.70%	44.5%
correlation VOL2 P2		-31.70%	37.9%	-42.70%	34.7%
correlation VOL2 CLK		28.90%	55.7%	-20.40%	77.9%
correlation MTT CLSG		8.80%	156.8%	-9.60%	165.6%
correlation MTT VOL		28.10%	32.6%	18.20%	55.5%
correlation MTT SI		-12.90%	70.6%	-12.00%	79.0%
correlation MTT P2		5.60%	208.9%	6.70%	185.1%
correlation MTT CLK		19.00%	72.1%	20.10%	73.1%
correlation MTT VOL2		-8.80%	111.1%	-22.50%	43.2%
Residual unknown variability					
σ_{prop}		0.0188	3.80%	0.0192	3.60%
σ_{add}		4.48	2.00%	4.48	2.00%

Table 4.3: Summary of 2GMM parameter estimates obtained before (base model) and after (final model) the allometric introduction. Typical values for parameters are in original units. Given that between-subject variability is modeled as log normal, variance measures are reported as approximate coefficients of variation (CV), whereas the covariance terms are in terms of correlation.

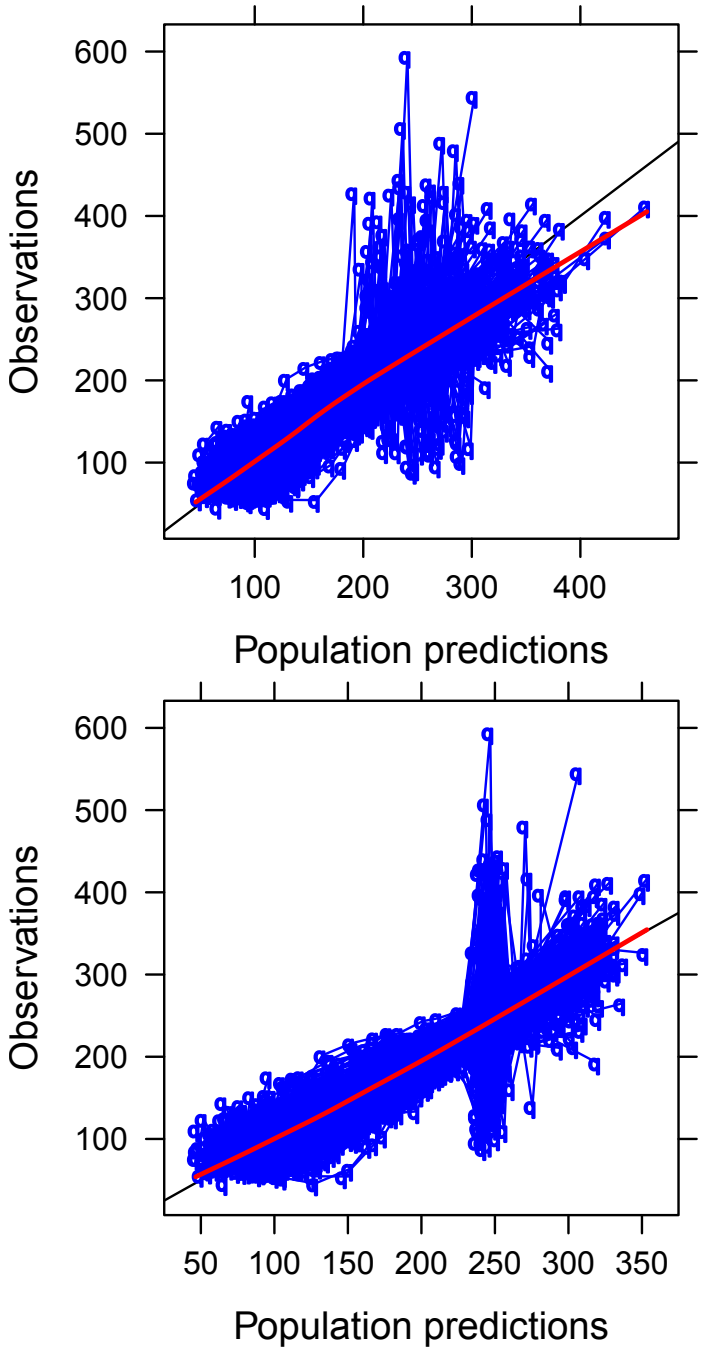

Figure 4.6: 2GMM Population predictions in the base model (on the top) and on the final model (on the bottom) after the allometric scaling introduction

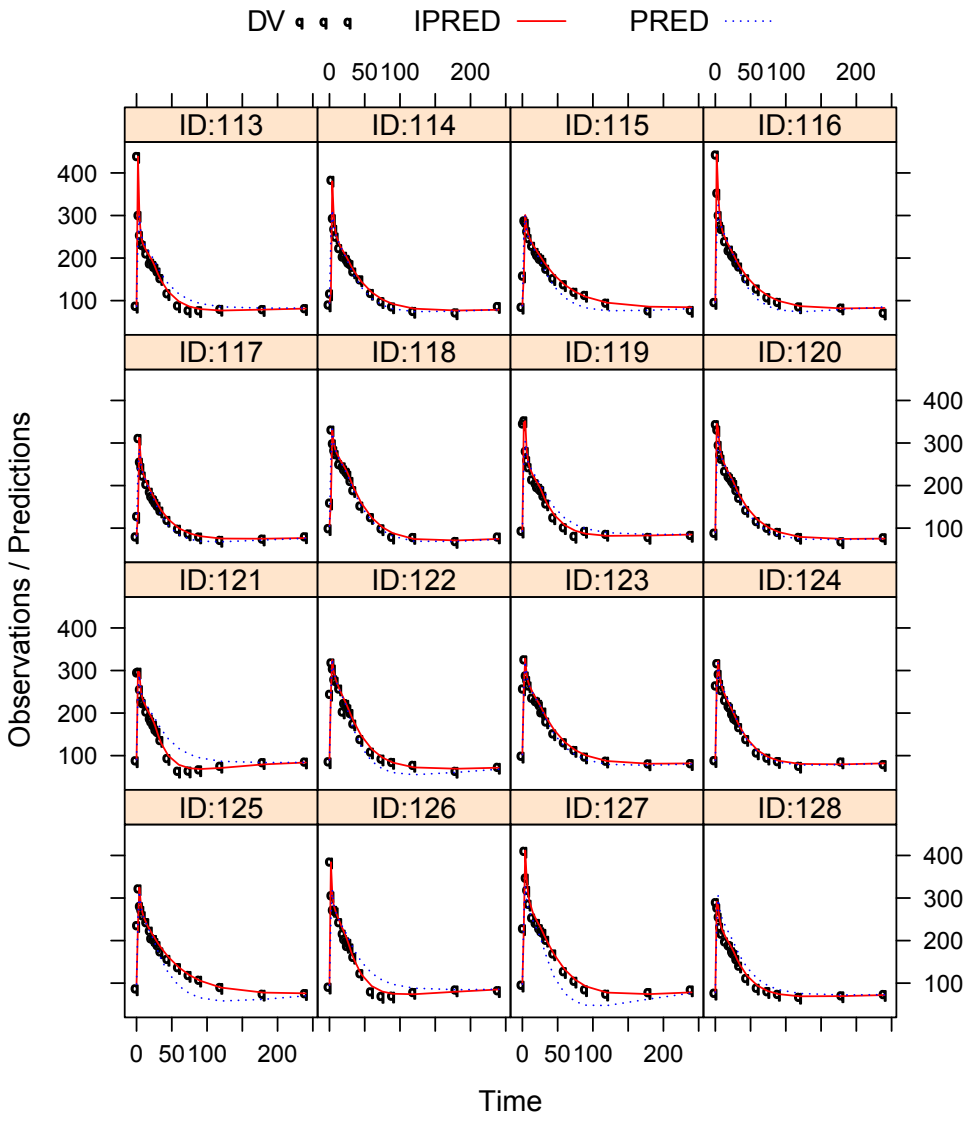

Figure 4.7: The 2GMM individual and the population fit of some random subjects. The dots are the observations, the red line is the individual fit whereas the blue dashed line is the population prediction.

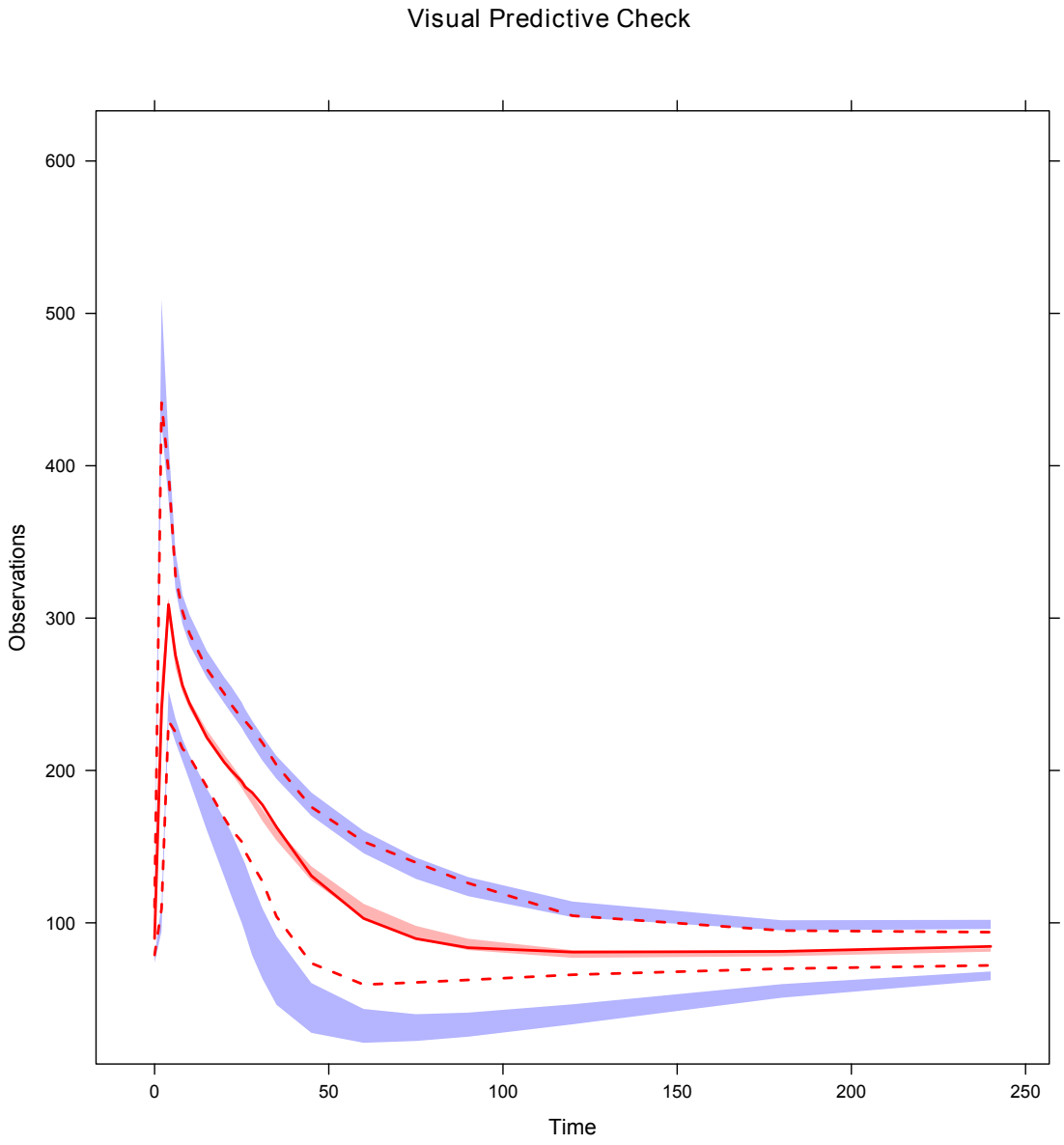

Figure 4.8: The 2GMM VPC of the final model.

4.4 Disussion

It has been shown that the IVGTT one compartment glucose minimal model implemented in the traditional approach (WNLS) presents some pitfalls in the modeling of the glucose kinetics [38] and that this under modeling can be fixed by using a two compartment glucose model. In this paper we transpose the problem in the population approach by implementing the 2GMM with the NLMEM technique and by comaparing it with the 1GMM implemented by Denti et al [2, 3]. In particular we exploit the potential of the NLMEM that uses the information spread on the set of subjects as a sort of prior during the estimation process to avoid the use of the Bayesian a priori information and to add further modeling parts to better explain the data in the first part of the experiment. Note that with the individual estimation approach this would not be possible due to identifiability problems. In fact with this approach not only the use of a priori information that might be not suitable to the population under analysis is necessary but also the possibility of adding other degree of freedom to the model (parameters) is denied. The 2GMM here developed aims to describe the glucose kinetics from minute 0 until the end of the experiment. This is a very important future since it was shown the importance of describing correctly the glucose dynamics to have more reliable physiological indexes (S_I and S_G). The 2GMM improvement introduced in the fit when compared to the 1GMM is evident in the first part of the experiment (from minute 0 to roughly minute 20). This is expectable since the second compartment that we add is a diffusive that means that the process that it explains is a fast one. Note that the 1GMM was implemented by excluding the first samples of glucose (usually prior to minute eight) depending on each subject glucose profile that means that among all the fit that we can obtain with the 1GMM this is the best because the glucose samples exclusion was personalized. In the 2GMM the exclusion is no more a problem since each subject profile is modeled from minute 0 so another advantage of using the 2GMM apart from having the description of the entire experiment is avoiding the time consuming and tricky personalized exclusion of samples. From the comparison of the physiological indexes between the 1GMM and the 2GMM we can say that the trend that was previously reported in literature [38] using the individual approach is caught also by using the population approach: there is an overestimation of S_G with the 1GMM and an underestimation of SI with the 1GMM.
If we look at the allometric scaling introduction in the 2GMM is interesting to note the big improvement in the model fit due to insertion of the covariate information in the parameters: the drop of function is statistically significant, the BSV decreases and especially the population fit with respect to the base model is improved (see Fig. 4.6). Some correlations were estimated with an elevated RSE but the condition number of

the model is low meaning there is no severe collinearity and its consequent probable overparameterization. It's interesting to note that the descriptor of the diffusion parameters (CL_K and V_2) is the lean body mass (LBM) that is the mass of the body without the fat (storage lipid). The diffusion phenomena in the body is known to be insulin independent so the dependence of its parameter from a descriptor that is not dependent on the glucose storage might be not determined by chance. This second compartment of the non accessible glucose pool might stand for the description of the insulin independent tissues whereas the main compartment whose volume (V) is described by the body weight might stand for the insulin dependent tissues. Obviously this conclusions are data dependent and other studies should be carry on to corroborate this physiological hypothesis. Finally the VPC (Fig. 4.8) shows that the model is able to simulate profiles with the same variability of the observed data. As we can see though there are some observable mismatching between the observed and the simulated data in particular between the CI of the simulated 5^{th} percentile and the 5^{th} percentile of the observed data. This can be assigned to the individual known input function in the model (insulin) that does not always interact properly with the individual parameters realization. In particular, there is no additional information in the model that can link the set of individual parameters to the proper forcing function in order to obtain always reasonable physiological outputs [44].

4.5 Conclusions

In this study a two compartment IVGTT glucose minimal model was developed using the NLMEM. This technique helped us to avoid the use of Bayesian information and to introduce a delay term at the beginning of the data that aims to describe the dose infusion of two minutes, the distribution of the glucose dose in the body and possible technical problems during each individual experiment. Moreover its performance was compared to the one obtained in Denti et al using the one compartment glucose minimal model and the benefit of the second compartment was clear because it allows to describe the data from minute 0 and it improves the fit in the first 20-30 minutes of the experiment. The same trend of overestimation of SG and underestimation of SI that was found using the single subject estimation process was detected using the population approach. Moreover the introduction of the weight predictor using the allometric scaling theory helped us to furtherly improve the fit, to reduce the BSV in the parameters and to detect possible physiological interesting relationships. These relations needs further investigations to be corroborated. To conclude this optimization of the IVGTT glucose minimal model is the

first step to build an integrated IVGTT system that describes both the glucose and the insulin kinetics without splitting it in two separated subsystems.

Covariate selection for the IVGTT C-peptide minimal model

5.1 Introduction

The quantification of insulin secretion is crucial to assess β-cell function in different pathophysiological states. The C-peptide minimal model (CMM) allows to quantitatively evaluate the β-cell response to a glucose stimulus [19, 45]. In particular it allows to reconstruct the prehepatic insulin secretion profile and to quantify the indices of glucose control on first-phase, second-phase and basal insulin secretion. This is possible because the C-peptide is a substance cosecreted with insulin in an equimolar way but, conversely from insulin, is not extracted by the liver and has a constant peripheral clearance. The intravenous glucose tolerance test (IVGTT) is a widely used test to calculate the β-cell sensitivity. By now, the CMM has been identified using the traditional Weighted Least Squares approach (WLS) applied on the experimental data of each single subject. Very often, in epidemiological studies, it is of interest to obtain also a description of the parameter distribution across the population. This information can be obtained through different techniques starting from the simplest i.e. a straightforward sample statistics (mean and covariance) on the individual parameter estimate set to the most explicative and at the same time complex nonlinear mixed-effects modeling (NLMEM) approach.

The aim of this work is to revise the CMM proposed by Toffolo et al [19, 45] by exploiting the population approach. This technique is able to deal with individual data sparseness by borrowing the lack of information from the entire population. Moreover the individual parameter identifiabiality is changed with respect to the individual approach because it can be improved by resorting to the population knowledge that creates a prior that facilitate the estimation process. In this article we introduce a transit model [41] to describe a delay in the first part of the data that is due to glucose signal that is infused from minute zero with a 2 minute of infusion that slow down the activation of the insulin production and of its cosecreted signal, the C-peptide. Moreover, in this paper, once the CMM model was optimized through the population approach, we exploit the potentials of the NLMEM population technique by inferring a covariate analysis in order to better explain the random variability in parameters and eventually its cause in order to improve the predictive performance of the model.

5.2 Material and methods

1. *Data*

   The data, provided by the Clinical Research Center at the Mayo Clinic, Rochester, MN, USA, originates from an insulin modified IVGTT protocol performed on 204 nondiabetic subjects (118 M /86 F, mean age 55.53 ± 21.66 mean BMI 26.62 ± 3.39 kg/m^2). Blood samples were collected at -120, -30, -20, -10, 0, 2, 4, 6, 8, 10, 15, 20, 22, 25, 26, 28, 31, 35, 45, 60, 75, 90, 120, 180 and 240 min for measurement of glucose, insulin and C-peptide concentrations. Additional patient information, so called covariates, was also collected with the purpose of investigating which physiological characteristics were significant as predictors of glucose-insulin metabolism. In particular, for each subject were collected thirteen different covariates: age (AGE), sex (SEX), height (BH), weight (BW), basal levels of glucose (GBSL) and insulin (IBSL), total body fat (TBF), percentage of total body weight (%TBF), lean body mass (LBM), visceral (VAF) and total abdominal body fat (TAF), and finally the derived indexes body mass index (BMI) and body surface area (BSA). As far as TBF, %TBF and LBM are concerned, these covariates were assessed using dual-energy X-ray absorptionmetry (DEXA) as described in Basu et al [46], whereas VAF and TAF were assessed using single-slice computed tomographic (CT), scan at the level of L2/L3 were employed as explained in Jensen et al [47]. Twelve out of the thirteen covariates are listed in Tab. 5.1. and graphic summaries of their distributions, also showing regressions between the most correlated pairs, can be

seen in Fig. 5.1. Three subjects had some missing values for VAF, TAF, and %TBF; therefore, their values were assumed to be the population median.

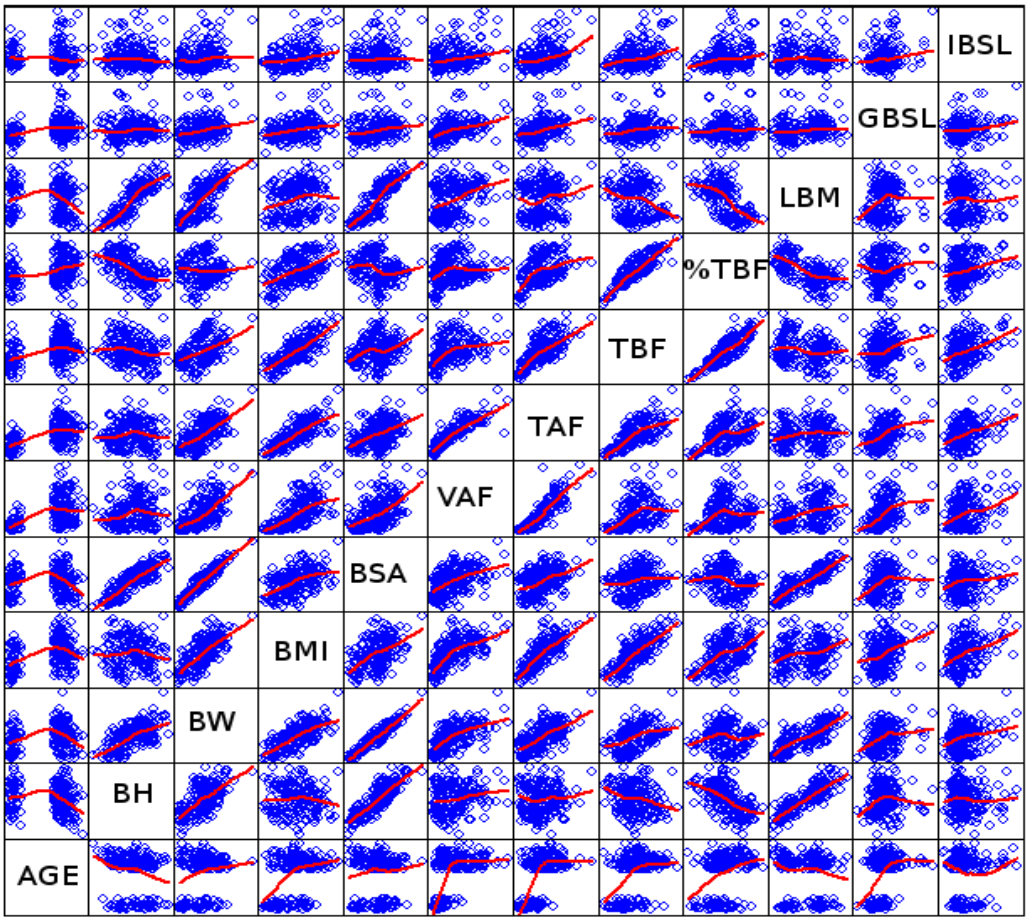

Figure 5.1: Regressions between the most correlated covariates are also shown, and a smoothed tendency line is superimposed to depict the trend of the relation

2. *The C-peptide minimal model*

   The CMM was revised by adding a delay term in the activation process of the secretion of insulin due to the glucose signal. In particular a transit model [41] was inserted in the original formulation of the model to delay the initial first phase of secretion by using a cascade of first order models with a single transfer rate k_{tr}.

Covariate	Name	Units	Mean	Min	1stQ	Median	3rdQ	Max
AGE	Age	years	55.53	18	27	65	71	87
BH	Body height	cm	170.86	145	163	171	178	194
BW	Body weight	kg	77.95	53	68.9	79	87	129
VAF	Visceral abdominal fat	cm^2/CT slice	141.84	11.86	62.54	125.09	206.73	478.23
TAF	Total abdominal fat	cm^2/CT slice	301.76	43.94	193.28	292.32	407.66	837.5
TBF	Total body fat	grams	23413.06	4884	17364	22520	28420	46986
%TBF	percentage of total body fat	%	32.41	7.3	25.8	31.6	39.75	56.7
LBM	Lean body mass	kg	49.53	30.1	38.5	51.84	58.68	74.58
GBSL	Basal Glucose	mg/dl	91.36	72.86	86.76	90.49	95.02	125.25
IBSL	Basal Insulin	pmol/l	27.48	5.52	19.05	24.66	32.10	78.36

Table 5.1: Continuous covariates for the glucose-insulin system measured in our 204 subject database. Statistics include minimum and maximum value, 1^st and 3^rd quartiles, and mean and median.

The deviation from the basal model is described by the following equations:

$$\begin{aligned} CP_1'(t) &= -(k_{01}+k_{21})\cdot CP_1(t) + k_{12}\cdot CP_2(t) + m\cdot X(t) && CP_1(0)=0 \\ CP_2'(t) &= -k_{12}\cdot CP_2(t) + k_{21}\cdot CP_1(t) && CP_2(0)=0 \\ X'(t) &= -m\cdot X(t) + Y(t) + X_0\cdot \frac{(k_{tr}\cdot t)^n}{n!}\cdot e^{-k_{tr}\cdot t} && X(0)=0 \\ Y'(t) &= \begin{cases} -\alpha\cdot(Y(t)-\beta\cdot(G(t)-G_b)) & Y(0)=0, \quad \text{if } G(t)-G_b>0 \\ -\alpha\cdot(Y(t)) & Y(0)=0, \quad \text{if } G(t)-G_b\le 0 \end{cases} \end{aligned} \tag{5.1}$$

CP_1 and CP_2 (pmol/l)are the C-peptide concentration in the accessible and in the peripheral compartments respectively whereas X (pmol/l) and Y (pmol l^{-1} min^{-1}) are respectively the C-peptide amount and provision in the β-cells. Note that the level of basal C-peptide is estimated (CP_b) whereas the glucose basal is fixed to the average of the four samples before the beginning of the IVGTT measured at time -120, -30, -20, -10 min and the sample at time 0. The parameters k_{ij} (min^{-1}) describe the C-peptide kinetics, in particular k_{12} and k_{21} are the transfer rate parameters between the two compartments and k_{01} is the irreversible loss. These kinetic parameters are fixed to population values following the method proposed in Van Cauter et al [20]. The remaining parameters α (min^{-1}), β ($mgdl^{-1}pmol$ l^{-1} min^{-1})and m (min^{-1}) represent the secretion parameters whereas k_{tr} (min^{-1}) and n are referred to the transit model and they are the constant transfer rate (k_{tr}) between the n compartments of the cascade. Note that k_{tr} can be expressed as a function of n and of the mean transit time or the time of delay of the secretion in the following way:

$$k_{tr} = \frac{n+1}{MTT} \tag{5.2}$$

In this article we estimate n and MTT. X_0 (pmol/l) is the stored amount of C-peptide immediately releasable after a glucose stimulus and it represents the first phase secretion. The second phase of secretion instead depends on the provision Y which in turn is controlled by the glucose concentration through the parameter β and G_b that represent respectively the sensibility to glucose and the glucose threshold above which there is insulin production. The provision comprehends the insulin production coming from the new synthesis and from the conversion of the stable insulin to labile.

3. *The derived indexes*
   The model allows calculating three fundamental indexes that explain the β-cell sensitivity to glucose respectively in the basal state, in the first phase and in the second phase of secretion. The basal sensitivity to glucose is described by the following index:
   $$\phi_b = \frac{k_{01} \cdot CP_{1b}}{G_b} \tag{5.3}$$
   where G_b is the basal glucose concentration. The first and second phase secretion of insulin are described respectively by the following indexes:
   $$\begin{aligned} \phi_1 &= \frac{X_0}{\Delta G} \\ \phi_2 &= \beta \end{aligned} \tag{5.4}$$
   where ΔG is the maximum increment of the plasma glucose concentration. Finally there is a global index of β-cell sensitivity to glucose that is defined as the average increase above basal of pancreatic secretion over the average glucose stimulus above the threshold level G_b:
   $$\phi_t = \phi_2 + \frac{\phi_1 \cdot \Delta G}{\int_0^\infty (G(t) - G_b)\, dt} \tag{5.5}$$

4. *Population modeling assumptions*
   In the population analysis by NLMEM the data are described by the model:
   $$y_{ij} = f(\mathbf{p_i}, x_{ij}) + \epsilon_{ij} \qquad 1 \leq i \leq m \qquad 1 \leq j \leq n_i \tag{5.6}$$
   where y_{ij} are is the jth observation (in our case C-peptide concentration) of the ith subject at some known time instant x_{ij}. Here, m is the number of individuals and n_i is the number of observation of individual i. $\mathbf{P}_i$ is the vector of model parameters for the ith individual. The model parameters across the population are assumed to

be lognormal distributed coherently with previous literature [2]. In particular the parameters can be described:

$$p_{ki} = \theta_k e^{\eta_{ki}} \tag{5.7}$$

where p_{ki} is the kth model parameter of the ith subject, θ_k is the typical value of the kth parameter common to the entire population and η_{ki} is the random effect of the kth model parameter of the ith subject. The random effect $\boldsymbol{\eta}_i$ are assumed to be independently distributed with zero mean and Gaussian:

$$\boldsymbol{\eta}_i \sim N(0, \boldsymbol{\Omega}) \tag{5.8}$$

with Ω being a positive definite covariance matrix. The $\boldsymbol{\Omega}$ matrix comprises only the significant correlations between the parameters that are the following: $X_0 - \beta$, $X_0 - \alpha$, $\beta - \alpha$, $\beta - CP_b$, $\alpha - CP_b$ (Eq. 5.9). Given these definitions of typical value and random effect the first stage of variability, better known as Between-Subject Variability (BSV), is explained.

$$\Omega = \begin{bmatrix} \omega^2_{X_0} & \omega_{X_0-\beta} & \omega_{X_0-\alpha} & 0 & 0 \\ \omega_{X_0-\beta} & \omega^2_{\beta} & \omega_{\beta-\alpha} & \omega_{\beta-CP_{bsl}} & 0 \\ \omega_{X_0-\alpha} & \omega_{\beta-\alpha} & \omega^2_{\alpha} & \omega_{\alpha-CP_{bsl}} & 0 \\ 0 & \omega_{\beta-CP_{bsl}} & \omega_{\alpha-CP_{bsl}} & \omega^2_{CP_{bsl}} & 0 \\ 0 & 0 & 0 & 0 & \omega^2_{MTT} \end{bmatrix} \tag{5.9}$$

Note that the parameters m and n are not present in the $\boldsymbol{\Omega}$ matrix because they are assumed constant in the population. In particular m is estimated as a fixed effect θ that whereas n is fixed to a population value big enough but not enormous (n=150) to facilitate the computational process. The variability due to measurement and model errors, better known as the residual unknown variability (RUV), instead can be explained through ϵ_{ij} which is assumed to be independently distributed with zero mean and Gaussian:

$$\epsilon_{ij} \sim N(0, (\sigma_{prop} y_{ij} + \sigma_{add})^2) \tag{5.10}$$

where σ_{add} and σ_{prop} (combination of additive and proportional error) are additional parameters to estimate.

5. *The covariate analysis*
   Before starting with the covariate model building, we did a pre analysis that consists in examining the covariate data and check if there are any correlations between

them in order to select only independent covariates with unique information. The strongest correlation were deleted but at the same time were kept those predictors that were of interest from a clinical point of view. From this subset potentially all the covariate combinations, for each of the five model parameters, are possible candidates to be tested into model. This turns into a very time consuming analysis. So in order to further narrow down these combinations we applied a technique that aims to identify a potential selection of covariates for each parameter. This technique is a stepwise generalized additive model (GAM) as described in Mandema et al. [48] and it was performed using R [49] package Xpose [50]. To be sure about the final subset of covariates selected for each parameter an influential individual analysis was performed using the R package Xpose in order to test the robustness of the chosen predictors in case that the subjects that influence mostly the GAM fit are left out. If the GAM fit changes the predictors, the covariate final subset is the one obtained without the influential individual. In particular we looked at the Cook Distance and at the leverage that measures respectively the effect of deleting a given observation on the vector of the parameter estimates and how much the certainty in the fit depends on the data point (high value=high dependence) [51]. The cut-off to determine a critical observation was selected by visual inspection from the graphs and the values that are larger than the rest were tested. The GAM algorithm implemented in Xpose tests also nonlinear relationship between the covariate and the parameters through the use of a linear piecewise function with one cut off. In this article though only linear relationship were tested. Once the selection was completed, we did a forward and backward elimination in the computer program NONMEM. Starting from the basic model (without covariates), in the NONMEM selection all possible parameter covariate combinations are tried, and inclusion of covariate effects is based on the likelihood ratio test. The covariate relationship that gives rise to the largest Δ OFV is retained in the model, given that inclusion results in Δ OFV > 3.84 (corresponding to $P < .05$). The full model is established when no more covariates can be included according to this criterion. From the full model, the covariate relations were then deleted one at a time using a stricter criterion of significance Δ OFV > 10.83 (corresponding $P < .001$). The final covariate model was achieved when deletion of each covariate relation was significant.

Continuous covariates were investigated with the following covariate model:

$$p_{ki} = \theta_k e^{\theta_{k+l}(cov_i - cov_{median}) + \eta_{ki}} \qquad 1 \leq l \leq n_{cov} \tag{5.11}$$

where p_{ki} is the kth model parameter of the ith subject and n_{cov} are the number of covariates. This model guarantees the positivity of the parameter without constraining θ_{k+l}. The only categorical covariate that was present in the dataset was given as a dichotomous variable (sex: male/female). The coding will be illustrated using an indicator variable (IND), being 1 or 0 (e.g. male or female).

$$p_{ki} = \theta_k e^{\theta_{k+l}(IND_l)+\eta_{ki}} \qquad l = 1 \tag{5.12}$$

6. *Algorithms*
   All the model estimation analysis were carried out using the software NONMEM VII [29] whereas the covariate exploration were done using the R package Xpose [50]. The software NONMEM VII implements the NLMEM approach, which consists in obtaining the population parameters by maximizing a likelihood function. Because of the computational infeasibility of the exact solution, different approximations were proposed. Here we applied the First Order Conditional Estimation (FOCE) approximation with INTERACTION coherently with was found previously in literature [2] and in 3.

5.3 Results

1. *Base model analysis*
   In Fig. 5.2 is presented the individual and the population fit of the CMM using some random subjects. In Fig. 5.3 is presented the basic goodness of fit plot that consist in two correlation graphs between the individual or the population predictions vs the observations and two plots of the individual and of the population weighted residual. We can see that the population prediction fail sometimes in the description of the first part of the curve where the observations assume big concentrations but on the whole the fit is still reasonable as we can see from the matching of the bisector of the plane with the linear regression (the red line). The individual predictions are in a better agreement with the observation as the data are less spread in the plane and the linear regression matches well the bisector of the plane. As far as the residuals are concerned, both the individual and the population weighted residuals behave well in terms of pattern and amplitude apart from few outliers. The population estimates (see Tab. 5.3) in terms of fixed effects, random effects and RUV are estimated precisely with a relative standard error (RSE) that ranges from 1.2% of the RUV estimate σ_{PROP} to a RSE of 26.7%

of the $\mathbf{\Omega}$ estimate $\omega^2_{\beta-\alpha}$. The individual estimates are also estimated precisely with a coefficient of variation (CV%) that ranges from a CV% average value of 9% for the CP_b estimate to a CV% average value of 34% for the α estimate. Is important to underline that there is no shrinkage [37] in the EBE that otherwise would have invalidate the covariate analysis by for example inducing or hiding some false covariate relationship. In particular the η-shrinkage values range from a value of 1% relative to CP_b to a value of 13.1% relative to α. To sum up all the shrinkage values are below the limit of alarm of the 20-30%.

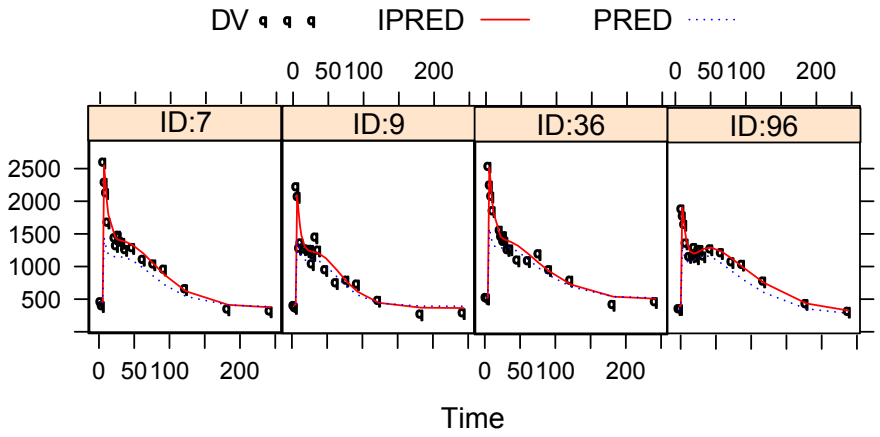

Figure 5.2: The individual and the population fit of some random subjects. The dots are the observations, the red line is the individual fit whereas the blue dashed line is the population prediction.

2. *Covariate model analysis*

   Once the CMM base model is optimized, the covariate model can be built up. Before starting with the covariate analysis, we perform a pre analysis to check the correlation among the covariates since we want them to add unique information to the model. The strongest correlations were deleted and moreover were kept those predictors that were of interest from a clinical point of view. The final set of covariates that is kept is the following: AGE, BMI, BSA, VAF, %TBF, LBM, SEX, GBSL and IBSL. Given the still high number of candidate predictors available a further exploratory analysis was carried out to narrow down a pool of potential candidate models to test using the GAM algorithm. The covariate selection obtained is illustrated in the first column of table 2. Note that the number 2 close to the covariate indicates a nonlinear relationship between the covariate and the parameters. To corroborate the results of the final subset of covariates to test, an influential analysis was carried out by means of leverage and Cook distance and

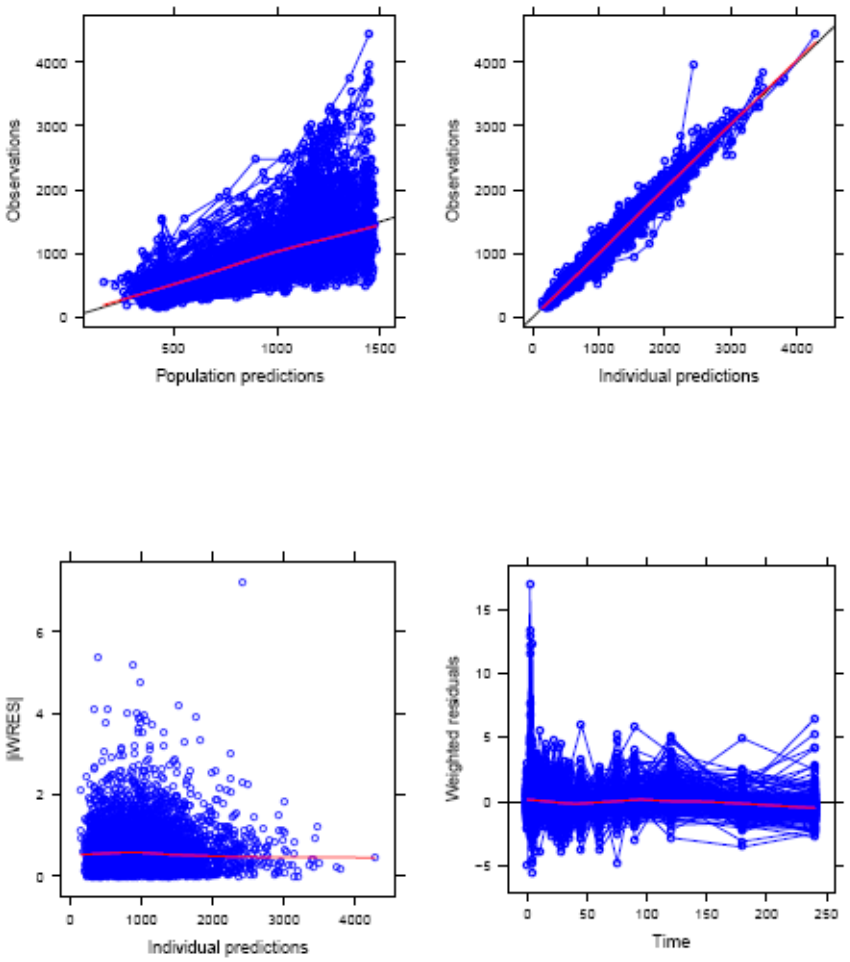

Figure 5.3: Plot of the individual and population predictions (at the top) and residuals (at the bottom).

Model parameters	GAM selected predictors	
	Pre influential analysis	Post influential analysis
β	IBSL BMI(2) VAF	IBSL BMI VAF
α	SEX GBSL AGE(2) VAF PTBF	GBSL AGE(2) VAF
X_0	GBSL IBSL AGE BSA	SEX GBSL IBSL AGE(2) PTBF
MTT	AGE(2)	AGE
CP_b	GBSL IBSL(2) AGE VAF PTBF	GBSL IBSL AGE VAF PTBF

Table 5.2: The GAM selection of covariates for each of the five CMM parameters before and after the influential analysis. (2) indicates a nonlinear relationship between the parameter and the covariate.

the outliers were detected by visual inspection (see Fig. 5.4 and 5.5). In particular from figure 5.4 we can see that subject with ID 1 presents a high Cook distance value with respect to the others and that subject with ID 66 instead presents a high leverage value with respect to the others. In Fig. 5.5 is presented the Cook distance in details calculated for each GAM term. In this figure only subject with ID 1 stands out from the others. The final subset of covariates for each CMM parameter is presented in the second column of Tab. 5.2.

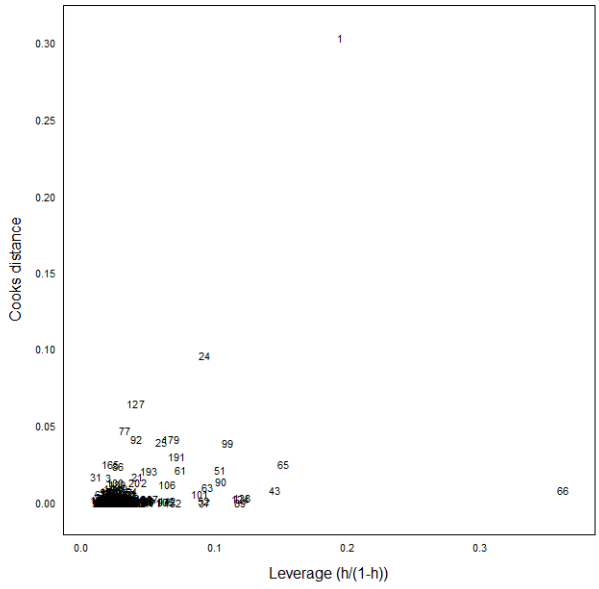

Figure 5.4: Cooks distance vs leverage for a GAM fit of the CP_b parameter. Data points are labeled by the ID number.

These screening results were included into the base model and the forward and backward selection in NONMEM was carried out. After forward inclusion and

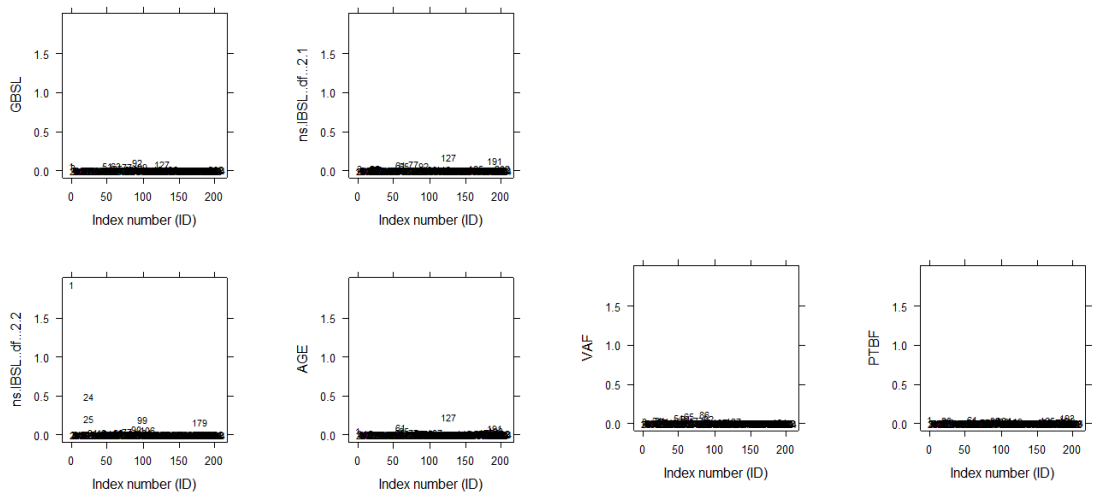

Figure 5.5: Cooks distance on each GAM term selected for the CP_b parameter. Data points are labeled by the ID Number.

backward, the full covariate model contained eight relations: $\beta \sim$ IBSL, $X_0 \sim$ GBSL-IBSL, $\alpha \sim$ GBSL-AGE, $CP_b \sim$ AGE-GBSL-IBSL. The significant relations identified by NONMEM were further examined for plausibility and relevance. Basal glucose and insulin (GBSL-IBSL) were identified to be plausible explanatory factors respectively for the parameters X_0-α and β-X_0-CP_b. Regarding the influence of AGE on α (negative relation) and on CP_b (positive relation), biological explanations can be given for these covariate relations in Basu et al [52] where it is claimed respectively that basal concentration of C-peptide where higher in elderly men and woman and that the dynamic response to glucose was lower in elderly men. The two AGE relations though assumed very small values with respect to the other and it was decided to left them out. The final parameter model is described in Eq. 2 as in Eq. 5.11 where COV (all caps) is a covariate (IBSL, GBSL, etc.) and ΔCOV represents the deviation of the covariate COV from its median value. The optimal parameter values for the base and the final covariate model are reported in Tab. 5.3, along with their precision. The drop of the objective function is statistically significant (around 240 points). Moreover there is the expected drop in the population variability that is evident looking at the omega matrix before and after the insertion of the covariates. In particular, the X_0 BSV moves from 54% to 42%, the β BSV from 41% to 34%, the α BSV from 75% to 72%, the CP_b BSV from 34% to 24% and finally the MTT BSV remains stable around 21% since it is

the only parameter without covariate relationship. This drop in the BSV means that the model has increased its descriptive capabilities and is able to explain a portion of the BSV in a deterministic way rather than attributing it to random differences among subjects. The clear trend between the individual etas and some covariates that was observable in the base model (see Fig. 5.6) is dramatically reduced as expected in the final covariate model.

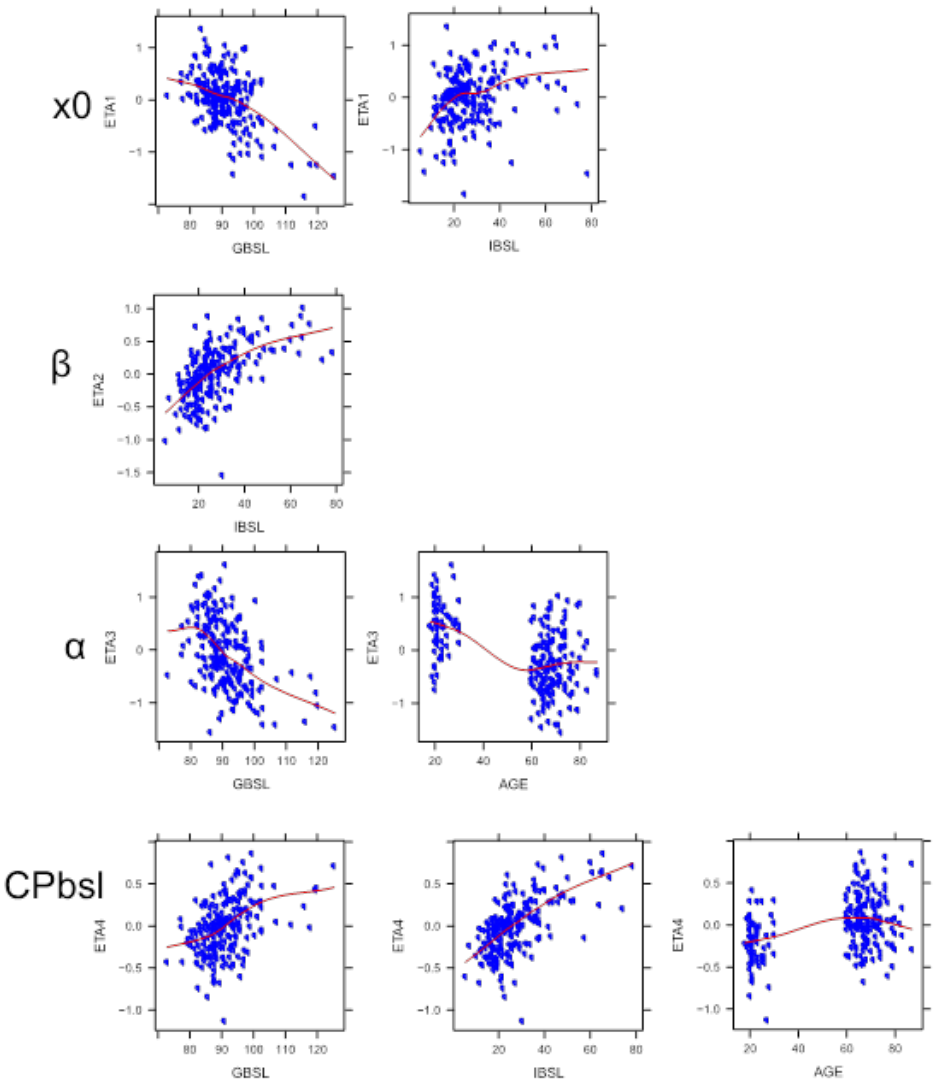

Figure 5.6: Individual random effects of four parameters in the base model versus the final selection of covariates after the forward and backward selection of NONMEM.

$$\begin{gathered}
\beta = \theta_\beta e^{\theta_{\beta\sim IBSL}\Delta IBSL+\eta_\beta} \\
\mathrm{X}_0 = \theta_{X0} e^{\theta_{X_0\sim IBSL}\Delta IBSL+\theta_{X_0\sim GBSL}\Delta GBSL+\eta_{X_0}} \\
\alpha = \theta_\alpha e^{\theta_{\alpha\sim GBSL}\Delta GBSL+\eta_\alpha} \\
\mathrm{CP}_b = \theta_{CP_b} e^{\theta_{CP_b\sim GBSL}\Delta GBSL+\theta_{CP_b\sim IBSL}\Delta IBSL+\eta_{CP_b}} \\
\mathrm{MTT}{=}\theta_{MTT} e^{\eta_{MTT}}
\end{gathered}$$

(5.13)

Shrinkage of the final model was calculated and was below the generally accepted upper threshold of 20 / 30% [53, 37]. In particular it ranges from a value of 1.2% of the parameter β to a value of 14.5% relative to the parameter α. In Fig. 5.7 is presented the basic goodness of fit plot. The population prediction compared to the one obtained in the base modeled is improved: the higher observation are better predicted and there is less underestimation. The individual prediction is satisfactory as in the base model. As far as the residuals are concerned, both the individual and the population weighted residuals behave well apart from few outliers.

To assess the ability of the model to capture the variability observed in the dataset, a visual predictive check (VPC) [50] was performed with NONMEM and PsN [43] as can be seen in Fig. 5.8 . The final population parameters were used to simulate 1000 replicates of the dataset, and the observations were stratified by percentiles for each time point. The model performance of simulating profiles similar to the observed data is good as it can be seen in Fig. 5.8 since the CI of the simulated percentiles follow well the percentiles of the observed data.

Model parameters	Units	base model		final modes	
		population estimates	RSE %	population estimates	RSE %
Fixed Effects					
X_0	pmol/l	1170	4.70%	1120	3.50%
β	pmol dl l^{-1} mg^{-1} min^{-1}	0.508	3.30%	0.483	2.60%
α	min^{-1}	0.105	6.40%	0.107	6.10%
CP_b	pmol/l	440	2.70%	421	2.00%
MTT	min	2.44	1.60%	2.51	0.1%
n	-	150	-	150	-
m	min^{-1}	1.99	7.10%	2.13	4.50%
Covariate Influence					
$X_0 - GBSL$		-	-	-0.0463	9.10%
$X_0 - IBSL$		-	-	0.0188	14.10%
$\beta - IBSL$		-	-	0.018	12.40%
$\alpha - GBSL$		-	-	-0.0364	23.50%
$CP_b - IBSL$		-	-	0.0147	10.50%
$CP_b - GBSL$		-	-	0.0138	15.00%
Random effects					
Interindividual Variability					
ω X_0		54.10%	4.95%	42.00%	6.17%
ω *beta*		41.40%	5.57%	34.50%	4.90%
ω α		75.30%	8.57%	71.70%	8.35%
ω CP_b		33.90%	5.63%	24.00%	5.08%
ω MTT		20.30%	4.41%	21.70%	5.82%
correlation β X_0		23.80%	19.37%	16.00%	35.58%
correlation α X_0		46.40%	14.72%	43.20%	18.97%
correlation α β		-26.50%	26.67%	-24.30%	30.89%
correlation $_b$ β		79.10%	9.39%	72.00%	17.33%
correlation $_b$ α		-45.30%	21.17%	-40.00%	31.28%
Residual unknown variability					
σ_{prop}		0.0847	1.20%	0.0844	1.20%
σ_{add}		47.7	2.80%	47	2.60%

Table 5.3: Summary of parameter estimates obtained before (base model) and after (final model) the covariates introduction. Typical values for parameters are in original units. Given that between-subject variability is modeled as log normal, variance measures are reported as approximate coefficients of variation (CV), whereas the covariance terms are in terms of correlation. Coefficients for the covariates are in logarithmic units; therefore, as a first approximation they can be interpreted as proportional changes in the minimal model parameter per unit change of the covariate.

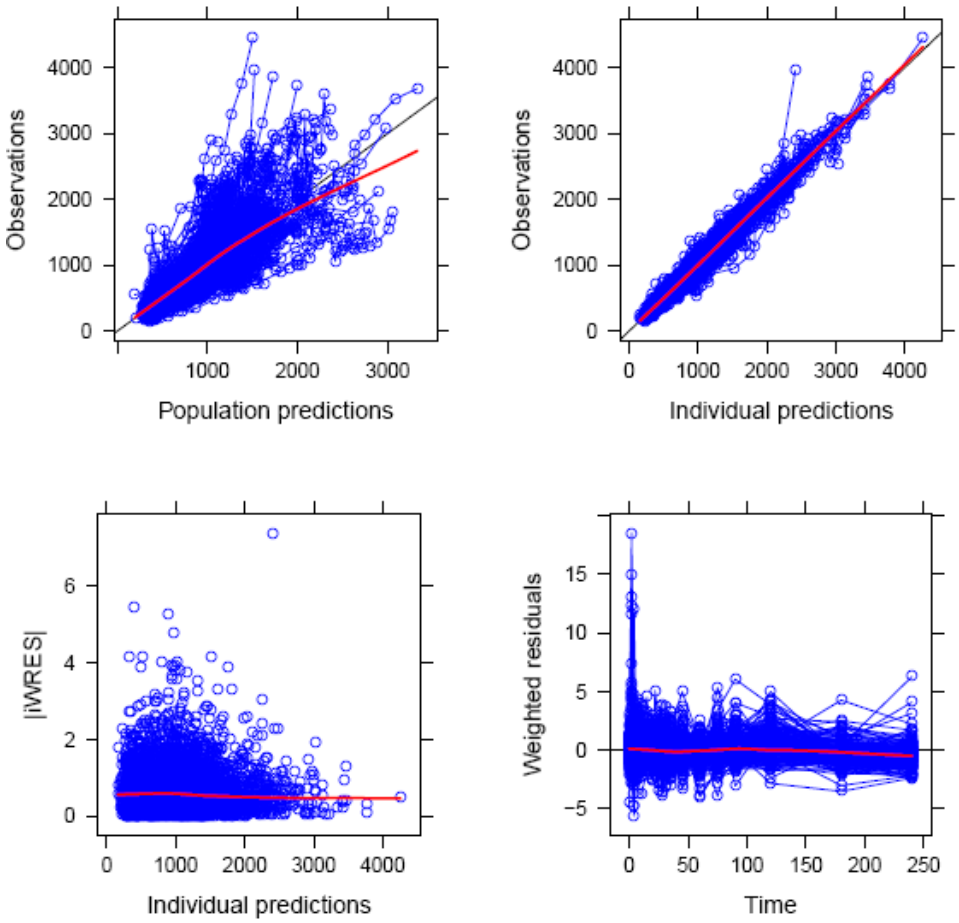

Figure 5.7: Plot of the individual and population predictions (at the top) and residuals (at the bottom)

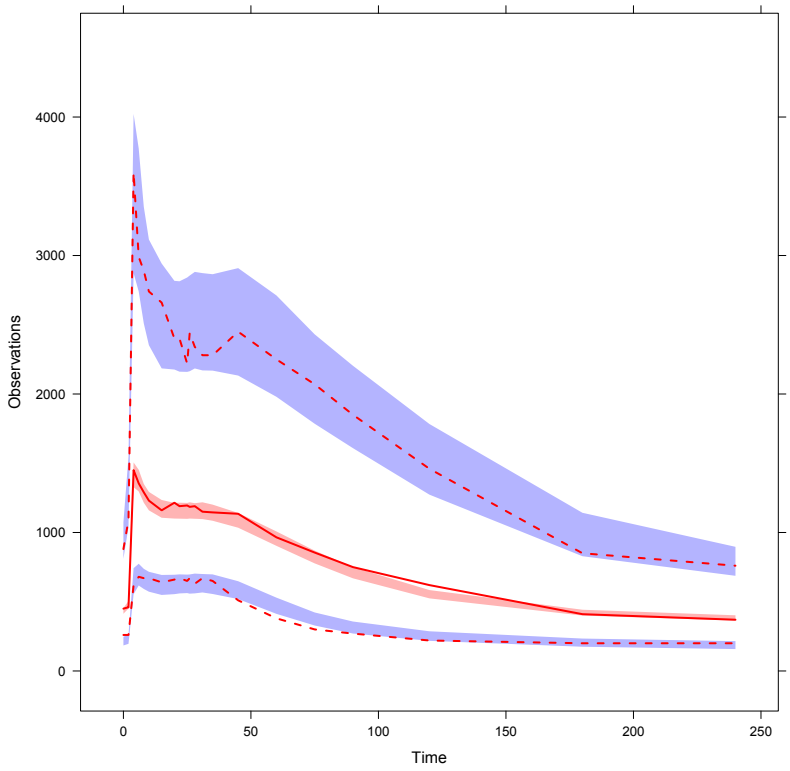

Figure 5.8: Visual predictive check of the final model.

5.4 Discussion

This article is the natural extension of the Denti et al work [3] in an IVGTT data rich protocol context where the sources of biological variability were investigated by introducing the covariates on the glucose minimal model once the model was optimized. The first part of the analysis consists on revising the CMM model by exploiting the NLMEM potentials. We introduced a delay term that enables the model to be more flexible in the first part of the data and to take into account the delay due to the glucose signal. In particular it was delayed the first phase of secretion that corresponds to stored amount of C-peptide immediately releasable after a glucose stimulus above basal concentration. It is reasonable to think in fact that the glucose dose (330 mg/kg) given from minute zero of the experiment can take a time of infusion and of distribution in the body equal to the 2.5 minutes estimated that is the time before the first secretion of insulin begins. Moreover in the between subject variability of the delay (MTT) are taken into account also possible experimental mistakes during the infusion. The CMM base model implemented with this new feature gives satisfactory results at both individual and population level. In particular the individual fit describes well the observed data in all the dynamics whereas the population prediction sometimes underestimates the peak due to the fact that the delay parameter MTT in the population description is modeled just as the fixed effect common to the entire set of subjects and in this way it loses the flexibility in some subjects to catch the dynamic of the curve in the first temporal window. Moreover the parameter individual information is characterized well enough to allow a proper covariate search without leading to false parameter-covariate relations. It is important to note that the Van Cauter parameters are constructed from each subject anthropometric information that might bias the following covariate analysis. Remember that the aim of this work was to implement through the population approach the already validated C-peptide model in the single subject approach. Future work would be to try to identify the model without the use of these kinetics priors if possible. if this is not possible even by exploiting a powerful approach like the NLMEM it would be interesting to identify the Van Cauter C-peptide kinetics data through a population approach and then use this complete kinetics characterization as future priors in the C-peptide minimal model.

Moving to the covariate analysis, the methodology used for the selection of the possible covariate-parameter relations to test in NONMEM was the GAM fit supervised by an influential individual analysis that helped to identify false relations caused by just few influential subjects. This analysis did not changed dramatically the GAM fit results: only the covariate relations identified for the parameters α and X_0 are partially different

whereas the remaining three parameters kept the same predictors with just some changes in the suggested relations to test (from nonlinear to linear). The GAM analysis included more predictors than the final ones selected by the following forward and backward NONMEM analysis but even if it did not single out the most parsimonious model, it still provided a very good guess, allowing dramatic reduction in time and improving the efficiency of the covariate selection process.
The optimal model obtained after the NONMEM forward and backward selection includes in the final model some covariates whose relations with their corresponding parameters we will try now to describe through possible physiological explanations. In particular the predictors of the basal level of the C-peptide are the basal levels of glucose and the basal level of insulin. These two relations detected are positive. Insulin basal level obviously is a positive predictor of the basal levels of the C-peptide since C-peptide is a cosecreted substance with insulin. The basal glucose relation instead is a consequence of the glucose basal higher levels in elderly subjects. In Basu et al [52] in fact was found that both the fasting C-peptide and glucose levels (but not insulin levels) are higher in elderly women and men. The parameter β has as a predictor the basal insulin with a positive relation that means that subjects with higher IBSL have more insulin secretion. In other words if two healthy subjects that have the same level of basal glucose undergo to the same glucose load, the subject with higher insulin basal level produce more insulin because the tissue are probably more insulin resistant and to absorb the same quantity of glucose it takes more insulin than the other subject. The covariates selected for the parameter α is basal glucose related in a negative way with the parameter. In particular the higher the basal level of glucose the lower the insulin production which is a plausible relation since the glucose stimulus is measured subtracting to the glucose signal the basal level. Finally the covariate relations selected for the parameter X_0 are the basal level of insulin and glucose. The physiological explanation for these last two might bound to the meaning of this parameter that represents respectively the insulin that is releasable because is present at the basal conditions (IBSL) and because there is a change in glucose levels (GBSL) so the smaller GBSL is the bigger the change is. We can conclude that the final selection might be physiologically plausible even if further clinical study are necessary to validate completely the work. If we look at the drop of BSV of each parameter in terms of relative deviation, it turns out that only the covariates GBSL, IBSL on the parameter CP_b are able to explain more than 30% of between subject variability of CP_b in the model without covariates whereas the other predictors in the remaining four parameters explain no more than the 22%. In particular the relative deviation for the parameter $_0$ is 22%, for β is 17% and for α is 5%.

So far it was discussed the CMM capability to describe the real data variability but at the same time it is important as well to check the model capability to simulate reasonable C-peptide data. Looking at the VPC analysis that was made in the final covariate model, the simulation performance of the model is on the whole satisfying: the CI of the percentiles of simulated profiles follow the dynamics of the percentiles of the observed data meaning that the simulated profiles are reasonable. We can conclude that for dataset fast screening purposes or for sparse dataset turns to be more convenient take into the analysis the relations discovered between the covariates and the parameters to reduce the BSV and to help the estimation process.

5.5 Conclusions

In this study, a population PK analysis was performed on a C â peptide rich dataset collected after an insulin modified IVGTT. The model that was used is a revision of the already published CMM [19] made by exploiting the potentials of the population approach. In particular a delay was introduced in the first part of the experiment to take into account the time between the injection of the glucose dose and its distribution and the following secretion of insulin. The results are satisfactory at both individual and population level so this work paves the way for further studies that aim to further narrow down the protocol in order to better deal with the typical data poor epidemiological study condition. Furthermore, in this article, we suggest a population CMM that incorporates in its estimates physiological information such as sex and age, easily measurable anthropometric data such as height and weight, body fat amount and distribution, and information on the basal levels of glucose and insulin. The introduction of the covariates underlines the model parameters dependence on the basal levels of both glucose and insulin. Since in clinical practice is easier to be in a data poor condition, this suggests that these relations have to be taken into account to introduce additional information that can improve the estimation process. At the same time our covariate model suffers from several limitations like the use of the Van Cauter kinetics parameters as an individual a priori knowledge that might blur the covariate analysis made. Another limitation that was not taken into account into this analysis is the existence of more complex and possibly nonlinear relationships between the covariates and the parameters that should be investigated. Finally, since the amount of variability in the data is limited, and therefore the possibility of statistical artifacts and model misspecification cannot be excluded, it would be important to validate and corroborate our results by repeating the analysis on different datasets.

An integrated model to describe the glucose and insulin system during an IVGTT

6.1 Introduction

The glucose and insulin minimal models [17, 21] are widely used tools to study the glucose insulin systems. The system in these two minimal models is decomposed in two subsystems where glucose and insulin are respectively used as known input and output or vice versa depending on which part of the system is chosen to be described. This modeling choice was introduced in the metabolic field as a strategy to better identify the minimal models. So far these models were both identified separately using the classic weighted nonlinear least square (WNLS) that due to a posteriori identifiability problem resorts often to Bayesian a priori knowledge to make the estimation step possible. In this article we want to integrate the glucose and insulin minimal models by exploiting the Nonlinear mixed effects approaches (NLMEM). Denti et al [2] showed already the advantages of the NLMEM in the estimation of the glucose minimal model. The NLMEM in fact resort to the population information spread in the collection of subjects that creates a prior that facilitate the estimation process. In this way the NLMEM are able to overcome some of the identifiabilty problem in the single subject approach and to deal with individual data sparseness by borrowing the lack of information from the entire

population.
In this case the NLMEM approach enables the integration of the two models that otherwise, in the individual context, would be not feasible for the big number of parameters. The rationale of the work was first to optimize from a populatin point of view the two minimal models separated and once this is done move to the integration of the two models. As far as the glucose minimal model is concerned this process was already done in chapter 4 with the two compartment glucose model formulation whereas the insulin minimal model has to be implemented in a population context from scratch. The insulin minimal model was implemented adding a delay term that describes, as in the IVGTT C-peptide minimal model, the time that takes the glucose signal to activate the insulin secretion from the beginning of its infusion. Moreover a second compartment was added to describe better the insulin kinetics and the compartment of the model representing insulin in the β-cell was deleted as it was unnecessary with this new formulation of the model. Finally an allometric scaling was introduced also in the insulin model to explain in a deterministic way part of the variability in the parameters. The main advantage of having an integrated glucose insulin system implemented in NLMEM is to have the complete characterization of the joint probability distribution of the parameters of an healthy population. From this distribution the entire glucose and insulin system can be simulated unlike the two minimal models where just a part of the system could be described by the simulation while the other one is known.

6.2 Material and Methods

1. *Data*
   The data, provided by the Clinical Research Center at the Mayo Clinic, Rochester, MN, USA, originates from an insulin modified IVGTT protocol performed on 204 nondiabetic subjects (118 M /86 F, mean age 55.53 $\pm$ 21.66 mean BMI 26.62$\pm$ 3.39 kg/m2) that underwent an intravenous injection of glucose (0.3 g/kg body wt) followed by a square wave (from 20 to 25 min) of insulin infusion (0.02 U/kg body wt). Blood samples were collected at -120, -30, -20, -10, 0, 2, 4, 6, 8, 10, 15, 20, 22, 25, 26, 28, 31, 35, 45, 60, 75, 90, 120, 180 and 240 min for measurement of glucose, insulin and C-peptide concentrations. Different weight information were collected to improve the parameter estimation process by adding some individual information the so called covariate. In Tab. 6.1 are summed up the weight descriptors characteristics.

2. *The integrated model*

Covariate	Name	Units	Mean	Min	1stQ	Median	3rdQ	Max
BW	Body weight	kg	77.95	53	68.9	79	87	129
VAF	Visceral abdominal fat	cm^2/CT slice	141.84	11.86	62.54	125.09	206.73	478.23
TAF	Total abdominal fat	cm^2/CT slice	301.76	43.94	193.28	292.32	407.66	837.5
TBF	Total body fat	grams	23413.06	4884	17364	22520	28420	46986
%TBF	percentage of total body fat	%	32.41	7.3	25.8	31.6	39.75	56.7
LBM	Lean body mass	kg	49.53	30.1	38.5	51.84	58.68	74.58

Table 6.1: Continuous covariates for the glucose-insulin system measured in our 204 subject database. Statistics include minimum and maximum value, 1^{st} and 3^{rd} quartiles, and mean and median.

The model building strategy was first to focalize on the two subsystems separated and then once the two minimal models were refined integrate them. The glucose minimal model with the two compartments was implemented as in the chapter 4 whereas the insulin minimal model revision exploiting the population approach was built from scratch. In particular we apply the NLMEM to the already published model [21] estimated with the traditional approach WNLS and we revised it using the potentials of the new approach. In the following two paragraphs are described the final formulations of the two models.

The glucose minimal model (GMM)

The 2GMM [18] was revised by adding a delay term in the appearance of glucose in plasma due to the infusion and distribution of the glucose in the body. In particular a transit model was inserted in the original formulation of the model by using a cascade of first order models with a single transfer rate k_{tr1}. The final model is described by the following equations:

$$\begin{aligned} Q_1'(t) &= -(S_G + X(t)) \cdot Q_1(t) + S_G \cdot Q_{1b} - k_{21} \cdot Q_1(t) + k_{12} \cdot Q_2(t) \\ &\quad + D \cdot BW \cdot \frac{(k_{tr1} \cdot t)^{n1}}{n1!} \cdot e^{-k_{tr1} \cdot t} \qquad Q_1(0) = G_b \cdot V \\ Q_2'(t) &= k_{21} \cdot Q_1(t) - k_{12} \cdot Q_2(t) \qquad Q_2(0) = \frac{k_{21}}{k_{12}} \cdot G_b \cdot V \\ X'(t) &= -p2 \cdot X(t) + p2 \cdot S_I \cdot (I(t) - I_b) \qquad X(0) = 0 \end{aligned} \tag{6.1}$$

where Q_1 and Q_2 is the glucose mass in plasma (mg) in the accessible and non accessible pool of the glucose system, G_b is the basal glucose concentration (mg/dl), I is insulin plasma concentration (pmol/l) and I_b is its basal value, X is insulin action (min^{-1}) and D is the dose (330 mg/kg). The parameters of the model are the following: the glucose effectiveness S_G (min^{-1}), the insulin sensitivity S_I

(min^{-1} $pmol^{-1}$ l), the insulin action p2 (min^{-1}), the volume V (dl), the glucose two compartment transfer rate k_{21} and k_{12} (min^{-1}), the transit model transfer rate k_{tr1} (min^{-1}) and the number of compartments n1. Note that k_{tr1} can be expressed as a function of n1 and of the mean transit time (MTT1) (min) or the time of delay of the secretion in the following way:

$$k_{tr1} = \frac{n1+1}{MTT1} \tag{6.2}$$

In this article we estimate n1 and MTT1. Note that the parameters S_G, k_{21} and k_{12} were expressed as clearances because by definition are more informative than their corresponding transfer rates. Moreover between the accessible and the non accessible compartment was supposed a diffusion process meaning that at the equilibrium state the concentration are the same so as a consequence also the clearance between those two compartments. To sum up the final set of unknown parameters are p=[cl_{S_G}, S_I, V, p2, cl_{k1}, V_2, n1, MTT1] where cl_{S_G} (dl/min) is the clearance of S_G, cl_{k1} (dl/min) is the clearance of the parameters that was supposed to be equal in the two compartments due to the diffusion hypothesis and V_2 (dl) is the volume of the non accessible compartment. Note that the model compartments were expressed in mass to have the parameters do not depend implicitly on weight information and to be able to introduce this information through the allometric scaling.

The insulin minimal model (IMM)

The IMM was revised and its final formulation is the following:

$$\begin{aligned}
I_1'(t) &= -n \cdot I_1(t) + Y(t) + k_{12} \cdot I_2(t) - k_{21} \cdot I_1(t) + U(t) \\
&\quad + X_0 \cdot V_I \cdot \frac{(k_{tr2} \cdot t)^{n2}}{n2!} \cdot e^{-k_{tr2} \cdot t} \qquad I_1(0) = I_b \cdot V_I \\
I_2'(t) &= k_{21} \cdot I_1(t) - k_{12} \cdot I_2(t) \qquad I_2(0) = I_b \cdot V_{I2} \\
Y'(t) &= \begin{cases} -\alpha \cdot (Y(t) - \beta \cdot (G(t) - G_b) \cdot V_I - n \cdot I_b \cdot V_I) \\ Y(0) = (n \cdot I_b \cdot V_I) \qquad \text{if } \beta \cdot (G(t) - G_b) \cdot V_I - n \cdot I_b \cdot V_I \geq 0 \\ -\alpha \cdot (Y(t)) \\ Y(0) = (n \cdot I_b \cdot V_I) \qquad \text{if } \beta \cdot (G(t) - G_b) \cdot V_I - n \cdot I_b \cdot V_I < 0 \end{cases}
\end{aligned} \tag{6.3}$$

where I_1 and I_2 are the insulin accessible and non accessible pool mass in plasma (pmol), U(t) is the squared infusion (pmol/min) and Y is the provision of new insulin (pmol/min). The model parameters are the following: n is the rate constant of insulin disappearance (min^{-1}), k_{12} and k_{21} (min^{-1}) are the rate transfer between the accessible and the non accessible pool, V_I (l) is the insulin distribution volume, X_0 (pmol/l) is responsible for the first insulin secretion, I_b (pmol/l) is the basal insulin level, α (min^{-1}) is a rate constant towards Y tends to a steady state value that is linearly related to glucose concentration G (mg/dl) through the parameter β (min^{-1} pmol dl l^{-1} mg^{-1}) above the basal glucose threshold G_b (mg/dl). Note that as in the IVGTT C-peptide the first insulin secretion is delayed through a transit model that is implemented as a cascade of n2 first order models with a single transfer rate k_{tr2}. This delay takes into account the glucose signal time of distribution in the body before it can activate the β-cell to secrete insulin. Note that k_{tr2} can be expressed as a function of n2 and of the mean transit time or the time of delay of the secretion in the following way:

$$k_{tr2} = \frac{n2+1}{MTT2} \tag{6.4}$$

In this article we estimate n2 and MTT2. Note that the parameters n, k_{12} and k_{21} are expressed as clearances and like in the glucose minimal model between the accessible and the non accessible compartment was supposed a diffusion process meaning that at the equilibrium state the concentration are the same so as a consequence also the clearance between those two compartments. The final set of unknown parameters are the following p=[cl_n, cl_{k2}, V_I, V_{I2}, X_0, α, β, MTT2, n2, I_b] where cl_{k2} (l/min) is the clearance of the parameters that was supposed to be equal in the two compartments due to the diffusion hypothesis and V_{I2} (l) is the volume of the non accessible compartment.
Note that in the integrated model the forcing function for the GMM is substituted with the estimated kinetic of the accessible insulin compartment (I_1/V_I) whereas the IMM forcing function is substituted with the estimated glucose kinetic of the accessible glucose compartment (Q_1/V). Both the signals are fitted simultaneously. Note also that the glucose and insulin basal values in the integrated model are both estimated parameters. So the finalset of unknown parameters is the following **p**=[cl_{S_G}, S_I, V, p2, cl_{k1}, V_2, n1, MTT1, G_b, cl_n, cl_{k2}, V_I, V_{I2}, X_0, α, β, MTT2, n2, I_b].

3. *Population modeling assumptions*

Nonlinear mixed effects models (NLMEM) are able to quantify both the population and the individual parameters and to identify by a hierarchical approach the biological sources of intra-individual and inter-individual variability. More specifically, in a first step, the data are described by:

$$y_{ij} = f(\mathbf{p_i}, x_{ij}) + \epsilon_{ij} \qquad 1 \leq i \leq m \qquad 1 \leq j \leq n_i \tag{6.5}$$

where y_{ij} are is the jth observation of the ith subject at some known time instant x_{ij}. Here, m is the number of individuals and n_i is the number of observation of individual i. $\mathbf{P}_i$ is the vector of model parameters of the ith individual. The variability due to measurement and model errors, better known as the residual unknown variability (RUV), is explained through ϵ_{ij} which is assumed to be independently distributed with a zero mean and Gaussian distribution:

$$\epsilon_{ij} = N(0, (\sigma_{prop} y_{ij} + \sigma_{add})^2) \tag{6.6}$$

The variance model is described for both the measures of glucose and insulin as a combination of a proportional and an additive error model where σ_{prop} and σ_{add} are additional parameters to estimate. In a second step, the model parameters are represented as function of some physiologically meaningful attributes that do not vary across the population ($\boldsymbol{\theta}$, fixed effects, i.e. values that are common to all subjects) and some others that do ($\boldsymbol{\eta}_i$, random effects, i.e. values typical of a specific subject). In our model we chose the function:

$$p_{ki} = \theta_k e^{\eta_{ki}} \tag{6.7}$$

where p_{ki} is the kth model parameter of the ith subject, θ_k is the typical value of the kth parameter common to the entire population and η_{ki} is the random effect of the kth model parameter of the ith subject. The random effect $\boldsymbol{\eta}_i$ are assumed to be independently distributed with a zero mean and Gaussian distribution:

$$\boldsymbol{\eta}_i \sim N(0, \boldsymbol{\Omega}) \tag{6.8}$$

with $\boldsymbol{\Omega}$ being a positive definite covariance matrix. With this formulation the second stage of variability, better known as Between-Subject Variability (BSV), is explained. The omega set up matrix for the integrated model is the following:

$$\boldsymbol{\Omega} = \begin{bmatrix}
\omega^2_{P2} & \omega_{P2-S_I} & \omega_{P2-cl_n} & \omega_{P2-I_b} & \omega_{P2-\beta} & \omega_{P2-\alpha} & 0 & 0 & 0 & 0 & 0 & 0 & 0 & 0 & 0 & 0 \\
\omega_{P2-S_I} & \omega^2_{S_I} & \omega_{SI-cl_n} & \omega_{SI-I_b} & \omega_{SI-\beta} & \omega_{SI-\alpha} & 0 & 0 & 0 & 0 & 0 & 0 & 0 & 0 & 0 & 0 \\
\omega_{cl_n-P2} & \omega_{cl_n-S_I} & \omega^2_{cl_n} & \omega_{cl_n-I_b} & \omega_{cl_n-\beta} & \omega_{cl_n-\alpha} & 0 & 0 & 0 & 0 & 0 & 0 & 0 & 0 & 0 & 0 \\
\omega_{I_b-P2} & \omega_{I_b-S_I} & \omega_{I_b-cl_n} & \omega^2_{I_b} & \omega_{I_b-\beta} & \omega_{I_b-\alpha} & 0 & 0 & 0 & 0 & 0 & 0 & 0 & 0 & 0 & 0 \\
\omega_{\beta-P2} & \omega_{\beta-S_I} & \omega_{\beta-cl_n} & \omega_{\beta-I_b} & \omega^2_{\beta} & \omega_{\beta-\alpha} & 0 & 0 & 0 & 0 & 0 & 0 & 0 & 0 & 0 & 0 \\
\omega_{\alpha-P2} & \omega_{\alpha-S_I} & \omega_{\alpha-cl_n} & \omega_{\alpha-I_b} & \omega_{\alpha-\beta} & \omega^2_{\alpha} & 0 & 0 & 0 & 0 & 0 & 0 & 0 & 0 & 0 & 0 \\
0 & 0 & 0 & 0 & 0 & 0 & \omega^2_{G_b} & \omega_{G_b-X_0} & 0 & 0 & 0 & 0 & 0 & 0 & 0 & 0 \\
0 & 0 & 0 & 0 & 0 & 0 & \omega_{X_0-G_b} & \omega^2_{X_0} & 0 & 0 & 0 & 0 & 0 & 0 & 0 & 0 \\
0 & 0 & 0 & 0 & 0 & 0 & 0 & 0 & \omega^2_{S_G} & 0 & 0 & 0 & 0 & 0 & 0 & 0 \\
0 & 0 & 0 & 0 & 0 & 0 & 0 & 0 & 0 & \omega^2_{V} & 0 & 0 & 0 & 0 & 0 & 0 \\
0 & 0 & 0 & 0 & 0 & 0 & 0 & 0 & 0 & 0 & \omega^2_{V_I} & 0 & 0 & 0 & 0 & 0 \\
0 & 0 & 0 & 0 & 0 & 0 & 0 & 0 & 0 & 0 & 0 & \omega^2_{cl_k1} & 0 & 0 & 0 & 0 \\
0 & 0 & 0 & 0 & 0 & 0 & 0 & 0 & 0 & 0 & 0 & 0 & \omega^2_{V_2} & 0 & 0 & 0 \\
0 & 0 & 0 & 0 & 0 & 0 & 0 & 0 & 0 & 0 & 0 & 0 & 0 & \omega^2_{cl_k2} & 0 & 0 \\
0 & 0 & 0 & 0 & 0 & 0 & 0 & 0 & 0 & 0 & 0 & 0 & 0 & 0 & \omega^2_{MTT1} & 0 \\
0 & 0 & 0 & 0 & 0 & 0 & 0 & 0 & 0 & 0 & 0 & 0 & 0 & 0 & \omega_{MTT1-MTT2} & \omega^2_{MTT2}
\end{bmatrix}$$

where the effort was to keep just the most explanatory terms of the Ω matrix. Note that the omega matrix set up of the IMM when was first built alone was supposed diagonal because the preliminary work of optimization is just a prerequisite of the integration. As far as the GMM parameter description is concerned, the parameter n1 is not present in the Ω matrix because is assumed constant in the population as described in the previous chapter 4. As far as the IMM is concerned, the parameter n2 is fixed to a population value big enough but not enormous (n2=200) to facilitate the computational process. The value n2 was chosen as the smallest that through a simulation do not change dramatically by visual inspection the insulin profiles. Moreover the volume of the non accessible pool of insulin V_2 was modeled simply as a fixed effect common to the entire population because it adds no significant improvement in terms of drop of function.

4. *Allometric scaling*

   An allometric scaling was introduced to explain in a deterministic way part of the BSV of the model parameters through the use of different weight information and consequently to reduce the estimated BSV. Note that all the model compartments were expressed in mass to better deal with the introduction of weight information with allometric scaling in the sense that the parameters do not depend implicitly on weight information. As far as the GMM is concerned the same allometric scaling as in chapter 4 was used whereas for the IMM the scaling was selected in the following way: a linear regression between the volume parameter (only V_I because it varies in the population) and the different weight predictors (body weight, lean body mass, visceral abdominal fat...) of the dataset was done due to the allometric linear relationship. For the clearance parameters the predictor selected in the volume was introduced as a descriptor.

5. *Algorithms*

   All the model estimation analysis were carried out using the software NONMEM 7.2.0

[29] that implements the NLMEM approach which consists in obtaining the population parameters by maximizing a likelihood function. Because of the computational infeasibility of the exact solution, different approximations were proposed. Here we applied the First Order Conditional Estimation (FOCE) approximation with INTERACTION coherently with was found previously in literature [2] and in chapter 3.

6.3 Results

Firstly we focus on the insulin minimal model optimization. Note that with respect to the model original formulation [21] a second insulin compartment of the non accessible pool was added that contributes to a statistically significant drop of the objective function. Moreover the compartment that in the original model represents the insulin amount in the β-cell was deleted because its role with this final formulation through a simulation analysis was seen to be irrelevant in the data description. In Fig. 6.1 are presented two correlation graphs between the individual or the population predictions versus the observations: on the whole the fit is good as we can see from the matching of the bisector of the plane (black line) with the regression line (the red line). In Fig. 6.2 are presented the individual (red line) and the population (blue dashed line) fits of some random subjects.

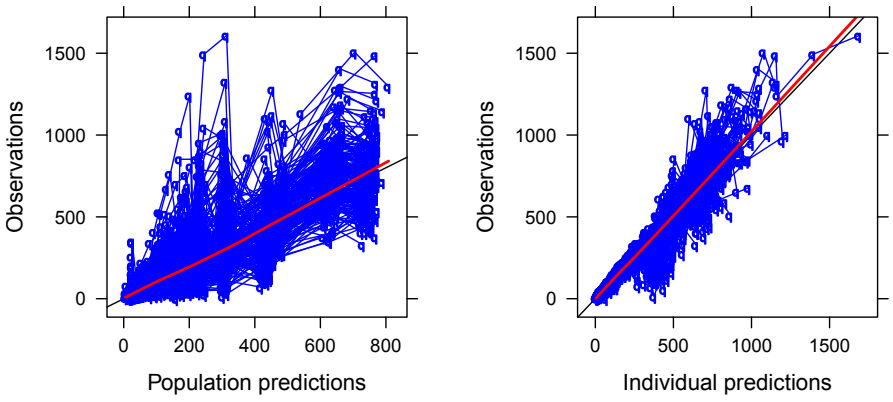

Figure 6.1: Scatterplot of the observation versus the IMM population prediction (left) and the individual prediction (right).

In Fig. 6.3 are presented the individual weighted residuals and the conditional weighted residuals [53] where we can see that the residuals in term of amplitude and pattern are satisfactory apart from few observations. In particular note that the conditional weighted residuals have a small trend at the end of the experiment but it is still well

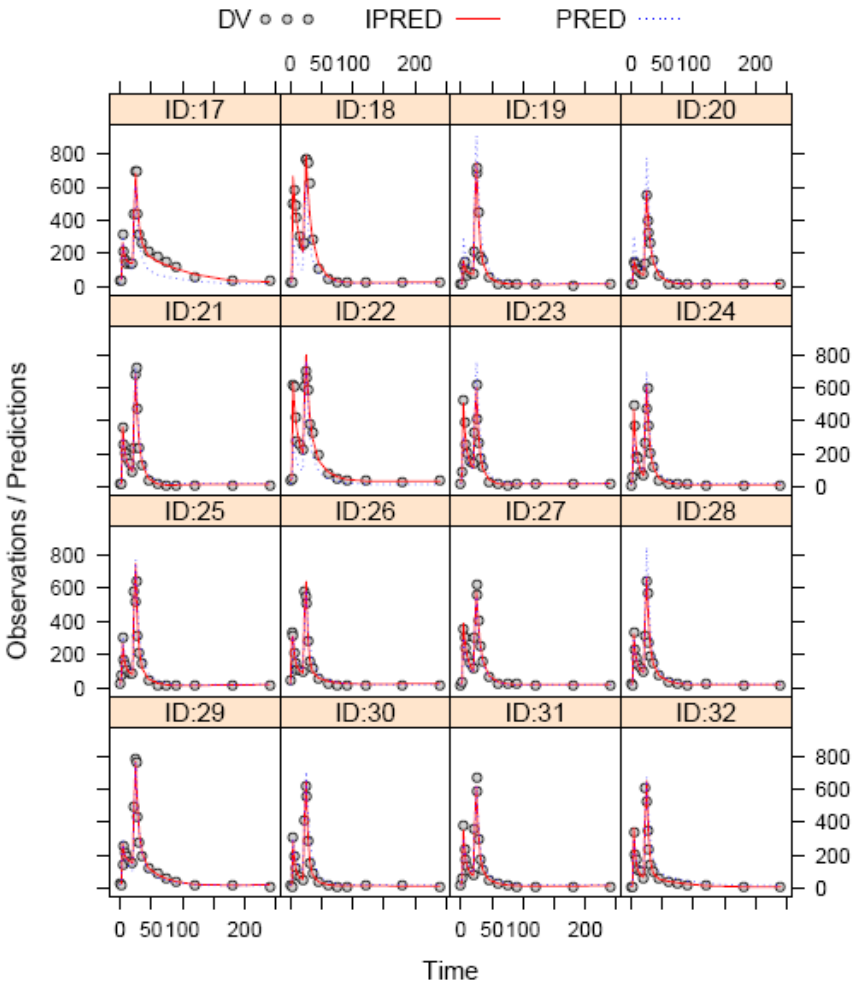

Figure 6.2: Individual profiles. IMM individual prediction (red line) and population prediction (blue dashed line) versus time for some randomly selected subjects. Dots represent the observed concentration.

scorrelated and the residual amplitude is small.

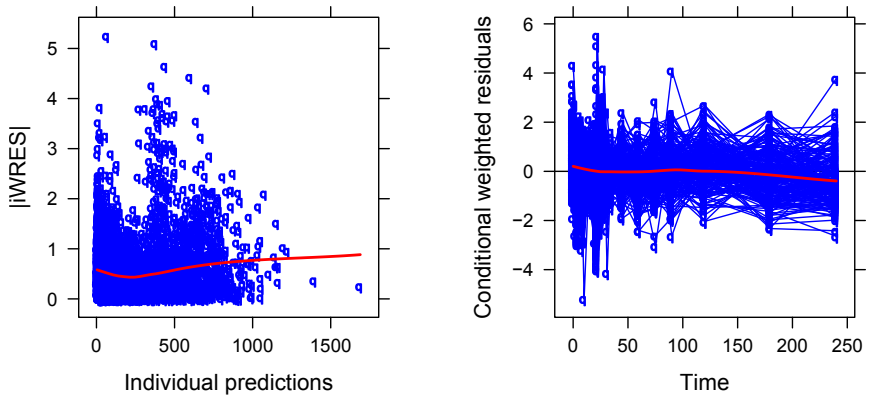

Figure 6.3: IMM individual and conditional weighted residuals.

The population estimates are all estimated precisely as it can be seen from Tab. 6.2 where are presented all the estimates with their relative standard error (RSE%). An allometric scaling was introduced in the volume and clearances parameters. In particular BW was the predictor with the strongest correlation with the parameter V_I in the regression analysis and so it was chosen as the predictors also for two clearances parameters (cl_n and cl_k2). So the final model parameter formulation is the following:

$$\begin{aligned} cl_{ni} &= \theta_{cln} \cdot exp(\eta_{clni}) \cdot \left(\frac{BW_i}{BW_{median}}\right)^{0.75} \\ cl_{K2i} &= \theta_{clk2} \cdot exp(\eta_{clk2i}) \cdot \left(\frac{BW_i}{BW_{median}}\right)^{0.75} \\ V_{Ii} &= \theta_{V\,i} \cdot exp(\eta_{V\,Ii}) \cdot \left(\frac{BW_i}{BW_{median}}\right) \\ V_{I2i} &= \theta_{V\,I2} \cdot \left(\frac{BW_i}{BW_{median}}\right) \end{aligned} \tag{6.9}$$

In Tab. 6.2 are presented the model parameter estimates with their relative standard error and it is clear how the weight information in the final model helped to reduce the parameter BSV by explaining it in a deterministic way. In particular the most important BSV reductions are: V_I BSV swift from 21.1% to 15.8% and the cl_{k2} BSV moves from 45.2% to 38.9%. The drop of objective function is statistically significant and it is around 60 points.

In Fig. 6.4 is presented the VPC [43] of the insulin minimal model. The graph yields that the model is able to catch the data variability as the CI of the percentiles of the simulated profiles are on the whole able to follow the percentiles of the observed data.

Model parameters	Units	base model		final modes	
		population estimates	RSE %	population estimates	RSE %
Fixed Effects					
X_0	pmol/l	366	7.6%	366	7.7%
cl_n	l/min	1.48	2.70%	1.51	3.10%
V_I	l	9.25	2.40%	9.48	1.90%
α	min^{-1}	0.177	11.40%	0.18	12.10%
β	min^{-1} pmol l^{-1} dl mg^{-1}	0.0837	7.20%	0.0841	7.00%
$MTT2$	min	2.45	1.10%	2.46	1.10%
n2	-	200	-	200	-
cl_k2	l/min	0.217	7.30%	0.22	7.30%
V_{I2}	l	6.29	6.90%	6.32	6.70%
I_b	pmol/l	22.3	6.10%	22.4	6.30%
Random effects					
Interindividual Variability					
ω X_0		73.10%	4.9%	73.40%	5.1%
ω cl_n		22.00%	7.5%	23.00%	7.1%
ω V_I		21.10%	8.2%	15.80%	10.7%
ω α		81.1%	13.4%	80.80%	13.6%
ω β		44.90%	10.5%	43.60%	10.4%
ω $MTT2$		7.90%	9.8%	8.00%	9.9%
ω cl_k2		45.20%	13.10%	38.90%	15.0%
ω I_b		43.50%	6.9%	43.10%	7.0%
Residual unknown variability					
σ_{prop}		0.188	0.90%	0.189	0.90%
σ_{add}		1.79	8.80%	1.78	9.00%

Table 6.2: Summary of the insulin minimal model parameter estimates obtained before (base model) and after (final model) the allometric introduction. Typical values for parameters are in original units. Given that between-subject variability is modeled as log normal, variance measures are reported as approximate coefficients of variation (CV), whereas the covariance terms are in terms of correlation.

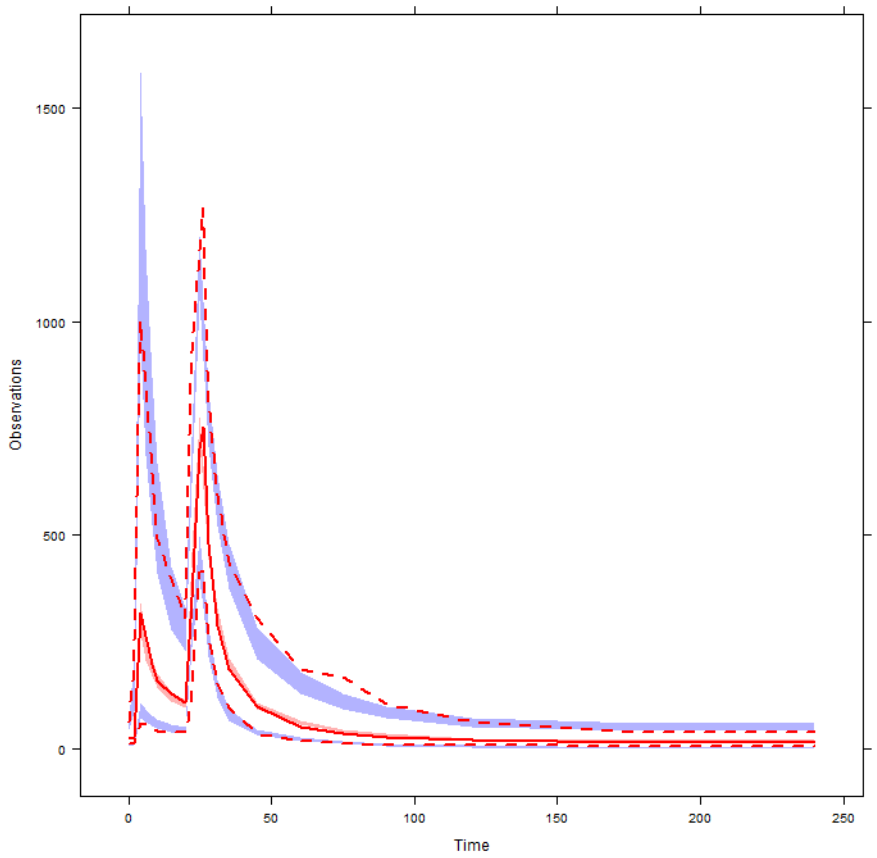

Figure 6.4: The VPC of the insulin minimal model.

After the insulin minimal model has been improved by the NLMEM we focus on the integration of the two subsystems. In Fig. 6.5 and in Fig. 6.6 are presented the integrated model population and individual predictions of the glucose and the insulin versus the observed data. For both the population and the individual predictions the match between the regression line and the bisector of the plane is good.

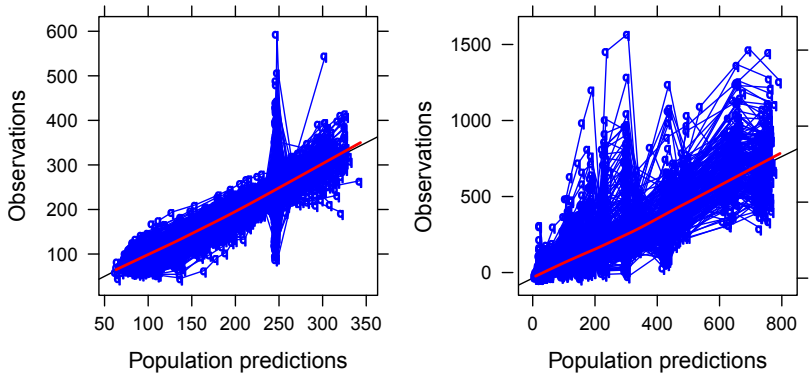

Figure 6.5: Scatterplots of the observation versus the glucose (left) and insulin (right) integrated model population predictions.

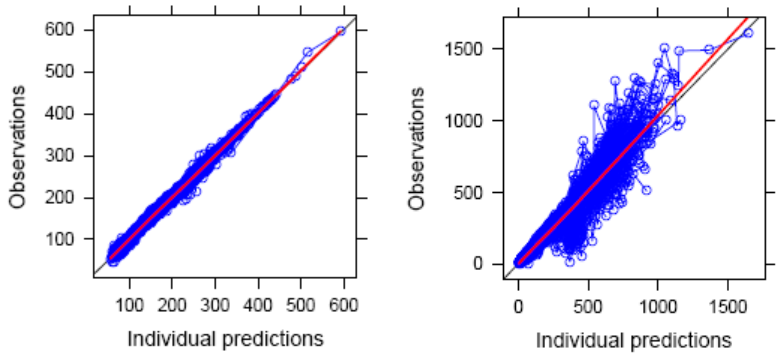

Figure 6.6: Scatterplots of the observation versus the glucose (left) and insulin (right) integrated model individual predictions.

In Fig. 6.7 and in Fig. 6.8 are presented the individual (absolute value) and the conditional weighted residuals of both the glucose and insulin signals. The fit is reasonably good if we consider the pattern and the amplitude of both the residuals. Looking at the glucose and insulin conditional weighted residuals we can see an opposite trend at the end of the experiment in the average line going respectively up for the glucose signal and down for the other signal. In Fig. 6.9 is presented the individual (red line) and the

population (blue dashed line) fit of some random subjects for both the insulin at the top of the figure and glucose at the bottom of the figure. In Tab. 6.3 are presented the

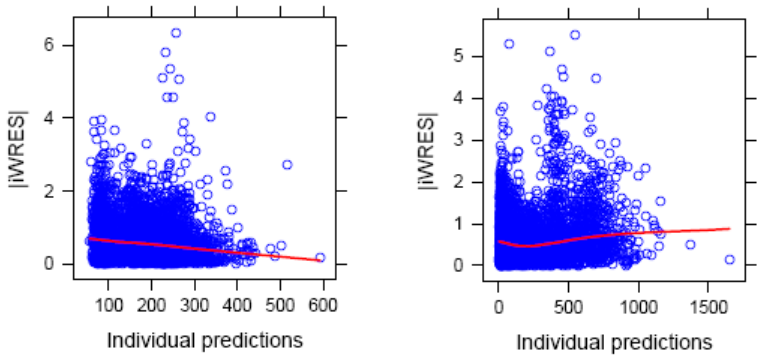

Figure 6.7: The absolute value of the glucose (on the left) and insulin (on the right) integrated model individual weighted residuals.

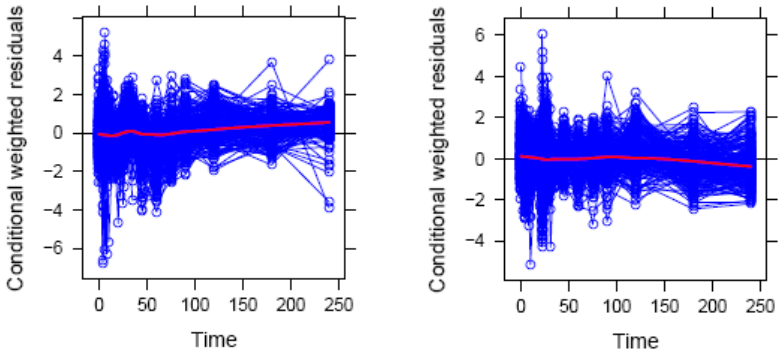

Figure 6.8: The integrated model glucose (on the left) and insulin (on the right) integrated model conditional weighted residuals.

integrated model population parameter estimates with their relative standard error. All the parameters are estimated with satisfactory precision apart from two correlations that due to their small value are poorly estimated.

In Fig. 6.10 is presented the VPC of the glucose and the insulin profiles.The graph yields that the model is able to catch the data variability as the CI of the percentiles of the simulated profiles are on the whole able to follow the percentiles of the observed data.

In order to deal with the clear trend that is present in the conditional weighted residuals at the end of the experiment we tried to model the basal levels of glucose and insulin with a very simple and raw model but at the same time efficacious: a line model.

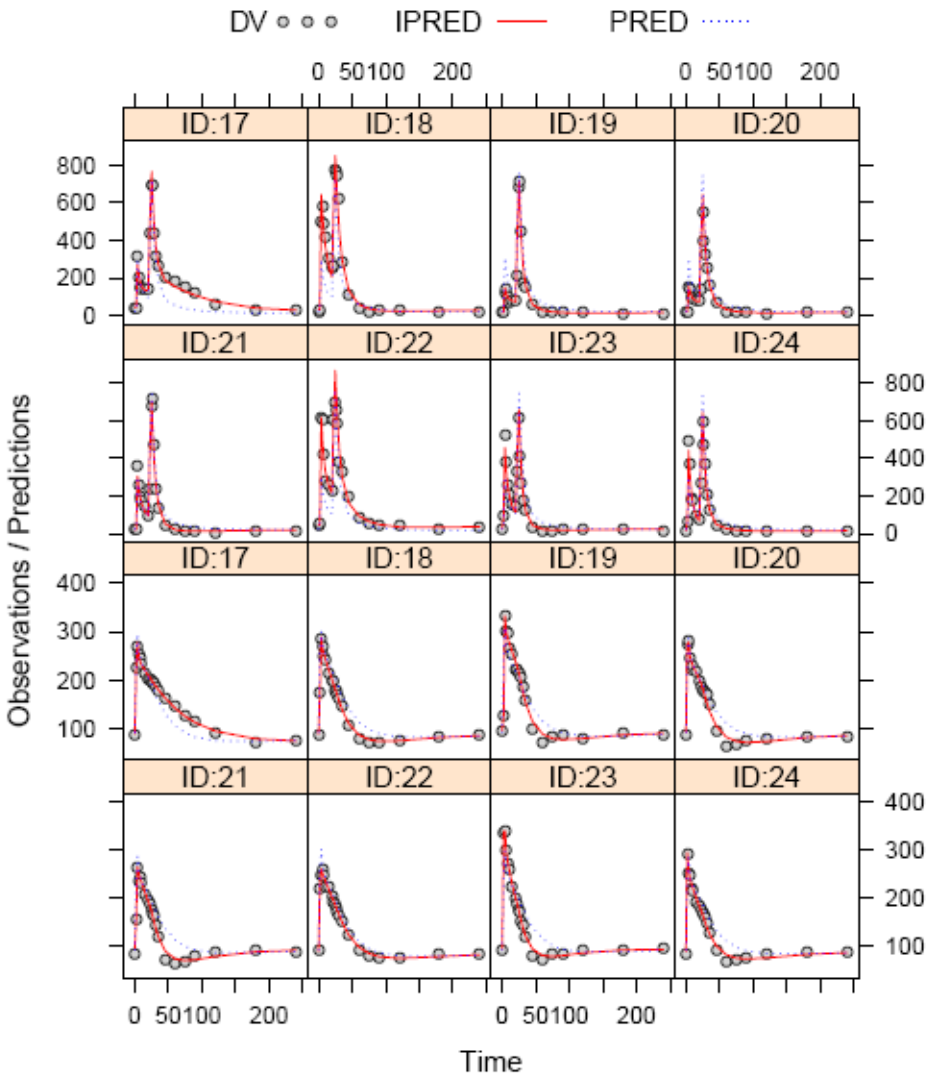

Figure 6.9: Insulin (top figure) and glucose (bottom part of the figure) individual profiles. Individual prediction (red line) and population prediction (blue dashed line) versus time for some randomly selected subjects. Dots represent the observed concentration.

		integrated model				integrated model	
Model parameters	Units	population estimates	RSE %	Model parameters	Units	population estimates	RSE %
Fixed Effects				*Random Effects*			
Cl_{S_G}		2.33	2.40%	Interindividual Variability			
V	dl	75	3.00%	ωcl_{S_G}		16.10%	14.70%
S_I	$min^{-1}\ pmol^{-1}\ l$	129	7.80%	ωV		20.70%	5.20%
p2	min^{-1}	0.0262	6.30%	ωS_I		59.70%	8.90%
ck_{t1}	dl/min	25.4	7.70%	$\omega P2$		42.80%	11.20%
V_2	dl	64.5	2.40%	$\omega \mathrm{cl}_{k1}$		58.70%	8.40%
MTT1	min	2.02	0.90%	V_2		15.20%	12.30%
n1	-	100	-	$\omega MTT1$		8.90%	7%
G_b	mg/dl	91.8	0.701%	ωh		5.60%	8.00%
X_0	pmol/l	357	8.70%	ωX_0		72.80%	6.30%
CL_n	l/min	1.56	2.40%	$\omega \mathrm{cl}_n$		19.30%	9.30%
V_I	l	9.74	1.70%	ωV_I		11.50%	13.40%
α	min^{-1}	0.128	10.50%	$\omega \alpha$		66.80%	15.20%
β	$min^{-1}dlmg^{-1}pmol^{-1}$	0.0902	6.80%	$\omega \beta$		43.60%	10.60%
MTT2	min	2.48	1.40%	MTT2		9.40%	15%
n2	-	200	-	$\omega \mathrm{clk}_2$		55.80%	16.40%
ck_2	l/min	0.139	11.20%	ωI_b		41.20%	6.10%
V_{I2}	l	5.59	13.60%	correlation P2-S_I		79%	9.85%
I_b	pmol/l	23.5	4.50%	correlation P2-cl_n		29.90%	44.15%
				correlation P2-I_b		-23.40%	51.28%
				correlation P2-β		-19.40%	62.89%
				correlation P2-α		65.80%	17.93%
Residual unknown variability				correlation S_I-cl_n		60.90%	12.38%
$\sigma_{propglu}$		0.0189	3.80%	correlation S_I-I_b		-63.70%	10.50%
σ_{addglu}		4.810	2.20%	correlation S_I-β		-61.40%	13.52%
$\sigma_{propinsu}$		0.189	1.10%	correlation S_I-α		31.30%	47.60%
$\sigma_{addinsu}$		0.847	31.60%	correlation cl_n-I_b		-59.60%	13.15%
				correlation cl_n-β		-29.30%	48.81%
				correlation cl_n-α		2.10%	766.67%
				correlation I_b-β		87.40%	5.88%
				correlation I_b-α		0.60%	2066.67%
				correlation β-α		19.60%	84.69%
				correlation G_b-X_0		-56.70%	14.96%
				correlation MTT1-MTT2		66.60%	13.11%

Table 6.3: Summary of the parameter estimates obtained in the integrated model. Typical values for parameters are in original units. Given that between-subject variability is modeled as log normal, variance measures are reported as approximate coefficients of variation (CV), whereas the covariance terms are in terms of correlation.

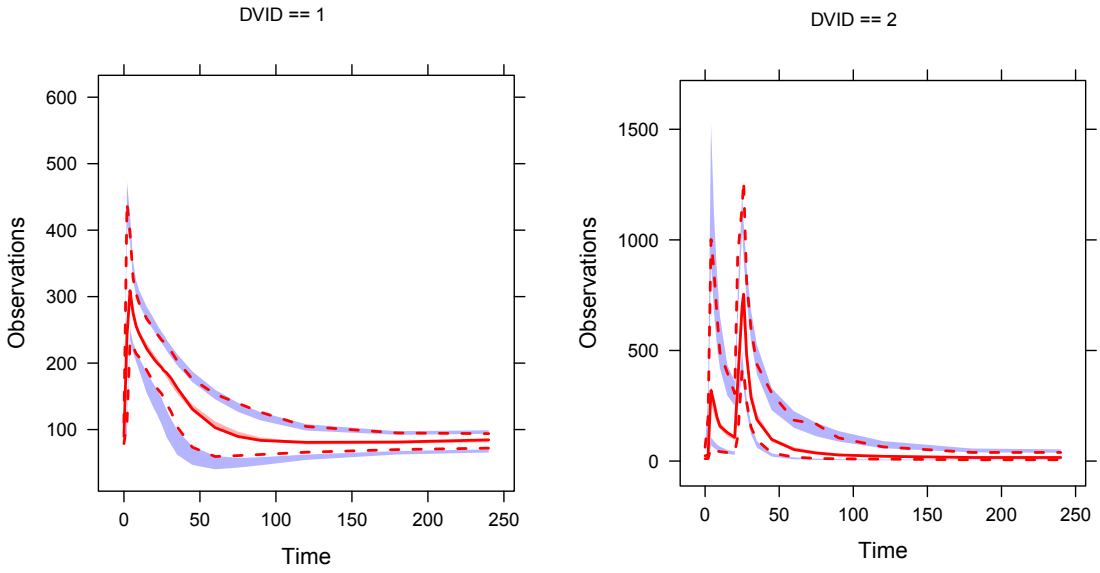

Figure 6.10: The stratified VPC of the integrated model: glucose profiles(on the left) and insulin profiles (on the right).

In particular we introduced two more parameters, the two slopes of the line models (glucose and insulin), to the integrated model formulation. Note that the basal level are the corresponding line intercepts. The trend in the residuals with this expedient disappears as we can see in Fig. 6.11 and the drop of function due to the two parameters introduction is statistically significant (around 25 points).

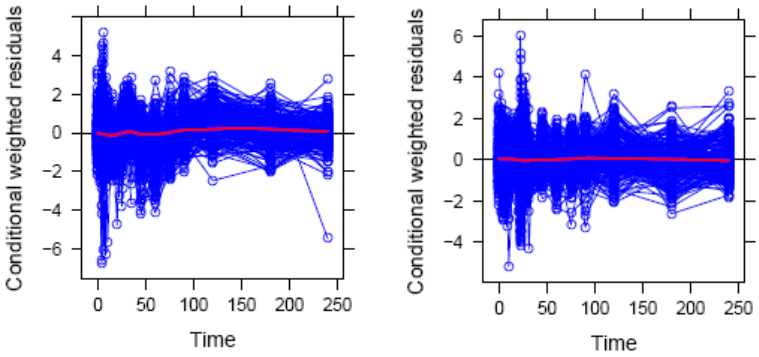

Figure 6.11: The conditional weighted residuals of glucose (on the left) and insulin (on the right) of the integrated model with baseline modeled as a line.

6.4 Discussion

Before integrating the insulin and glucose subsystems we decided to optimize the two models on their own. Note that with optimization we intend the process of model building exploiting the population approach that is a different context then from the individual approach where these models were first built. The GMM was refined in chapter 4 whereas the IMM was implemented from a population point of view in this chapter.
As far as the IMM is concerned we did some changes in the model structure with respect to the previously published insulin model [21]. In particular we added a delay term through a transit model [41] consistently with the IVGTT C-cpeptide minimal model to describe the delay of the insulin first secretion due to the glucose signal. Then we added a second compartment that is a non accessible pool of insulin. The second compartment meaning might be explained physiologically through a temporary binding of the insulin hormone with its receptor as it is modeled in Wanant et al [54]. This binding step marks the beginning of the insulin signaling pathways that will lead to mediate the glucose uptake and metabolism. Finally we deleted from the original model formulation the compartment of the insulin amount in β-cell. Note that no straight proper comparison about the model structure can be made with the C-peptide minimal model (CMM) although in the IMM was introduced similarly a delay term. In fact, firstly the IMM has a protocol enriched with the insulin injection that enables a better parameters estimation (the insulin disappearance) and the CMM does not. Secondly the CMM kinetics between the two main compartments are fixed to prior knowledge [20] and the IMM kinetics are not.The last step of the IMM analysis is the introduction of the covariates in the clearance and volume parameters following the allometric scaling theory in order to reduce the parameters variability. With these changes in the model structure the IMM is able to catch the insulin kinetic in a satisfactory way at both individual and population levels as the model fit and residuals show (Fig. 6.1, 6.2, 6.3). The VPC analysis (Fig. 6.4) brings to the same conclusions: the model is able to describe the data variability as the CIs of the simulated percentiles follow the percentiles of the observed data. These results allow us to finally move towards the integration of the GMM with the IMM.
Although the big number of parameters the integrated model is able to estimates all the parameters and to allow the calculation of the covariance step. In this way all the precision of the estimates are present without the need to resort to any bootstrap. Is important to note that the parameters, in particular the fixed effects, do not deviate dramatically from the estimates obtained in the two separated subsystems meaning again that the new integrated model formulation is stable. The reduction of the matrix was necessary to furtherly stabilize the model estimation. To exclude the covariance terms

first a model with a full matrix was run and only the more relevant terms were kept in the final model. Both the glucose and insulin are fitted well as we can see from the plots (Fig. 6.6, 6.5) and from the residuals (Fig. 6.7, 6.8). With respect to the fit obtained with the two separated subsystems, the integrated model performance seems to behave better. Looking for example at the integrated GMM conditional results with respect to the results obtained in the GMM standalone, we can see that the conditional weighted residuals are smaller and that the population prediction versus the observed data are more centered with the bisector of the plane. Moreover the parameters BSV decreases in the integrated model meaning that the parameters are less variable in the parameter space. This is due to the fact that the model has increased its degree of flexibility (e.g. the glucose basal now is modeled) and that the covariance matrix gives the possibility at the two part of the system to interact in a proper way. The VPC of the integrated model underlines the model capability of describing the variability in the observed data. With respect to the VPCs of the corresponding minimal models implemented as separated subsytems (see Fig. 4.8, 6.4)there is a clear improvement in the integrated model VPC. In this case in fact the model is able to simulate both the glucose and the insulin kynetics without the need of using forcing functions that might be misleading during the simulation step of the VPC [44]. Finally is interesting to note the opposite trend in the conditional weighted residuals in the glucose and insulin fit at the end of the experiment that can be fixed modeling the insulin and glucose basal levels. In fact the basal levels at time 0 with respect to the levels at time 240 are systematically lower in the subjects and taking into consideration this feature clearly prevent the trend in the residuals (Fig. 6.11). The physiological reasons for this lowering of the basal levels needs to be investigated furtherly but might be due to the fact that the patient is without food for the following four hours after the glucose intake or that maybe is hydratate during the experiment.

6.5 Conclusions

In this study we propose an integrated model to study the insulin and glucose system exploiting the NLMEM potentials. We come up with a model that is able to describe the glucose and insulin kinetics at the same time without using Bayesian a priori information and without the need of dividing the system in two subsystems for identifiability reason. Moreover we add some modeling part that improved the model performance. We started from optimizing separately the glucose and insulin minimal model and once this is done we integrated the two. In this way we achieved a model that is able to simulate both the

profiles without using forcing functions. The simulation step then is not dependent on any observed data and is achievable simply knowing the population parameter distribution and the measurement error. Moreover we came up with a complete characterization of a healthy population parameter distribution during an IVGTT.

The MTT glucose minimal model on a synthetic dataset

7.1 Introduction

The glucose-insulin regulatory system can be investigated by fitting an adequate mathematical model to data obtained following intravenous injection of a bolus of glucose, e.g. during an intravenous glucose tolerance test (IVGTT) or after ingestion of glucose, e.g. an oral glucose tolerance test (OGTT), or a mixed meal tolerance test (MTT). Between the three different tolerance tests, the oral MTT perturbations are no doubt more physiological as they are closer to mimic the usual modality and pathway to introduce a glucose perturbation in the human body. However, MTT data require a more complex mathematical model than IVGTT ones since the quantification of insulin action during an oral protocol requires assessment of the systemic rate of appearance of the ingested glucose. In particular, from MTT data, the model presented in [22] is widely used to estimate insulin sensitivity (SI), i.e. one important metabolic index used in clinical and epidemiological studies of diabetes and hyperglycemia, and the rate of appearance of the glucose time curve (Ra_{meal}) (see reviews [12, 55]). This model requires the estimation of eleven parameters, seven of which are used to describe the Ra_{meal} through a piecewise linear model (PL). In this chapter we propose some new formulations

of Ra_{meal} that will be compared to the well established PL. In particular, our effort is to find a parametric function capable not only to perform comparably to the PL description but also to be more conservative in terms of number of parameters. This because mainly of the computational time burden and feasibility in the implementation. In data rich pathophysiological studies the oral glucose minimal model (OGMM) is identified by weighted nonlinear Least Squares (WNLS) applied on each single subject experimental data. However in epidemiological studies, usually a data poor context, it is important to estimate the parameters from the population data, though is useful to obtain the description of the parameter distribution across the population. Here we exploit the potential of the nonlinear mixed effects modeling (NLMEM) techniques [29] to identify the OGMM and characterize a healthy population that underwent an MTT. Denti et al [2] already explored the advantages of population technique analyzing the glucose minimal model after an intravenous injection of glucose. This article faces a more challenging problem: describe a less controlled test as the MTT with a more complex model that characterize both the glucose and the Ra_{meal} profiles. The population approach allows borrowing information across all subjects simultaneously, quantifying population features directly and subsequently deriving individual parameter estimates. In this way the WNLS parameter numerical unidentifiability due to sparse data (few and noisy data per individual) can be circumscribed by resorting to the population knowledge that creates a prior that facilitate the estimation process. In the NLMEM technique the individual parameter is seen as a realization of a distribution that is characterized by a typical value, the fixed effect, that is common to the entire population and by a certain variability, the between subject variability (BSV), that explains the spread of the parameter individual values among the population. Moreover in the NLMEM not only the parameter but also the error, the residual unknown error (RUV), is modeled as a realization of a normal distribution with zero mean. In this work we put into competition four different models that describe the Ra_{meal} coupled with the minimal glucose model and then select the best which simultaneously well describes the glucose data and Ra_{meal} and gives reliable SI estimates. The rationale for this is that the PL has seven parameters. From a NLMEM point of view, this is translated in the possible identification of both the fixed effect and the random effect for each parameter which turns out to be a very time consuming task and if the dataset is very sparse or even noisy the numerical identification might be not successful because of overparameterization.

7.2 Material and methods

Synthetic Data

The database consists of 144 synthetic nondiabetic subjects that were generated using Dalla Man et al [56, 57, 58] healthy state MTT simulator. In particular, starting from the 204 nondiabetic subjects [52] (118 M /86 F, mean age 55.53±21.66 mean BMI 26.62±3.39 kg/m2) that underwent an MTT at the Clinical Research Center Mayo Clinic, Rochester, MN, USA, the parameters of the joint probability distribution of the meal model were reconstructed. From this joint probability, virtual subjects can be generated simply by randomly sampling from the multivariate normal distribution and by adding on top some measurement error. Simulated plasma samples are available at -120, -30, -20, -10, 0, 5, 10, 15, 20, 30, 40, 50, 60, 75, 90, 120, 150, 180, 210, 240, 260, 280, 300, 360, 420 min for glucose, insulin and C-peptide concentrations with an MTT glucose dose of 1 ± 0.02 g/kg. Moreover also the Ra_{meal} flux is available.

Oral glucose minimal model (OGMM)

The model proposed by Dalla Man et al [22] is an extension of the classical IVGTT glucose minimal model [17] by coupling to it a parametric function that describes the glucose rate of appearance in plasma. The OGMM is described by:

$$\begin{aligned} Q'(t) &= -(S_G + X(t)) \cdot Q(t) + S_G \cdot Q_b + Ra_{meal}(\mathbf{p}, t) \qquad Q(0) = G_b \cdot V \\ X'(t) &= -p2 \cdot X(t) + p2 \cdot S_I \cdot (I(t) - I_b) \qquad X(0) = 0 \end{aligned} \tag{7.1}$$

where Q (mg/kg) is the glucose mass in plasma and Q_b (mg/kg) its basal value, G_b (mg/dl) is the basal glucose concentration in plasma, I (μ U/ml) is insulin plasma concentration and I_b (μU/ml) its basal value, X (min^{-1}) is insulin action, Ra (mg/kg $\cdot$ min) is the glucose unknown rate of appearance in plasma, V (dl/kg) is the volume distribution, S_G (min^{-1}) is glucose effectiveness, S_I (min^{-1} μU^{-1} ml) is insulin sensitivity and p2 (min^{-1}) is an insulin action parameter. Note that Ra_{meal} is a parametric function expressed as dependent of a vector of unknown parameters $\mathbf{p}$; the number of parameters depends on the parametric function chosen.

Note that the OGMM was also identified on its own by substituting in place of a parametric model the Ra_{meal} synthetic known flux. In this way the *reference estimates* (REF) of the parameters S_G, V, S_I and p2 were obtained.

Rate of appearance models

In total four models with different number of parameters and complexity were evaluated.

These models were identified also on their own using the synthetic Ra_{meal} data to obtain the *reference estimates* (REF) for the parameters of the four models.

1. *Piecewise Linear model (PL)*
   Ra_{meal} is described by a piecewise-linear function with a given number of breakpoints. In particular, they were more concentrated at the first part of the experiment where the signal varies more rapidly and more sparsely afterwards. The breakpoints chosen are at 0, 10, 30, 50, 90, 120, 180 and 420 min. The expression for Ra_{meal} is thus:
   $$Ra_{meal}(\mathbf{p},t) = \begin{cases} \alpha_{i-1} + \frac{\alpha_i - \alpha_{i-1}}{t_i - t_{i-1}} \cdot (t - t_{i-1}), & \text{if } t_{i-1} \leq t \leq t_i \\ 0, & \text{otherwise} \end{cases} \tag{7.2}$$
   where α_i are the unknown parameters and t_i are the breakpoints. Note that α_2 is was not estimated but derived using the following constraint on the area under the curve of Ra_{meal}:
   $$\int_0^\infty Ra_{meal}(\mathbf{p},t)\,dt = \frac{dose \cdot f}{BW} \tag{7.3}$$
   where dose is the dose expressed in mg, f is the fraction of the ingested dose (fixed to 0.9) and BW (kg) is the subject weight.

2. *Double exponential (DE)*
   This model is described by a rising and a falling curve. This model does not have predefined breakpoints and it has just two unknown parameters: α, the rate of the decaying exponential (the second part of Ra_{meal}) and β, the rate of the rising exponential (first part of the curve Ra_{meal}). Ra_{meal} is given by:
   $$Ra_{meal}(\mathbf{p},t) = D(\alpha+\beta)\frac{\alpha}{\beta}\left[e^{-\alpha t}(1-e^{-\beta t})\right] \tag{7.4}$$
   where α and β are the unknown parameters and D (mg/kg) is the MTT glucose dose.

3. *the lagtime model(LAG)*
   This model is derived from Nerella et al [59] where the absorption phase is modeled taking into account a delay. Ra_{meal} is described as follows:
   $$Ra_{meal}(\mathbf{p},t) = \frac{D \cdot K_a \cdot K_{el}}{K_a - K_{el}}\left[e^{-K_{el}\cdot(t-t_{lag})} - e^{-K_a\cdot(t-t_{lag})}\right] \tag{7.5}$$
   where K_{el} and K_a are the unknown parameters that describe respectively the falling and the rising parts of the Ra_{meal} curve, t_{lag} is the unknown parameter that

represents the delay in the absorption of glucose and D (mg/kg) is the MTT glucose dose. Note that, if the delay parameter is not considered in Eq. 7.5, Rameal corresponds to the leaving flux of the second compartment of a two compartments model that has a first compartment with a costant rate Ka and a dose injection D and a second compartment with a constant elimination rate Kel.

4. *The Mix Piecewise and Exponential model (LAG)*
   The fourth model is a combination of the piecewise linear model and a decreasing exponential. There are two absorption phases: the first more rapid that produces the peak of the curve and the second slower that contributes to the tail of the curve. In order to better describe the first part of the curve a piecewise linear model was chosen. Five breakpoints were used at the following time: 0, 20, 30, 40 and 50 min. They were more concentrated with the first points of the curve. To describe the second part of the curve a decreasing exponential was chosen. Ra_{meal} is given by:

$$Ra_{meal}(\mathbf{p},t) = \begin{cases} \alpha_{i-1} + \frac{\alpha_i - \alpha_{i-1}}{t_i - t_{i-1}} \cdot (t - t_{i-1}), & \text{if } t_{i-1} \leq t \leq t_i \ i = 1, ..., 4 \\ B \cdot e^{-\beta t}, & \text{otherwise} \end{cases} \tag{7.6}$$

   where α_1 , α_2 , α_3 and α_4 are the unknown parameters relative to the piecewise model and β is the unknown parameters of the exponential model. Note that B is constrained to be equal to $B = \frac{\alpha_4}{e^{-\beta \cdot 50}}$.

Nonlinear mixed effects modeling

Nonlinear mixed effects models (NLMEM) are able to quantify both the population and the individual parameters and identify by a hierarchical approach the biological sources of intra-individual and inter-individual variability. More specifically, in a first step, the data are described by:

$$y_{ij} = f(\mathbf{p}_i, x_{ij}) + \epsilon_{ij} \qquad 1 \leq i \leq m \qquad 1 \leq j \leq n_i \tag{7.7}$$

where y_{ij} are is the jth observation (in our case glucose concentration) of the ith subject at some known time instant x_{ij}. Here, m is the number of individuals and n_i is the number of observation of individual i. Pi is the vector of model parameters of the ith individual. The variability due to measurement and model errors, better known as the residual unknown variability (RUV), is explained through ϵ_{ij} which is assumed to be independently distributed with a zero mean and Gaussian distribution:

$$\epsilon_{ij} = N(0, (\sigma y_{ij})^2) \tag{7.8}$$

The variance model is described as a proportional error model where σ is an additional parameter to estimate. In a second step, the model parameters are represented as function of some physiologically meaningful attributes that do not vary across the population ($\boldsymbol{\theta}$, fixed effects, i.e. values that are common to all subjects) and some others that do ($\boldsymbol{\eta}_i$, random effects, i.e. values typical of a specific subject). In our model we chose the function:

$$p_{ki} = \theta_k e^{\eta_{ki}} \tag{7.9}$$

where p_{ki} is the kth model parameter of the ith subject, θ_k is the typical value of the kth parameter common to the entire population and η_{ki} is the random effect of the kth model parameter of the ith subject. The random effect $\boldsymbol{\eta}_i$ are assumed to be independently distributed with a zero mean and Gaussian distribution:

$$\boldsymbol{\eta}_i \sim N(0, \boldsymbol{\Omega}) \tag{7.10}$$

with $\boldsymbol{\Omega}$ being a positive definite diagonal covariance matrix. With this formulation the second stage of variability, better known as Between-Subject Variability (BSV), is explained. The omega set up for all the models implementation was diagonal. Moreover the PL final omega set up was further reduced since $\boldsymbol{\eta}$ relative to $\boldsymbol{\alpha}_4$ and to $\boldsymbol{\alpha}_5$ were negligible. This was dataset dependent. We suggest to test all the variability in each $\boldsymbol{\eta}$ before removing any term. To obtain the population parameters the joint likelihood function is maximized. Because of the computational nonfeasibility of the exact solution, different approximations are proposed. Here, on the basis also of the results obtained in chapter 3 and in Denti et al [2], we used the First Order Conditional Estimation (FOCE) approximation with INTERACTION implemented in NONMEM 7.2.0 [29]. The estimation process was facilitated with the introduction of some priors in the parameters S_G, V and p2 that were fixed to their population values respectively LN(0.0055,1.76), LN(2.03,0.0115) and LN(0.0111,0.273). For further information see the appendix.

Performance indices

In order to compare the four different OGMM Ra_{meal} parametric model coupling performances, the NLMEM approach potentials were exploited by analyzing both the individual and the population results.

As far as the individual information is concerned, the following aspects were considered: the whiteness of the individual weighted residuals, the Ra_{meal} individual prediction, the Akaike Criterion (AIC=WRSS+2M where M is the number of parameters), the individual estimates and their precisions. The Ra_{meal} individual prediction was evaluated by

comparing the medians of the pharmacokinetics descriptors calculated on the individual predictions (peak, time to peak, half-life and AUC) with the median of the descriptors calculated on the synthetic data curves. The individual estimates S_G, Vol, S_I and p2 were evaluated by comparing them with the REF individual estimates. In particular was compared the median of the relative deviations of the individual estimates from the REF individual estimated parameters. The relative deviations were calculated in the following way:

$$\delta p = \frac{(p_{REF} - p_{EST})}{p_{EST}} \tag{7.11}$$

As far as the Ra_{meal} individual estimates are concerned it was decided for comparison reason among the four Ra_{meal} models coupled with the OGMM to average for each model the absolute values of the medians of the relative individual deviations of the Ra_{meal} parameters from the REF estimates. Note that the REF estimates of the Ra_{meal} parameters were obtained fitting the models on only the Ra_{meal} synthetic data. In addition the individual estimates were compared to the reference values by Pearson correlation analysis.

As far as the population is concerned, the following aspects were taken into consideration using either the population predictions or the population estimates: the whiteness of the population weighted residuals calculated using the population predictions, the population Bayesian information Criterion (BIC), the Ra_{meal} population prediction, the population estimates and their precision and finally the RUV. To evaluate the population estimates it was considered the relative deviations of the population estimated parameters from the population REF estimates as in Eq. 7.11. Note that the analysis focus on S_I and not on S_G, V and p2, because it is the only parameter, except from the Ra_{meal} population parameters, that is free to vary in the parameter space whereas the others are fixed to their prior value. Note that for comparison reason among the four Ra_{meal} models coupled with the OGMM were averaged for each model the absolute values of the relative deviations of the Ra population parameters. Note that the REF values for the Ra_{meal} parameters of each of the four model were obtained fitting the four models on only the Ra_{meal} synthetic data. To evaluate the Ra_{meal} population prediction the root of the sum of the squared residuals (RRSS) was taken into consideration. In the following formula the RRSS for subjects i=1,..,m with samples j=1,...,n_i of the i-th subject were evaluated:

$$RSSS = \sqrt{\sum_{i=1}^{m}\sum_{j=1}^{n_i}(Ra_{ij} - Ra_{ij}(j, \mathbf{p}))^2} \tag{7.12}$$

Note that since the measurement error is equal for all the four couplings model, the RUV estimate assume the meaning of a measure of the model misspecifications.

7.3 Results

All the analysis were carried out using the software NONMEM 7.2.0 [29]. All the run minimized successfully with their own covariance step and the estimated parameter observed the imposed distribution. The histograms of the logarithm of the individual REF estimates are presented in Fig. 7.1: the gaussianity of the distributions is respected.

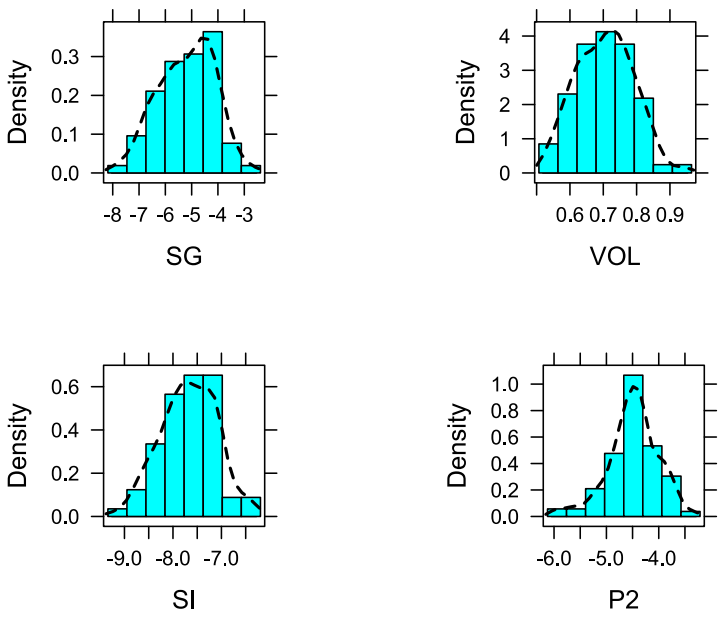

Figure 7.1: Histograms of the logarithm of the individual REF estimates

Individual results

1. *Model fit*
   The goodness of the model fit was evaluated by inspection of the weighted individual residuals obtained from each subject and after averaged. Fig. 7.2 shows the average of the weighed individual residuals and the standard deviation for the four rate

of appearance Ra_{meal} models in the 0-240 min time interval where the signal varies the most. All the four models present a reasonably good fit: the average individual weighted residuals did not show systematic deviations from zero even if they were not always within the range [-1 +1]. On the basis of the AIC, the most parsimonious model is the OGMM coupled with the DE (median AIC value 24.05) and immediately after the OGMM with the LAG (median AIC value 28.054) whereas the OGMM coupled with PL and MPLE clearly underperform (median AIC value of respectively 44.02 and 36.03).

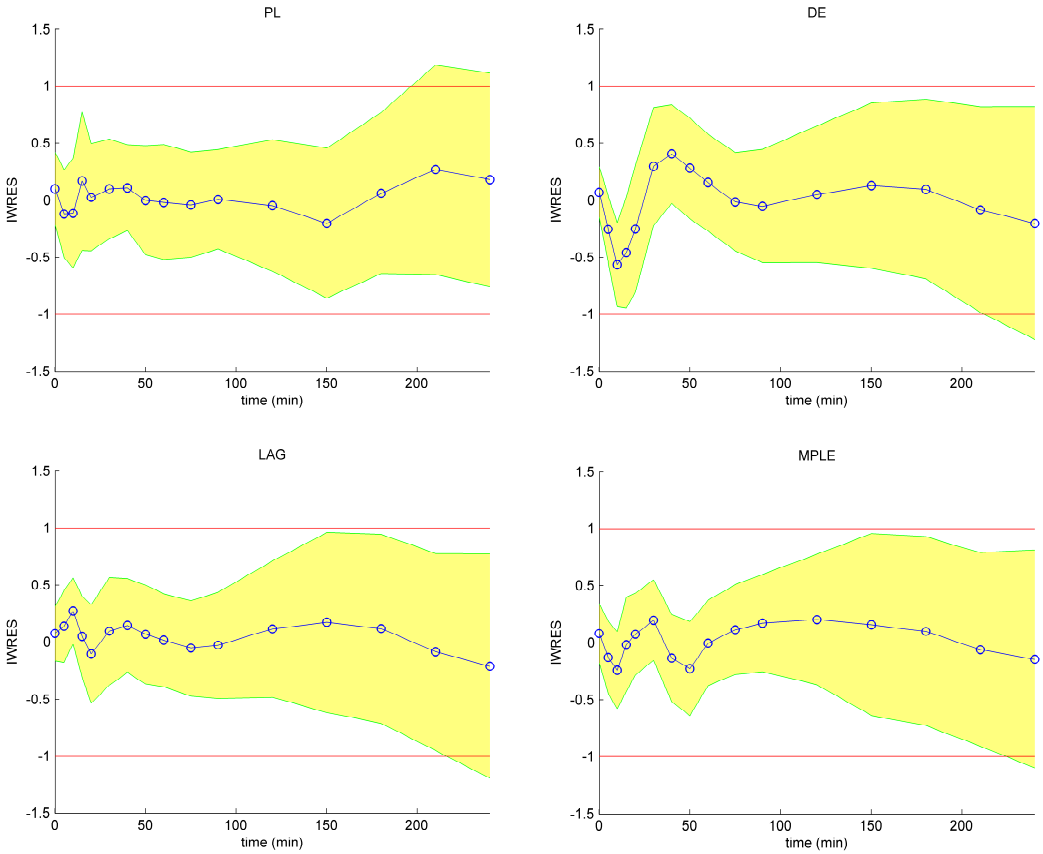

Figure 7.2: Mean (blue line) ± standard deviation of individual glucose weighted residuals in the 0-240 time interval.

2. *Ra_{meal} individual prediction*

   The individual predicted rate of appearance kinetics has been summed up by four features, i.e. the value of the peak, the time to peak, the half-life and the area under the curve (AUC). In Tab. 7.1 the medians of these indexes for each model are reported together with the median reference values (REF) obtained from the

synthetic Ra_{meal} data.

model	*cmax [mg kg^{-1} min^{-1}]*	*tmax [min]*	*t 1/2 [min]*	*AUC*
REF	7.68	30	89	962.46
PL	6.99	20	107	1004.30
DE	5.63	40	162.5	1022.72
LAG	6.31	20	139.5	1021.96
MPLE	6.72	30	52.5	795.87

Table 7.1: Medians of some pharamcokinetic indexes for each Ra_{meal} model calculated on the predicted kinetics and on the Ra_{meal} synthetic data.

From the results the best performances is when the OGMM is matched with the PL. The OGMM coupled with the MPLE and the OGMM with the LAG model performance is comparable. Instead the worst characterization is from the OGMM coupled with the DE that is not able to describe the kinetics of the curve.

3. *Individual estimates and their precision*
The medians of the relative deviations of the individual estimates from the REF individual estimates for the four OGMM parameters (S_G, V, S_I, p2) are presented as percentages in Tab. 7.2. In the same table are presented also the averaged values of the medians of relative deviations of the parameters for each Ra_{meal} model. The OGMM matched with the LAG is the couple that performs better in average. Moreover in Fig. 7.3 are shown the correlation plots between the S_I REF estimates and the S_I individual estimates obtained with the OGMM coupled with four Ra_{meal} models. The OGMM coupled with DE seems to perform slightly better than the LAG and PL ($R_{DE} = 0.92$, $R_{LAG} = 0.91$, $R_{PL} = 0.91$ p < 0.01). The OMM coupled with the MPLE perform the worst ($R_{MPLE} = 0.85$) but still has an acceptable value.

model	Δ S_G	Δ V	Δ S_I	Δ *p2*	Δ *Ra*
PL	4.24%	-0.98%	-10.96%	17.37%	7.77%
DE	13.13%	0.40%	-12.35%	-1.51%	15.48%
LAG	6.47%	-0.98%	-7.88%	-0.87%	21.32%
MPLE	37.87%	0.17%	7.35%	8.44%	14.81%

Table 7.2: Medians of the relative deviations of the individual estimates from the REF estimates.

Remembering that Vol, S_G and p2 are parameters constrained to the prior information while S_I is not, the parameter that is estimated in all the models with more

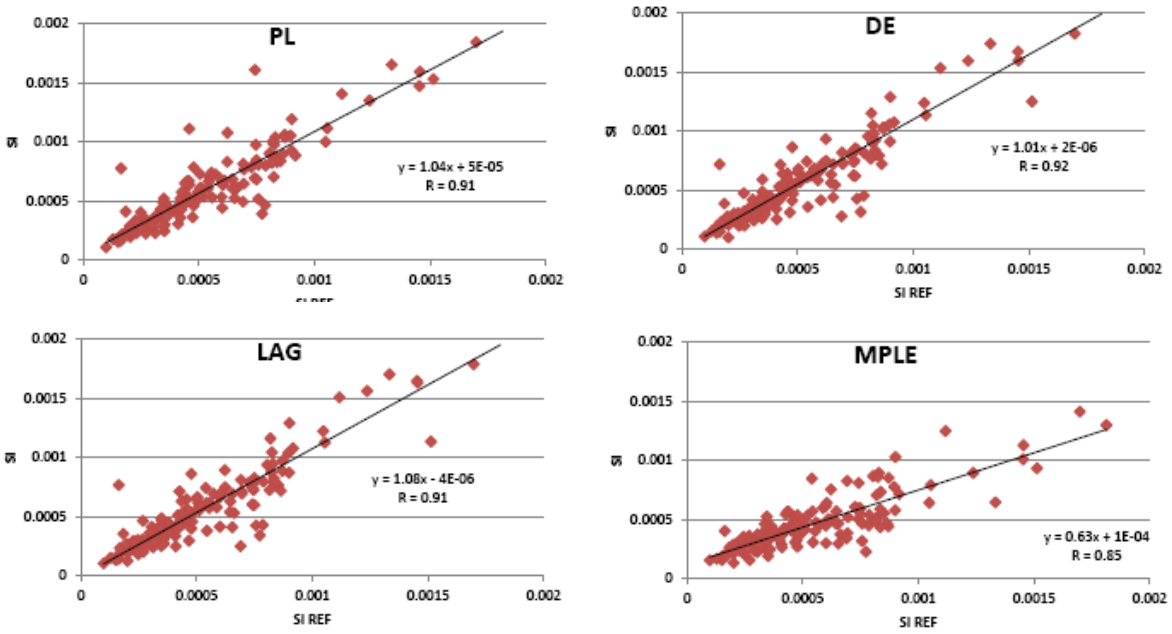

Figure 7.3: Correlation plots between the REF individual SI estimates and the individual SI estimates obtained with the four Ra_{meal} models coupled with the OGMM.

precision is Vol with median values of coefficient of variation (CV) around 10%. S_G is the most poorly estimated parameter and PL and LAG models seem to estimate it with more precision than the other models (73-74%). S_I and p2 are estimated with highest precision in the LAG with median CV respectively equal to 15% and 20% and with little less precision in DE and PL (median values respectively of 17% and 20% and for PL 17% and 23%). The median CV of the Ra_{meal} parameters were averaged in each of the four Ra_{meal} models to compare their performance. The CV averaged values of the four models are all in all comparable ranging from a 28% of both the LAG and the DE parameters to a 40% of the MPLE parameters.

Population results

1. *Model fit*

   The ability of the model OGMM to fit when different rate of appearance models are assumed was evaluated by BIC and by inspection of the population weighted residuals. Fig. 7.4 shows the mean and the standard deviation of the population weighed residuals in a time interval of 0-240 min where the signal varies the most. Note that the OGMM coupled with the PL has a different scale. All the four

models present a reasonably good fit: the population weighted residuals did not show systematic deviations from zero and the amplitude is relative small. As far as the BIC analysis is concerned the DE is the model that stands out with a BIC value of 30.61. The BIC for the LAG model is 37.15, while PL and MPLE instead perform worst with BIC values of respectively 62.96 and 49.78.

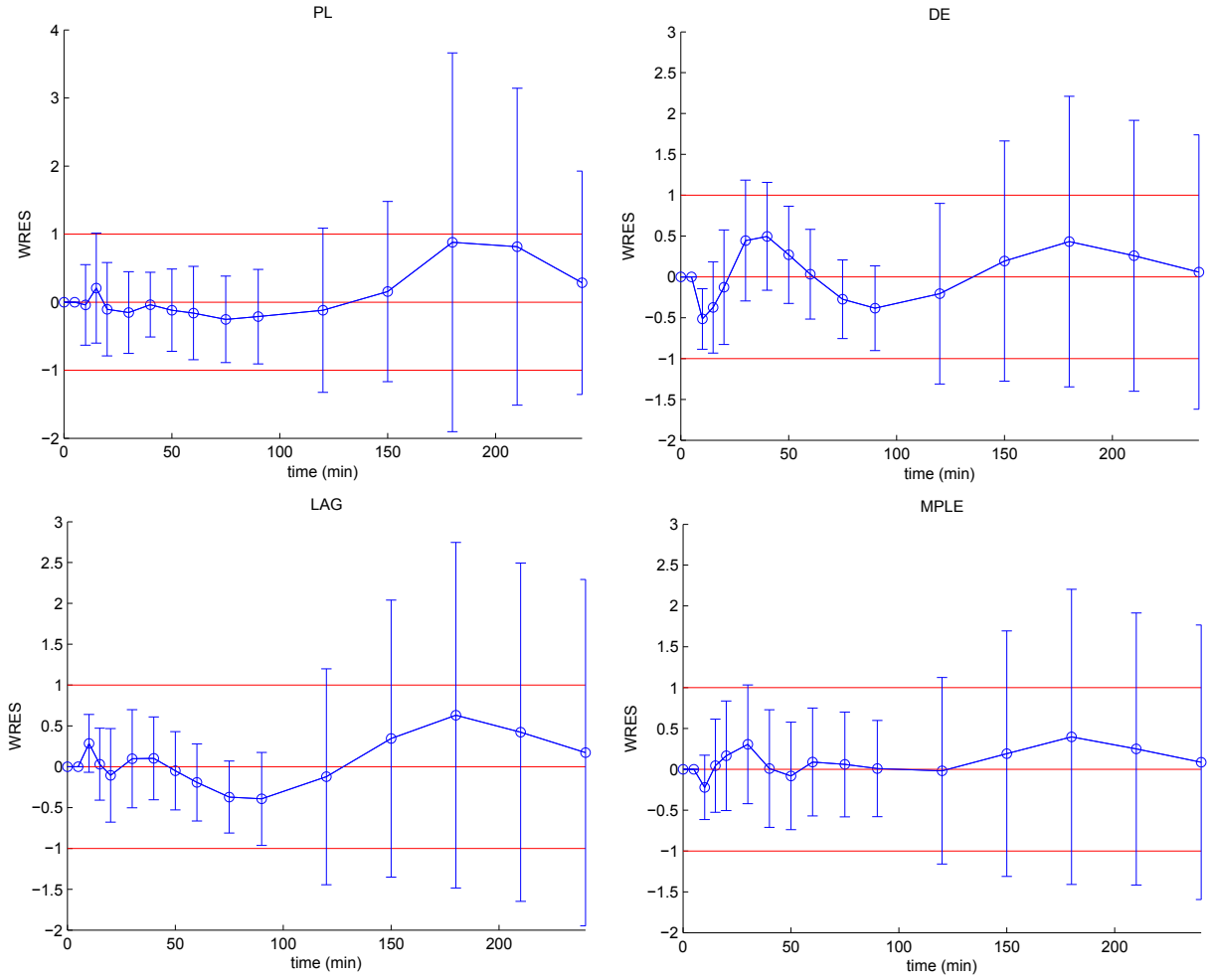

Figure 7.4: Mean ± standard deviation of population glucose weighted residuals in the 0-240 time interval.

2. *Rate of appearance model prediction*

   The rate of appearance prediction was evaluated by means of root of the sum squared residuals (RRSS) as explained in the performance indexes section (Eq. 7.12). The OGMM coupled with the LAG performs best with an RRSS of 64 whereas the OGMM with the PL, DE and MPLE have a RRSS of respectively 68,

69.5 and 71.2.

3. *Population estimates and their precision*

Tab. 7.3 shows the relative deviations reported as percentages of the S_I parameter and of the average of the absolute values of the population parameters for each Ra_{meal} model in terms of both the fixed effect (θ) and BSV (Ω) from the REF population estimates. The OGMM coupled with the DE behaves on the whole the best: both the S_I and the Ra parameters are close to their reference. The OGMM coupled with the LAG and with the MPLE behave the worst.

model	Δ S_I (θ)	Δ S_I (Ω)	Δ Ra_{meal} (θ)	Δ Ra_{meal} (Ω)
PL	-8.71%	0.29%	6.79%	84.82%
DE	-5.66%	-12.32%	13.90%	22.72%
LAG	-14.16%	-20.82%	24.02%	58.95%
MPLE	16.99%	7.04%	16.22%	142.87%

Table 7.3: The relative deviations of fixed effects ($\Delta\theta$) and random effects ($\Delta\Omega$) of the S_I and the Ra$_{meal}$*populationparameters*.

Tab. 7.4 shows the S_I estimate relative standard error (RSE) and the average of the population parameters RSE for each Ra_{meal} model in terms of both the fixed effects (θ) and the BSV (Ω). The OGMM coupled with the LAG model and with the DE produce estimate with the lowest relative standard error.

model	S_I (θ)	S_I (Ω)	Ra_{meal} (θ)	Ra_{meal} (Ω)
PL	5.2%	14.1%	7.5%	45.9%
DE	4.80%	13.1%	4.4%	22.7%
LAG	2.4%	14.9%	1.9%	26.3%
MPLE	5.3%	18.1%	7.3%	30.8%

Table 7.4: The S_I and the average Ra_{meal} RSE for both the fixed effects (θ) and random effects (Ω).

4. *RUV Evaluation*

As far as the RUV is concerned we present the estimated CV, the root of the RUV, in the four models. The model that has the smallest value and possibly less model specification is the PL (5.56%) model whereas the DE is the worst performing

model (7.96%). The MPLE and the LAG have a RUV of respectively 6.78% and 7.45%.

7.4 Discussion

OGMM requires to use as input function the rate of appearance of the meal dose into the plasma pool. This flux is not trivial to be measured and requires the use of the triple tracers technique [60]. A more attractive alternative is to use the OGMM with a parametric model in order to estimate not only the parameters of the OGMM but also the parameters that describe the rate of appearance. The present study attacks the problem of defining the best match between the OGMM and different rate of appearance parametric models. This implies finding the match that not only has the best fit glucose data but also has the best prediction of Ra_{meal} time curve and the best estimates of SI. Ideally the final choice should satisfies all these three criteria. Four different parametric models were detected to describe the Ra_{meal}: the PL, the DE, the LAG and the MPLE. First of all, it is interesting to discuss the peculiarity of each of these four models. The PL has the disadvantage of having seven unknown parameters that means estimating seven fixed effects and at least seven random effects. This large amount of parameters turns into very time consuming run and problems during the estimation step. The DE instead has the advantage of having just two unknown parameters that means a faster minimization step and a straightforward successful estimation. At the same time, the model fails to describe the Ra data as well as the others: the peak is always underestimated whereas the tail is always well modeled, see Tab. 7.1. The LAG model has the advantage to take into consideration the delay of the appearance of the glucose in plasma as it was done in [59]. But this positive characteristic turns into a disadvantage too: during the minimization process is frequently difficult to numerically identify the delay. In fact the gradients of the optimization function are usually high and this makes the model instable. Finally the mix of the piecewise and the exponential was thought to be the best compromise between the piecewise ability to describe the first part of the curve and the exponential decay ability to describe the tail of the curve. Merging this two models allows to have less parameters than the piecewise and so less problems during the minimization and the estimation step. Before looking at the individual analysis results, it is important to underline that the shrinkage analysis that it often used to evaluate the nonlinear individual mixed-effects results as written in Savic et al [37] is not reported since by fixing some parameters we introduced some known misspecifications to the original model. This turns into some relatively high shrinkage values (40%-50%) that

anyway do not invalidate the analysis but corroborate the importance of having the most correct priors as possible.

To sum up, from the *individual analysis*, we can conclude that there is not the best model but depending on the modeler purpose there is one or more option to choose. In particular, looking at the individual analysis, if the purpose is to model the glucose individual data the best choice would be the OGMM coupled with the LAG. In fact, as far as the weighted residuals are concerned the OGMM coupled with the DE behaves badly (there are some systematic deviation from zero) whereas the other three behaves comparably well. Looking at the AIC though, seems there is a difference in the remaining three: the LAG is the best choice. Considering the Ra description, the OGMM coupled with the PL seems to be the best performing model. Since the number of parameter is big the LAG is the best compromise for a good fit and with a parsimonious number of parameters whereas the DE model is not able to describe the kinetics of the curve. Looking at the individual parameters relative deviation from the REF values and at the individual estimates precision, the OGMM coupled with the LAG is the best choice. Looking at the individual description of the SI and its correlation with the REF estimates the best model is the OGMM coupled with the DE that precede the PL and the LAG model with an R_{DE} equal to 0.92 ($p < 0.01$).

Regarding the *population results*, if we consider the weighted residuals there is no model that performs better than the others whereas looking at the BIC criterion the best model is the DE. Regarding the Ra description the OGMM coupled with the LAG has the best performance. Considering the S_I and the Ra parameters population estimates and its deviation from the REF estimates the OGMM coupled with the DE model is the best performing model match. As far as the precision of the population estimates the OGMM coupled with the DE and the LAG, the parametric models with less parameters, have the RSE smaller than the other. The RUV, surprisingly, despite the possible overparameterization, has a smaller value with PL meaning that the model error present in PL is the smallest.

Finally in this chapter, we choose to do not present the VPC [43] analysis because of the inappropriateness of this test in models like the OGMM [44]. In the simulation step there are some observable mismatching between the observed and the simulated data. This can be assigned to the presence of one input function in the model (the insulin data) that when it comes to simulate from the population description does not interact properly with the individual realizations. In particular, there is no additional information in the model that can link the parameters distribution to the proper forcing function in order to obtain always reasonable physiological outputs (for more details see chapter 9). By

now what was done in this work was simply to avoid the use of this analysis as a tool to study the performance of the four different models.
To conclude if the aim of the study is to get the S_I individual estimates our suggestion is to use the OGMM coupled with the DE whereas if the aim is to get the description of the Ra or of the glucose level we suggest to use the OGMM coupled with the LAG.

7.5 Conclusions

In this study, a population PK analysis was performed on a glucose rich simulated dataset produced using the Dalla Man simulator [57, 58]. This work is the natural extension of Denti et al [3] as the potentials of NLMEM technique are exploited but this time in a more complex context such as the MTT to better characterize the glucose minimal model inter and intra subject variability. We relaborate Dalla man work [22] by testing four different models. The aim was to find a more parsimonious model than the already proposed PL model that can describe well the glucose and the Ra_{meal} data and that can give satisfactory S_I estimates. What comes up with this study is not an absolute best model but a good answer for each sub problems whether the question concerns a focus on the individual results or on the population results. Depending on the modeler purpose the choice can be one of the four models presented: the PL, the DE, the LAG and the MPLE coupled with OGMM. To describe the S_I individually the fastest and at the same easiest model to use would be the DE whereas to describe the Ra_{meal} kinetics both at the individual and at the population level the best model would be the OGMM coupled with the LAG. To describe individually the glucose data the OGMM coupled with the LAG performs well whereas at the population level the OGMM coupled with the DE is the best choice. To conclude, with this study, we characterize a healthy simulated population that underwent an MTT resulting in a illustration of the pros and cons of using different parametric model for Ra_{meal} description. This work paves the way to move from an in sylico context to a real one in order to describe a real healthy population adding the covariates information to characterize even better the estimates.

7.6 Appendix

The population priors for the parameter S_G, V and p2 were obtained in the following way. Firstly the population parameters S_G, V and p2 were estimated using the OGMM coupled with the Ra_{meal} known flux introduced as a forcing function. The distributions of these parameters are then used as prior knowledge to the a posteriori population identification of the OGMM coupled with the four parametric Ra_{meal} models. Note that

these priors are crucial for the numerical identification since they strongly influence the estimates.

The MTT C-peptide minimal model

8.1 Introduction

The C-peptide minimal model (CMM) during a meal tolerance test (MTT) [24] is a widely used tool to assess the pancreatic β-cell function. This is possible because insulin secretion can be inferred from plasma C-peptide since: 1) C-peptide is secreted equimolar with insulin, and 2) its extraction by the liver, at variance with insulin, is negligible. Moreover it has been proved [61] its applicability on a reduced sampling scheme that moves from a 21 samples protocol (7 hours) to a 7 samples one (2 hours). This result is particularly appealing for epidemiological studies and large scale clinical trials where the number of samples weight on the experiment expense. The CMM model so far has been estimated with the classical weighted nonlinear least square (WNLS) approach applied in each subject. Due to the complexity of the model, the parameters precision sometimes can become not satisfactory in "data poor" situations. In this optic it has been shown [2] that the nonlinear mixed effects modeling technique can improve the estimates with respect to the single subject technique not only in a rich data context but most of all in a reduced sampling scheme. The NLMEM assume the subject as a realization of the population and this assumption create a prior that improves the individual parameter estimation especially when the individual information per se is not enough to identify the parameter. The technique estimates both the individual and population parameters

by assuming two levels of variability: the variability within each subject (intra individual variability) due to model error or measurement error and the variability among the subjects (inter individual variability). In this article we exploit the NLMEM to identify the CMM in a rich and reduced protocol to characterize a healthy population. Moreover we test the robustness of the NLMEM technique on furtherly reduced protocols, firstly, by removing 25% and, then, by removing 50% of the original samples of the reduced protocol. Finally we compare the derived indexes of the pancreatic $\beta-$ cell function obtained in a healthy population with the indexes obtained in a prediabetic population and diabetic population.

8.2 Material and methods

Data

The healthy population data is formed by 203 nondiabetic subjects [52] (118 M /86 F, mean age 55.53 ± 21.66, mean weight 77.94 ± 13.24 kg) that underwent an MTT (10 kcal/kg, 45% carbohydrate, 15% protein and 40% fat) consisting of scrambled eggs, Canadian bacon, glucose Jell-O (containing 1.2 g/kg body weight dextrose) at the Clinical Research Center Mayo Clinic, Rochester, MN, USA. The pre diabetic population data are 44 subjects [62] (20 M/24 F, mean age 53.73±7.74, mean weight 91.01±18.4 kg) that underwent an MTT of scrambled eggs, 55 g Canadian bacon and Jell-O containing (75 g) at the Clinical Research Center Mayo Clinic, Rochester, MN, USA. The diabetic population instead is made up of 28 subjects (F/M mean age 55.±.4, mean weight 93.73±17.04 kg) twelve of which [63] received an MTT of scrambled eggs, Canadian bacon, 100 ml water, and Jell-O (1.2 g/kg body weight of glucose) and the other twelve [64] an MTT of scrambled eggs, 55g of Canadian bacon, 240 ml of water, and Jell-O containing 75 g glucose. All the patients were sampled at the Clinical Research Center Mayo Clinic, Rochester, MN, USA. Plasma samples were all collected at 0, 5, 10, 15, 20, 30, 40, 50, 60, 75, 90, 120, 150, 180, 210, 240, 260, 280, 300, 360, 420 minutes and plasma glucose, insulin and C-peptide were measured apart from the prediabetic dataset that did not have samples at minute 260 and 420 and the diabetic dataset that miss the sample at minute 420. These 21 samples constitute the full whereas samples at 0, 10, 20, 30, 60, 90 and 120 correspond to the reduced MTT protocol, respectively. Moreover the samples drawn before the beginning of the experiment were averaged with the sample at min 0 to form the basal values. In Tab. 8.1 are presented the main feature of the three datasets and the systematically missing samples for each dataset.

	number of patients	*weight (kg)*	*age*	*dose*	*missing samples*
healthy	203	77.94±13.24	55.53±21.66	1.2 g/kg	-
prediabetic	44	91.01±18.4	53.73±7.74	75 g	260-420
diabetic	28	93.73±17.04	55.1±9.4	75 g / 1.2 g/kg	420

Table 8.1: Summary of the main features of the three dataset and of their relative protocols.

The C-peptide oral minimal model

The C-peptide oral minimal (CMM) model is described by the following equations:

$$\begin{aligned} CP_1'(t) &= -(k_{01}+k_{21})\cdot CP_1(t) + k_{12}\cdot CP_2(t) + SR_n & CP_1(0) &= 0 \\ CP_2'(t) &= -k_{12}\cdot CP_2(t) + k_{21}\cdot CP_1(t) & CP_2(0) &= CP_b\cdot k_{21}/k_{12} \\ Y'(t) &= \begin{cases} -\alpha\cdot(Y(t)-\beta\cdot(G(t)-G_b)) & Y(0)=0, \quad \text{if } G(t)-G_b\geq 0 \\ -\alpha\cdot(Y(t)) \qquad Y(0)=0, & \text{if } G(t)-G_b<0 \end{cases} \end{aligned} \tag{8.1}$$

where CP_1 and CP_2 (pmol/l) are C-peptide concentration in the accessible and peripheral compartments respectively. K_{01}, k_{12} and k_{21} (min^{-1}) are the C-peptide kinetic parameters and they are fixed to population values following the method proposed in Van Cauter [20]. Note that this formulation represents the deviation from the basal model.

$$\begin{aligned} SR_n(t) &= SR_s(t) + SR_d(t) \\ SR_s(t) &= Y(t) \\ SR_d(t) &= \begin{cases} k\cdot\frac{dG}{dt}, & \text{if } \frac{dG}{dt}\geq 0 \\ ,0 & \text{if } \frac{dG}{dt}<0 \end{cases} \end{aligned} \tag{8.2}$$

SR_n is the pancreatic secretion controlled by the sum of two components the glucose concentration (static control SR_s) and its rate of increase (the glucose dynamic control SR_d). The static secretion is supposed to be equal to Y (pmol l^{-1} min^{-1}) that is the provision of new insulin. The uniquely identifiable parameters of the model are: k (pmol dl l^{-1} mg^{-1}) , *alpha* (min^{-1}) β (min^{-1} pmol dl l^{-1} mg^{-1}) and Cp_b (pmol/l). Once COMM parameters are estimated, three β-cell responsivity indexes can be derived: the static sensitivity (Φ_s, 10^{-9} min^{-1}) that measures the effect at steady state of a glucose stimulus on β-cell secretion, the dynamic sensitivity (Φ_d, 10^{-9} unitless) that measures the effect of the rate of change of glucose on secretion of the stored insulin and finally the total sensitivity (Φ_t, 10^{-9} min^{-1}) which measures the overall responsivity from Φ_s

and Φ_d.

$$\begin{aligned} \Phi_s &= \beta \\ \Phi_d &= k \\ \Phi_t &= \Phi_s + \frac{\Phi_d \cdot \Delta G}{\int_0^\infty (G(t) - G_b)\, dt} \end{aligned} \tag{8.3}$$

where ΔG is the maximal excursion of glucose above basal.

Population modeling assumptions

Nonlinear mixed effects models (NLMEM) are able to quantify both the population and the individual parameters and identify by a hierarchical approach the biological sources of intra-individual and inter-individual variability. More specifically, in a first step, the data are described by:

$$y_{ij} = f(\mathbf{p_i}, x_{ij}) + \epsilon_{ij} \qquad 1 \leq i \leq m \qquad 1 \leq j \leq n_i \tag{8.4}$$

where y_{ij} are is the jth observation (in our case glucose concentration) of the ith subject at some known time instant Xij. Here, m is the number of individuals and n_i is the number of observation of individual i. $\mathbf{P}_i$ is the vector of model parameters of the ith individual. The variability due to measurement and model errors, better known as the residual unknown variability (RUV), is explained through ϵ_{ij} which is assumed to be independently distributed with a zero mean and Gaussian distribution:

$$\epsilon_{ij} = N(0, (\sigma_{prop} y_{ij} + \sigma_{add})^2) \tag{8.5}$$

The variance model is described as a combination of a proportional and an additive error model where σ_{prop} and σ_{add} are additional parameters to estimate. In a second step, the model parameters are represented as function of some physiologically meaningful attributes that do not vary across the population (θ, fixed effects, i.e. values that are common to all subjects) and some others that do ($\boldsymbol{\eta}_i$, random effects, i.e. values typical of a specific subject). In our model we chose the function:

$$p_{ki} = \theta_k e^{\eta_{ki}} \tag{8.6}$$

where p_{ki} is the kth model parameter of the ith subject, is the typical value of the kth parameter common to the entire population and η_{ki} is the random effect of the kth model parameter of the ith subject. The random effect $\boldsymbol{\eta}_i$ are assumed to be independently

distributed with a zero mean and Gaussian distribution:

$$\boldsymbol{\eta}_i \sim N(0, \boldsymbol{\Omega}) \tag{8.7}$$

with $\boldsymbol{\Omega}$ being a positive definite covariance matrix. With this formulation the second stage of variability, better known as Between-Subject Variability (BSV), is explained. The omega matrix set up is full.

Analysis of the results and algorithms used
As a first step, we identify the CMM in the healthy population using the NLMEM approach and we compared its performance with the one obtained with the traditional WNLS estimation approach, referred to here as STS. Both the estimation were carried out using the software NONMEM [29]. The model at this step does not estimate the basal of the C-peptide coherently to what was done previously in literature [24] with the single subject approach. In particular we looked at individual and population estimates the first in terms of correlation and the second in terms of magnitude. Note that we calculated the geometrical mean and variance of the WNLS individual estimates for comparison reason with the NLMEM population estimates. Moreover eighteen subjects were excluded from this step of analysis because they need Bayesian a priori information for the individual estimation. Once we have shown the two techniques results comparability in a rich protocol, we can carry on our analysis using just the population approach. In particular we investigated the NLMEM potentials in a "data poor" context by identifying the CMM on the reduced protocol (R) and on the two furtherly discarded dataset obtained by removing the 25% (R1) and the 50% (R2) of the C-peptide original samples of the reduced protocol. In particular we looked at the percentages of discrepancy between the estimated population parameters (fixed effects and square root of the BSVs) in the reduced protocols and the "true values" estimated in the full protocol (REF). Moreover we evaluated the goodness of the individual estimates assessed by the square Root of the Mean Square Error (RMSE):

$$RMSE_k = \sqrt{\sum_{i=1}^{m} \frac{(p_{ki} - \hat{p}_{ki})^2}{m}} \tag{8.8}$$

where p_{ki} is the true parameter value (REF) for subject i (the parameter estimate in the full protocol), $\hat{p}_{ki}$ its estimate on a reduced protocol, and m is the number of subjects involved in the analysis. For readability purposes, these values were indicated as percentage of the true population mean of each parameter. Finally we looked at the

derived indexes performance through a correlation analysis between each reduced dataset and the full protocol. Pearson's correlation was used to evaluate univariate correlation. The samples removal was random and as a consequence some individual data profiles were more affected than others. This is a common situation in pharmacokinetics and pharmacodynamics studies where the information about some subjects might be very rich, while for others the sampling might be so unsatisfactory that individual estimates are impossible to obtain with the traditional estimation paradigm. The glucose concentration data, used in the model as a forcing function, was not undersampled. While this situation does not realistically reflect a practical experimental setting, where both glucose and C-peptide would be undersampled, here our purpose is testing the potentials of the NLMEM technique and we focus our attention mainly on the effect of sparse C-peptide sampling. Finally we compare the derived indexes of the β-cell function of insulin secretion in the three population: the healthy, the prediabetic and diabetic dataset. Analyses among the three subgroups were made using Kruskal-wallis followed, where appropriate, by a ranksum test. A P value of 0.05 was considered statistically significant. Note that all the analysis were carried out using the software NONMEM 7.2.0 [29] that implements the NLMEM approach which consists in obtaining the population parameters by maximizing a likelihood function. Because of the computational infeasibility of the exact solution, different approximations were proposed. Here we applied the First Order Conditional Estimation (FOCE) approximation with INTERACTION coherently with was found previously in literature [2] and in 3.

8.3 Results

As explained in the analysis of the results we firstly assessed the comparability of the new NLMEM results with the traditional WNLS approach results. As far as the population description is concerned using the full MTT dataset the BSV and the fixed effects are comparable (Fig. 8.1). However the BSV obtained with FOCE is smaller than the one obtained with STS method as previously reported in literature [26, 2].

At the individual level, the linear regression analysis between FOCE vs STS estimates results having a highest correlation of R=0.98 and a lowest correlation of R=0.92 (Fig. 8.2). In Fig. 8.3 are presented the boxplots of the three derived individual indexes for the two methods: is evident like in Fig. 8.1 the overestimation of the BSV using the STS technique. All in all as for the two previous points, the matching between the two estimation technique is good and this legitimize the transition to the population technique for the next analysis.

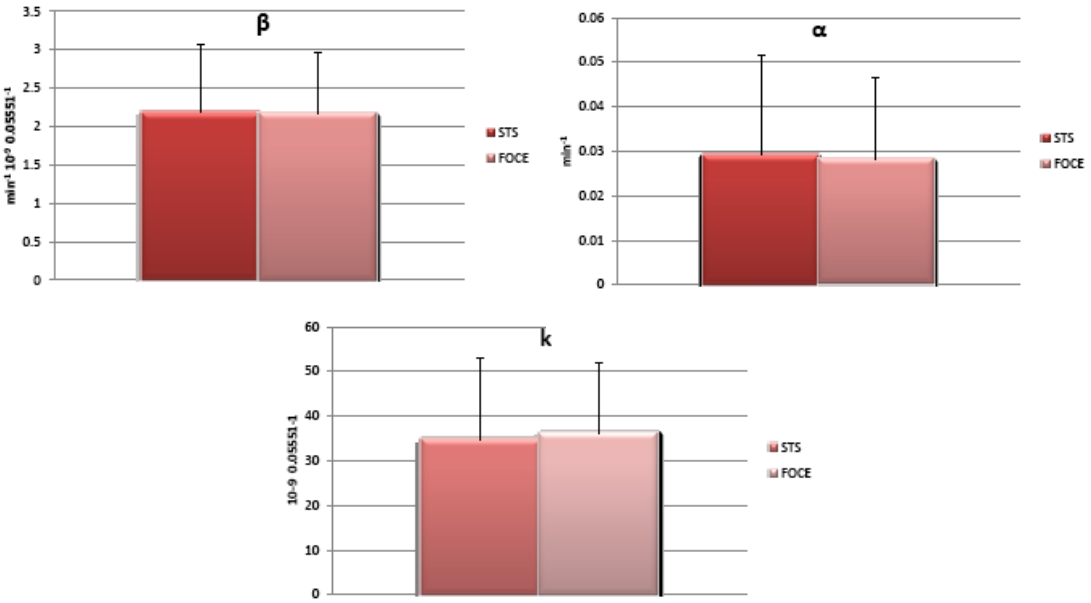

Figure 8.1: Bar plots of the population estimates using the individual (STS) and the population approach (FOCE).

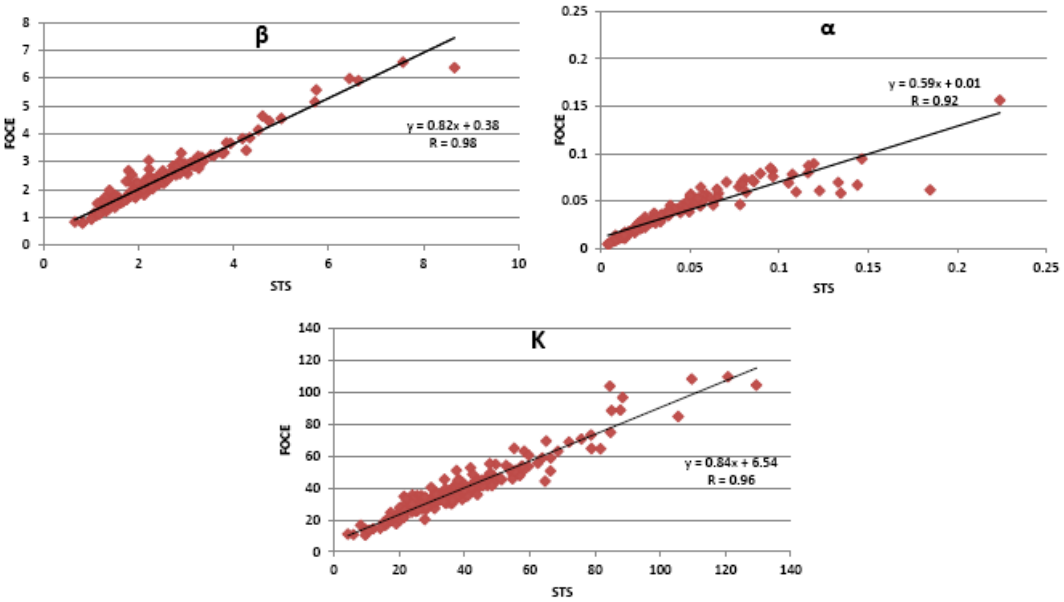

Figure 8.2: Correlation graphs of the individual parameters using the individual (STS) and the population approach (FOCE).

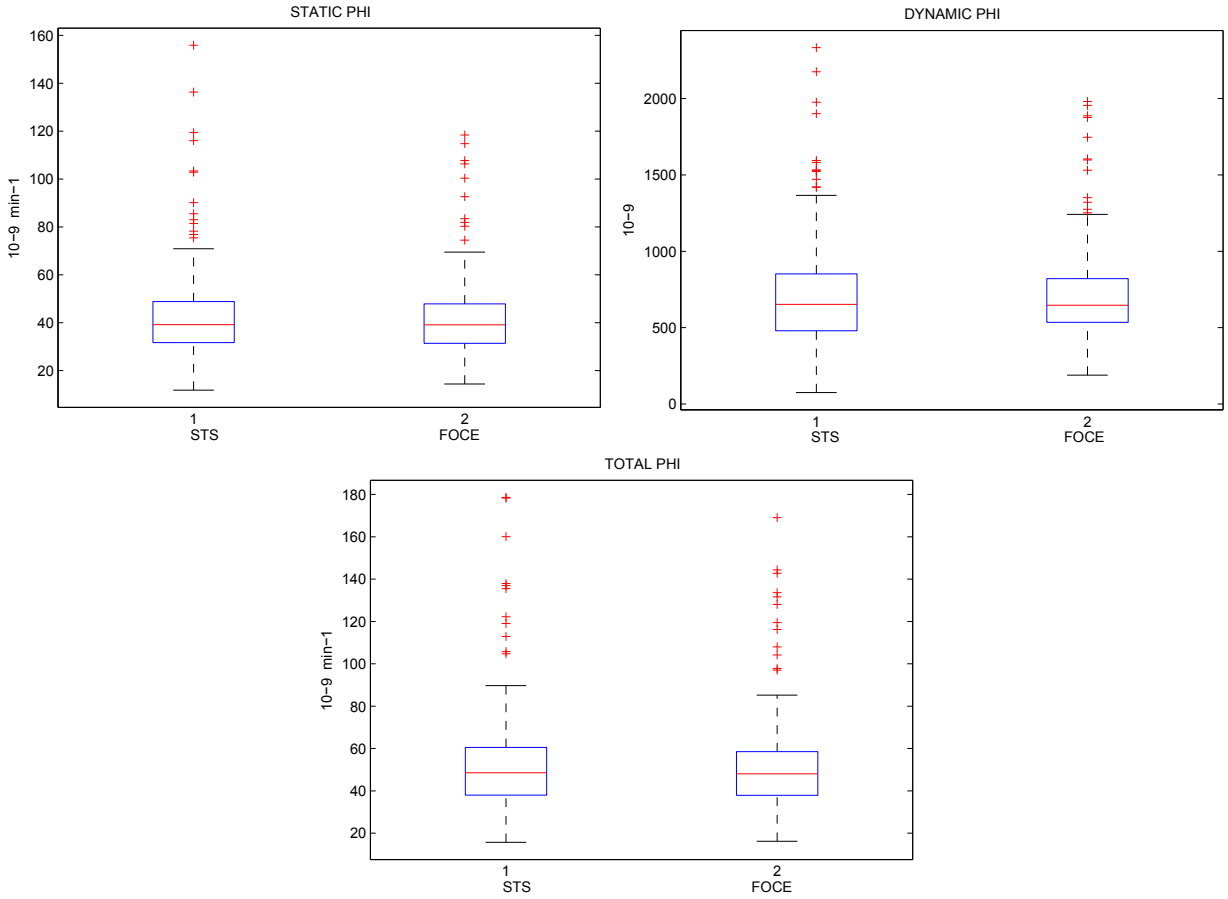

Figure 8.3: Boxplots of the derived secretion pancreatic indexes using the individual (STS) and the population approach (FOCE).

		C-peptide minimal model	
Model parameters	Units	population estimates	RSE %
Fixed Effects			
β		2.04	2.7%
α		0.0343	5.00%
K		34.4	3.20%
CP_b		453	3.30%
Random effects			
Interindividual Variability			
$\omega\ \beta$		33.30%	5.0%
$\omega\ \alpha$		59.80%	7.0%
ω K		37.00%	6.2%
$\omega\ CP_b$		37.70%	7.2%
correlation *beta* α		-35.60%	22.9%
correlation β K		79.80%	5.8%
correlation $\beta\ CP_b$		53.00%	18.2%
correlation α K		17.20%	42.6%
correlation $\alpha\ CP_b$		-61.60%	11.1%
correlation K CP_b		44.20%	19.3%
0.211 0.6049.9 3.20	*Residual unknown variability*		
σ_{prop}		0.211	0.60%
σ_{add}		49.9	3.20%

Table 8.2: Summary of the CMM parameters in the full protocol. Typical values for parameters are in original units. Given that between-subject variability is modeled as log normal, variance measures are reported as approximate coefficients of variation (CV), whereas the covariance terms are in terms of correlation.

The second step now is to explore the NLMEM potentials in a data poor condition but before doing so in Tab. 8.2 are briefly summarized the population parameters description of the CMM after a 21 samples MTT. Note that we included the basal level of the C-peptide as a parameter since it improve the fit significantly. All population estimates were estimated with good precision: apart from the correlation between α and k all the RSE% are below the 23%. η - Shrinkage values are under the limit of alarm 20-30% meaning that there is enough information in the data to estimate the parameters. In particular the shrinkage values range from the 3.1% of the k parameter to the 5.9% of the α parameter. Also the ϵ-shrinkage value is under the limit of alarm (5.8%) meaning that no overfit is taking place.

In Fig. 8.4 are presented the individual and the population fit vs the observation: the red line, the linear regression between the observation and the predictions, matches pretty well the bisector of the plane. In Fig. 8.5 are presented the individual population residuals and the population weighted residuals. The fit is reasonably good if we look at the pattern and the amplitude.

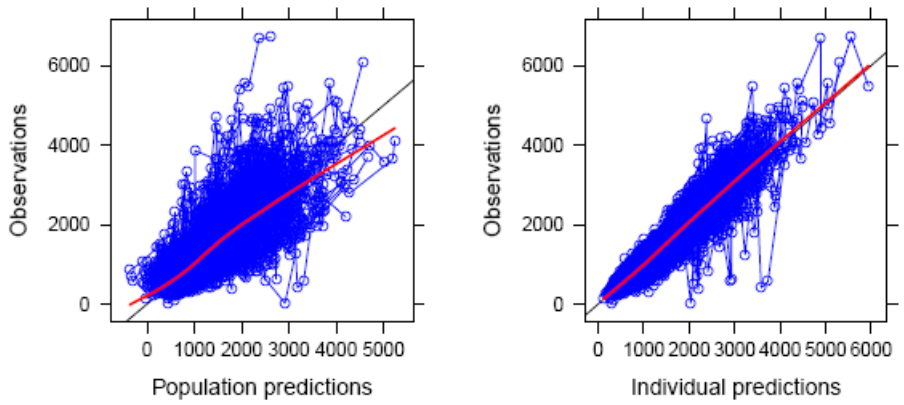

Figure 8.4: C-petide population (on the left) and individual (on the right) prediction versus observation in the full protocol.

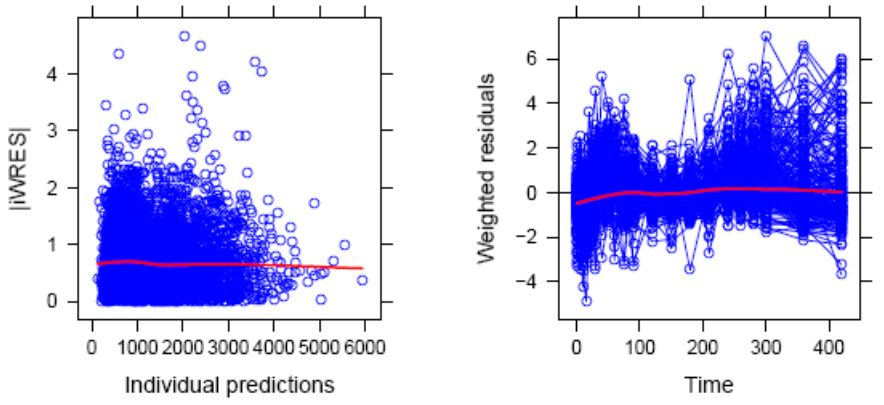

Figure 8.5: Individual weighted residuals (IWRES) on the left an population weighted residuals (WRES) on the right in the full protocol.

In Fig. 8.6 is presented the VPC of the CMM: The graph yields that the model is able to catch the data variability as the CI of the percentiles of the simulated profiles are on the whole able to follow the percentiles of the observed data apart from some clear mismatching on the 5^{th} percentile and on the 95^{th} percentile.

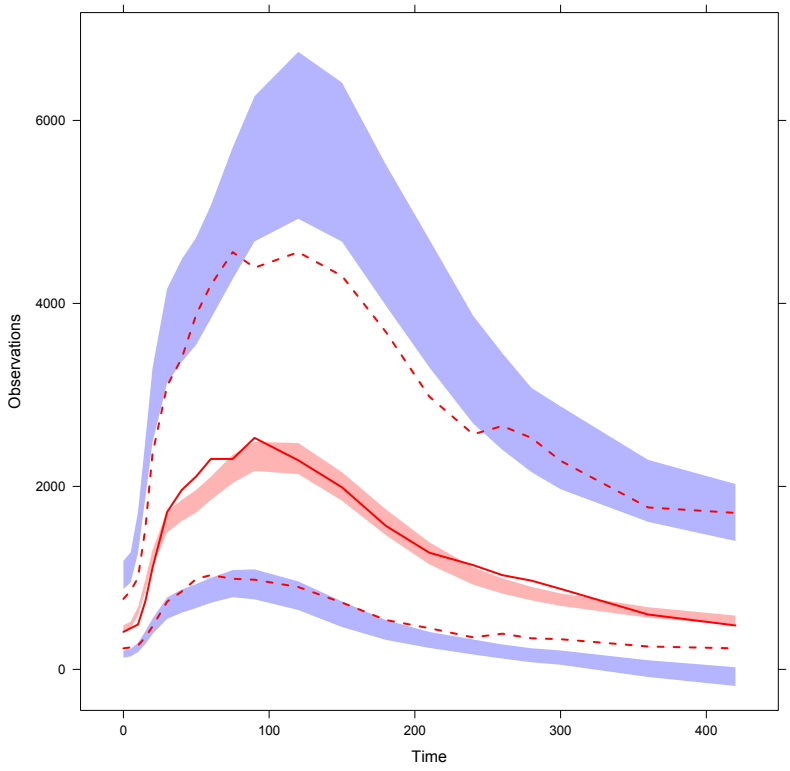

Figure 8.6: Vpc of the CMM in the full protocol.

As far as the CMM performance on the reduced protocols is concerned, the population parameters discrepancy values yield that apart from α the other parameters are reasonably close to the corresponding estimate in the full protocol (Tab. 8.3).

With the paucity of the data the discrepancy tend to become bigger apart from some cases like for example the parameter CP_b in the R2 dataset. This effect is a typical feature of the population approach, especially in a poor data context. In fact when there is not enough individual information (i.e. few samples per individual), a condition that is merely tolerated by the individual approach, a sort of constraint is generated between the individual estimates that tends to bring them together towards the population mean. This phenomenon is known in literature as shrinkage. Note that the shrinkage increase with the decreasing of the number of samples and that in particular it is close to the alert value for the parameter α already from the R dataset (18%) meaning that most

dataset	β	α	K	CP_b
R dataset	-4.4%	296.5%	-22.4%	-11.5%
	(-11%)	(60%)	(0.1%)	(-22%)
R1 dataset	-5.4%	346.1%	-23.3%	-12.6%
	(-12%)	(46%)	(-8%)	(-20%)
R2 dataset	-5.4%	471.4%	-30.5%	-11.7%
	(-7%)	(107%)	(17%)	(-16%)

Table 8.3: The distance of the estimated values for both the fixed effects and the square root of the BSV (in brackets) from the true values are reported as percentage differences normalized to the true values for the 3 datasets.

likely with the reduced sampling scheme there is not enough information in the data to estimate the parameter well. Moving the attention to the individual results, the RMSE present the same expected trend that is present in the population estimates: with the decreasing number of samples the RMSE increase (Tab. 8.4).

dataset	β	α	K	CP_b
R dataset	19.26%	459.81%	27.10%	25.63%
R1 dataset	20.91%	427.73%	29.88%	26.76%
R2 dataset	22.60%	541.42%	35.28%	27.81%

Table 8.4: Square root of the mean square error (RMSE) of the individual parameter estimates expressed as percentage of the true population mean for the three reduced datasets.

Looking at the β-cell responsivity indexes, the correlation analysis between each reduced dataset and the full protocol yields that there is a good match between the two even if we are in a sparse dataset as R2. Obviously with the paucity of data, the correlation decreases. In Fig. 8.7 are presented the correlation analysis for Φ_d and in Tab. 8.5 are presented the correlation values expressed as R.

The last part of the analysis consists on comparing the three β-cell derived indexes (Φ_s, Φ_d, Φ_t) among the three different categories (healthy-prediabetic-diabetic). The geometrical average values are plotted in Fig. 8.8. From the statistical analysis all the three indexes were significantly different in the three groups (healthy/ prediabetic/diabetic) apart from one case where the Φ_s was not statistically different between the healthy and the prediabetic patients.

dataset	Φ_s	Φ_d	Φ_t
R dataset	0.86	0.84	0.79
R1 dataset	0.92	0.92	0.86
R2 dataset	0.88	0.86	0.83

Table 8.5: R values from the correlation analysis between the derived indexes in the full protocol and the derived indexes on the three reduced datasets.

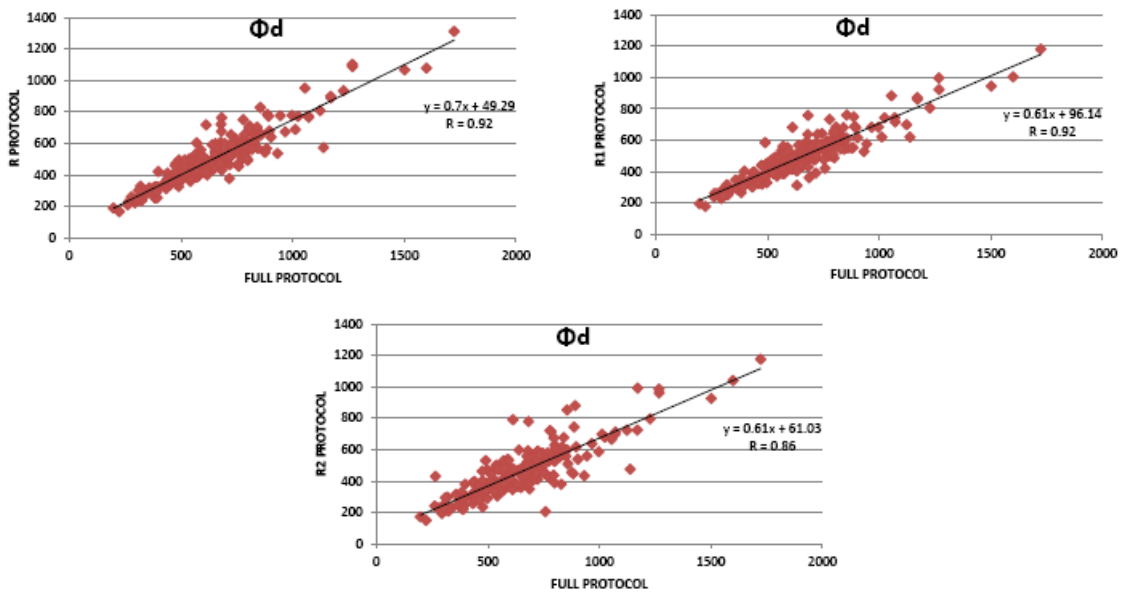

Figure 8.7: Correlation graphs between the Φ_d obtained in the full protocol and the three reduce dataset (R - R1 - R2).

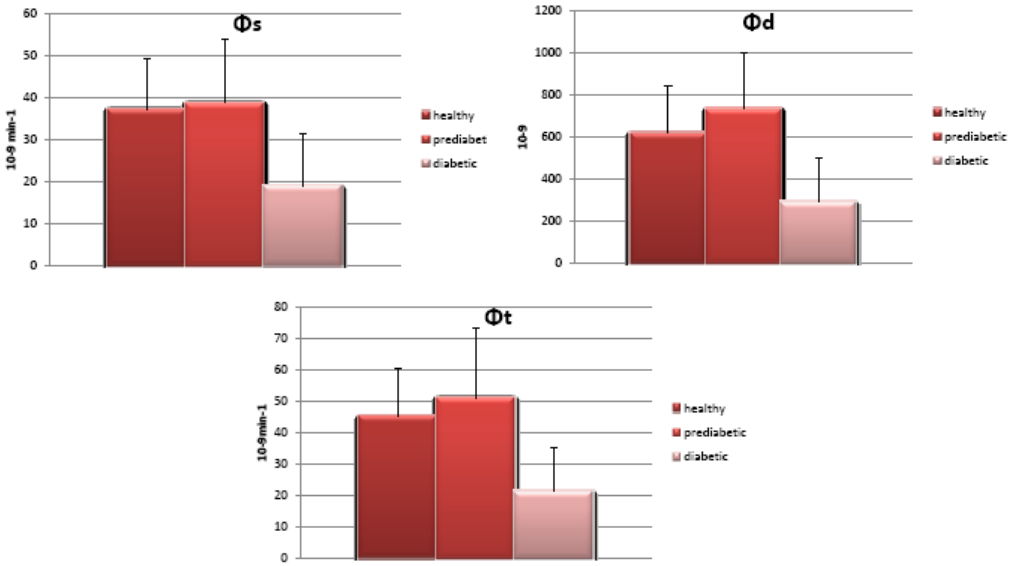

Figure 8.8: Bar graphs of the three β-cell indexes in the three categories .

8.4 Discussion

In this chapter we identify the CMM with the NLMEM approach in different populations. To do so, first we show the continuity in moving from the traditional individual approach to the population approach by comparing the results of the two techniques. Then we show the NLMEM benefits in a data poor context that corroborate the usefulness of applying the population approach instead of the traditional single subject estimation. Finally, once the model is optimized, we use it in different populations to determine whether is able to catch the different curve kinetics and distinguish among the groups.
Regarding the first part of the analysis, not only we proved the comparability of the results of the technique but also we show the superiority of the NLMEM technique. In particular during the single subject estimation (STS) eighteen patients were excluded because an a priori Bayesian information was needed to estimate their parameters and for comparison reason with the population approach, that does not use it, these subjects were left out from the first part of the analysis. In fact in the population approach this additive hint is not necessary because the lack of information is compensated by the information that is spread in the set of subjects that works like a prior during the estimation step. Note also that the population parameters variances in Fig. 8.1 and that the outliers of the population ϕ indexes that are present in Fig. 8.3 are less widespread than in the the individual approach. The results that we obtained on the comparison of

the two techniques yield that the NLMEM can be successfully used and that the results are coherent with what was previously found in literature and that this approach helps to get estimates less widespread.
Not only the population approach helped us to avoid the use of an a priori Bayesian information but also on the second part of the analysis we were able to estimate an additional parameter that is the basal value of the C-peptide. With this final formulation we identify the CMM on a full protocol and characterize a healthy population. At this step, a covariate analysis would be helpful to identify in a deterministic way some sources of the biological variability in the model. Some considerations have to be made on the VPC (Fig. 8.6). The model on the whole seems to reproduce well the observed data variability but at the same time has some problems in simulating the highest concentrations. This can be assigned to the individual known input function in the model (glucose) that does not always interact properly with the individual parameters realization. In particular, there is no additional information in the model that can link the set of individual parameters to the proper forcing function in order to obtain always reasonable physiological outputs [44].
The CMM on the reduced dataset (R) and on the furtherly discarded dataset (R1 and R2) behave reasonably well. It is important to point out that the CMM using the traditional single subject estimation would not be able to be identified on the R1 and R2 dataset. The most affected parameter by the poorer sampling is α that at the same time presents also a value of shrinkage close to the limit of alert already from the R dataset meaning that in the reduced sampling protocol there is not enough information in the data to determine it well. The other parameters both at the individual and at the population level are reasonably close to the true values and with the paucity of data this discrepancy becomes bigger as expected. Is important to notice though that the parameters from which the β-cell responsivity indexes are derived are less affected from the sampling scheme and there is a good match between the indexes calculated on the full protocol and the ones calculated on the reduced. In other words the CMM also in the reduced sampling dataset is able to describe the β-cell function consistently with the full protocol.
Finally we apply the NLME CMM on different population and we found that the Φ are statistically different in each population apart from Φ_s between the healthy and the prediabetic patients. It is important to note that the size of the healthy population (203) is really different from the diabetic (28) and prediabetic one (44). In order to have a robust characterization of these last two population parameter distributions more subjects need to be added in each dataset.

8.5 Conclusion

In this article we implement the CMM by using the population approach. By doing so we proved the comparability and at the same time the benefits of this technique with respect to the traditional single subject approach. We proved the feasibility of the population approach on severely discarded dataset. This paves the way to other studies that aim to further narrow down the reduced protocol in order to better deal with the typical data poor epidemiological study condition. Finally with the optimized C-peptide NLMEM we proved that the CMM implemented on different populations is able to describe the different kinetics and distinguish among the groups through the β -cell derived indexes.

The visual predictive check in model with forcing functions

9.1 Introduction

The nonlinear mixed effects models (NLMEM) are well established modeling techniques during drug development in PKPD analysis and epidemiological studies because they are able to quantify not only the individual and population parameters but also to identify the biological sources of inter-individual and intra-individual variability. Moreover the nonlinear mixed-effects approach is particularly appealing in "sparse dataset", the typical epidemiological study condition, where a complete statistical description is obtainable by borrowing the lack of information from the entire population thus potentially reducing the need for blood samples and invasive trials. In order to draw the correct clinical conclusions on a study it is really important to use the correct diagnostic to evaluate the NLMEM predictive performance. In these last two decades many sophisticated diagnostic tools have been proposed that rely on a graphical assessment or on a statistical elaboration of the model predictions compared with the observed dataset. These techniques are based on the individual-population estimates and residual or are based on simulation or numerical elaboration [53]. Recently a simulation based diagnostic has been particularly used for its simplicity: the visual predictive check (VPC) [43]. The idea of the VPC is to

assess by visual inspection whether the model is able to catch or not the variability of the observed data. To do so multiple simulations are runned keeping the structure of the observed dataset. Then the median of the 5th and the 95th percentiles of the simulated datasets are compared to the corresponding percentiles of the original data. To make the interpretation of the VPC less subjective the CI of the percentiles of the simulated data are used instead of just the percentiles [65]. Many VPC adaptations have been proposed by now [66, 67, 68] since the technique can be easily appreciated but still there are some pitfalls that have to be explored for example during the simulation step. This step is particularly critical because not always are simulated profiles that are consistent with the original dataset. In fact when models with time varying known input function or forcing functions (FF) are evaluated there is a potential mismatch between each set of simulated parameters and the associated individual FF which can cause an incorrect profile simulation.

These kind of models are well-known in the metabolic field where FFs are introduced as a strategy to better identify the glucose and C-peptide minimal models [17, 19, 22, 24] by decomposing the system in two subsystems where the glucose and the C-peptide are respectively used as known input (FF) and output or vice versa depending on which part of the system is chosen to be described [12]. In PKPD modeling problems instead FFs are used when there are no assumptions made on the PK model and usually when the "data rich" conditions are satisfied. In this case just the PD is fitted using the PK data as a known input function.

This study aims to overcome the VPC limitation on the simulation step by taking into account a correlation term that bounds the set of simulated parameters with the most appropriate FF. In particular we calculated for each set of simulated parameters (SIM) a weighted distance (the normalized Euclidean distance (NED) or the Mahalanobis distance (MD)) between the SIM and the previously estimated parameters (EST). This helped us to find the vector of EST parameters that was closer to SIM and consequently to match the EST corresponding FF to the SIM parameters in the simulation step. Moreover we proposed another approach that has been developed in case of low FF variability that is a common situation in PKPD experiments since the kinetics of the FF curves are less variable if compared to the ones measured in metabolic studies. This method adds an elaboration step before applying the MD. A clustering analysis detects the most important FF kinetics that are used to simulate a new dataset whose parameters are estimated, then the MD is applied. Note that this step is plausible because the FF main kinetics detected by the clustering analysis are a good approximation of the FF variability and as a consequence the population inter individual variability is not underestimated.

We assessed the techniques on four nonlinear metabolic models (the IVGTT and the ORAL glucose and C-peptide minimal models [17, 19, 22, 24]) and on a typical PKPD example such as the Warfarin model [69, 70].

9.2 Material and methods

NED and MD VPC

This newly proposed technique addresses the problem of generating reasonable simulated profiles from models with time varying known input function by better controlling the VPC simulation step. The classical VPC approach in fact does not take into account the relationship between the simulated parameters and the individual FF associated. NED and MD VPC approach instead create an external bound that drives the simulation firstly by calculating for each set of simulated individual parameters (SIM) a weighted distance between the SIM and all the previously estimated set of individual parameters (EST) on the observed data and then by searching for the minimum distance. When the minimum distance is detected the corresponding FF of the set of EST parameters can be associated to the set of SIM in the simulation step. The weighted distance used are the normalized Euclidean distance or the Mahalanobis distance. By definition NED and MD represent the distance between two random vectors $\mathbf{X}$=[X_1, X_2, ..., X_N] and $\mathbf{Y}$=[Y_1, Y_2, ..., Y_N] that belong to the same multivariate distribution with mean $\boldsymbol{\mu}$=[μ_1, μ_2, ... , μ_N] and covariance $\boldsymbol{\Sigma}$. In other words E[$\mathbf{X}$]= E[$\mathbf{Y}$]= $\boldsymbol{\mu}$ and $\boldsymbol{\Sigma}$=cov($\mathbf{X}$)=cov($\mathbf{Y}$). The covariance $\boldsymbol{\Sigma}$ matrix is diagonal when the NED is calculated whereas it takes into account the terms out of the diagonal when the MD is applied. In formulae the MD can be described as in the following equation:

$$\Delta^2 = (\mathbf{X} - \mathbf{Y})' \, \boldsymbol{\Sigma}^{-1} \, (\mathbf{X} - \mathbf{Y}) \tag{9.1}$$

Eq. 9.1 can be simplified in the following way (Eq. 9.2) when the NED is applied since only the diagonal terms are taken into consideration:

$$\Delta^2 = \sum_{i=1}^{N} \frac{(X_i - Y_i)^2}{\Sigma_{ii}} \tag{9.2}$$

Note that with the NED or MD VPC approach the error during the association process of the SIM with the FF is minimized but it is not completely removed. To avoid this kind of error an agglomerative hierarchical cluster analysis was done on the FFs before applying the MD or NED VPC. This cluster analysis has the purpose of detecting kinetically

similar FFs curves according to a distance measure. The algorithm chosen was Ward's minimum variance method that minimize the total within cluster variance as a rule to join two clusters. In particular it calculates the merging cost (Δ_w) of combining the possible combination of clusters that is the sum of squares increase. In formulae the Δ_w of combining the clusters A and B:

$$\Delta_w = \sum_{i \in A \cup B} \|\mathbf{x}_i - \mathbf{m}_{A \cup B}\|_2^{\,2} - \sum_{i \in A} \|\mathbf{x}_i - \mathbf{m}_A\|_2^{\,2} - \sum_{i \in B} \|\mathbf{x}_i - \mathbf{m}_B\|_2^{\,2} = \frac{n_A \cdot n_B}{n_A + n_B} \|\mathbf{x}_A - \mathbf{m}_B\|_2^2 \tag{9.3}$$

Where $\mathbf{m}_Y$ is the center of cluster Y, n_Y is the cardinality of Y and $\|\quad\|_2$ is the Euclidean distance. At the initial step, all clusters are singletons (clusters containing a single point). Then each agglomeration occurs at a greater distance between clusters than the previous agglomeration. We decided to stop clustering when the clusters are too far apart to be merged using a threshold criterion. After having identified each FF cluster, the cluster centroids are used instead of the individual FF to simulate a new dataset where individual (EST) and population estimates are obtained. The MD or the NED VPC approach then can be applied with smaller error of association than before. This approach can be applied though under the hypothesis of having a model with FF with variability relative small so that the kinetics detected in the cluster analysis are a good FF approximation and that the new generated dataset variability is consistent with the observed data.

APPLICATION

1. *Metabolic Examples*
   The glucose and c-peptide IVGTT and ORAL models [17, 19, 22, 24] are well known instruments to study the glucose insulin system. All these four models present at least one known input function. In particular both the IVGTT models have one FF whereas the two oral models present two FFs. The dataset consist of 120 healthy volunteers (71 males and 49 females age 62 ± 17.5 and bodyweight 79.2 ± 13.5 kg) that underwent both an IVGTT and an MTT. The insulin modified IVGTT consists on an administration of a dose of 330 mg/kg glucose at time 0 min and a dose of 0.02 units/kg of insulin at time 20 min. Blood samples are collected at -120, -30, -20, -10, 0, 2, 4, 6, 8, 10, 15, 20, 22, 25, 26, 28, 31, 35, 45, 60, 75, 90, 120, 180 and 240 min for measurement of glucose, insulin and C-peptide concentrations. The mixed meal (10 kcal/kg, 45% carbohydrate, 15% protein and 40% fat) contains 1 ± 0.02 g/kg glucose and plasma samples were collected at -120, -30, -20, -10, 0, 5 10, 15, 20, 30, 40, 50, 60, 75, 90, 120, 150, 180, 210, 240, 260, 280,

300, 360,420 min for the measurement of plasma glucose, insulin and C-peptide. Note that these models were implemented in their original formulation as in their corresponding articles. In particular the glucose IVGTT model is implemented as in [2], the glucose MTT model is implemented as in [22] without modeling the Rate of appearance, the C-peptide IVGTT is modeled as in [19] and finally the C-peptide MTT is built as in [24].

2. *PKPD Example (simulated data)*
   To demonstrate the approach feasibility on different fields apart from the metabolic one, we applied the method on a well known PKPD example such as the Warfarin model [69] where the PK of the drug is assumed to be the known input function and the PD of the effect, the prothrombin, is the fitted data. In particular the dataset is based on a simulation of 100 subjects obtained from the population estimates of 32 healthy subjects that underwent an oral single dose of Warfarin [1.5 mg/kg] [70, 71]. On these subjects 250 samples of Warfarin concentrations together with 232 samples of prothrombin complex activity (PCA) were measured. The model was implemented as a turnover model to characterize Warfarin delayed effect with an indirect mechanism of action due to the interaction between the drug and the endogenous enzymes (the prothrombin) [71, 72].

SOFTWARE
All the estimation steps were done using NONMEM 7.2.0 [29] whereas all the simulation steps were done using Matlab software [73].

9.3 Results

Metabolic Example
The following results are obtained using the glucose and C-peptide minimal models after and an intravenous or an oral dose of glucose. The IVGTT minimal models have one known input function whereas the MTT minimal models have two. In particular the IVGTT glucose and C-peptide have respectively the insulin and the glucose profiles as FF whereas the MTT glucose and C-peptide minimal models have respectively the insulin and the rate of appearance of the glucose in plasma and the glucose and its first derivative.

1. *IVGTT glucose and C-peptide minimal model*
   In Fig. 9.1 we present the classical VPC of the Glucose and C-peptide minimal model. We found implausible simulated curves and as a consequence the CI of the

percentiles have some problems in following the reference percentiles calculated on the observed data. Note that the VPC of the IVGTT glucose minimal model is presented from min 8 since the models explains the dynamics of glucose from that minute on.

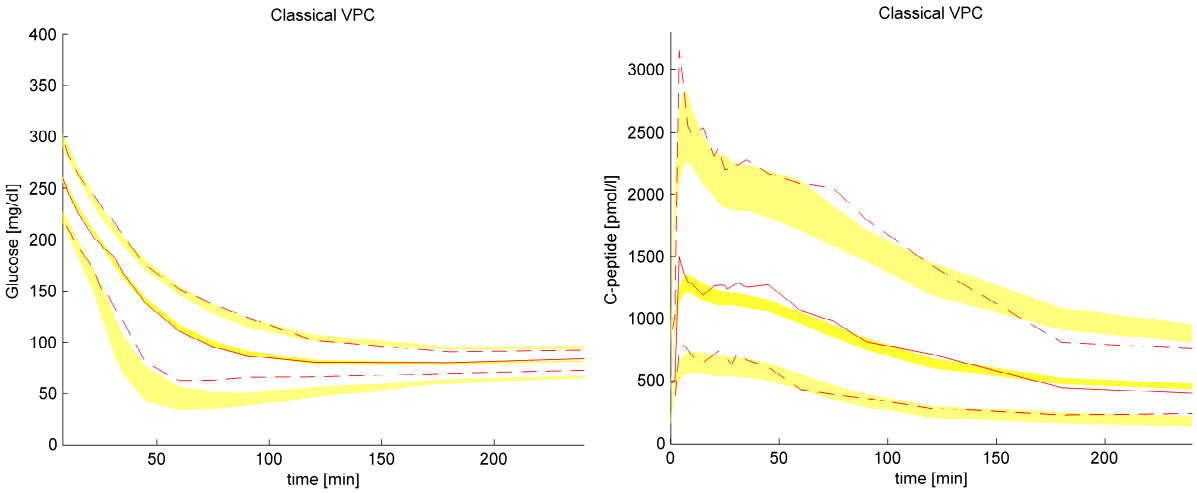

Figure 9.1: The classical VPC of the IVGTT glucose (on the left) and C-peptide (on the right) minimal models.

In Fig. 9.2 the VPC with NED and MD are presented applied both in the glucose and C-peptide minimal model. The CI of the simulated percentiles follow better the dynamic of the reference percentiles. There are no major differences in the performance between the VPC with MD and the NED technique. Finally in Fig. 9.3 are presented the classical VPC and the VPC with MD using as observed data the simulation with the FF obtained from the cluster analysis. In this way the effect of the correction with MD in the simulation step is more evident since we are testing the technique in a more controlled environment with less probability of failing during the matching.

2. *MTT glucose and C-peptide minimal model*
   In Fig. 9.4 we present the classical VPC of the Glucose and C-peptide minimal model. The simulated profiles without the correction were sometimes not physiological and as a consequence the CI of the percentiles do not match the reference percentiles calculated on the observed data. This time the difference between the simulated profiles and the observed one is more marked than the VPC on the IVGTT data.

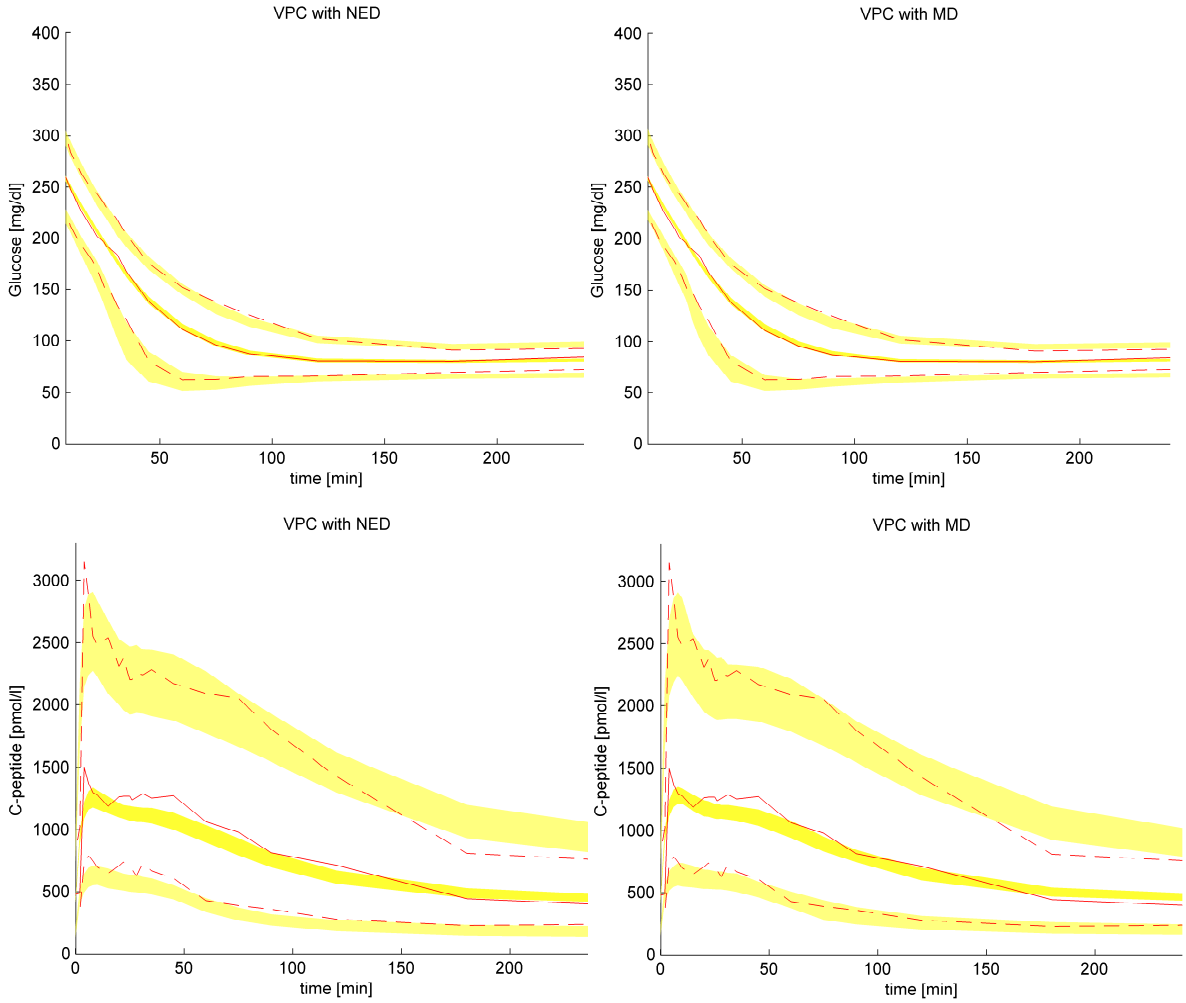

Figure 9.2: VPC with NED and MD of the IVGTT glucose (on the top figure) and C-peptide (on the bottom figure) minimal model.

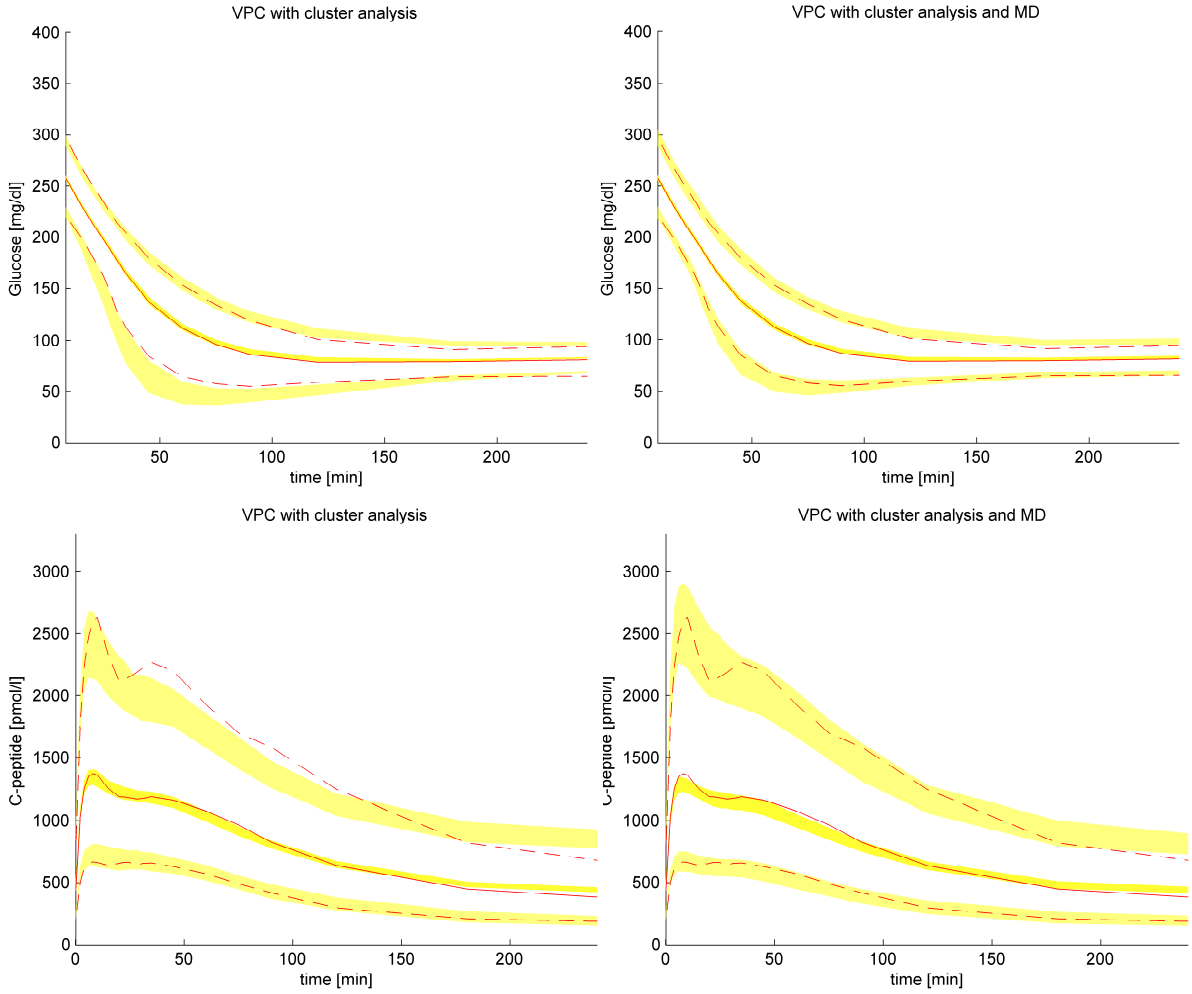

Figure 9.3: The classical VPC and with MD of the IVGTT glucose (on the top figure) and C-peptide (on the bottom figure) minimal model using simulated data obtained with FF resulted from a cluster analysis .

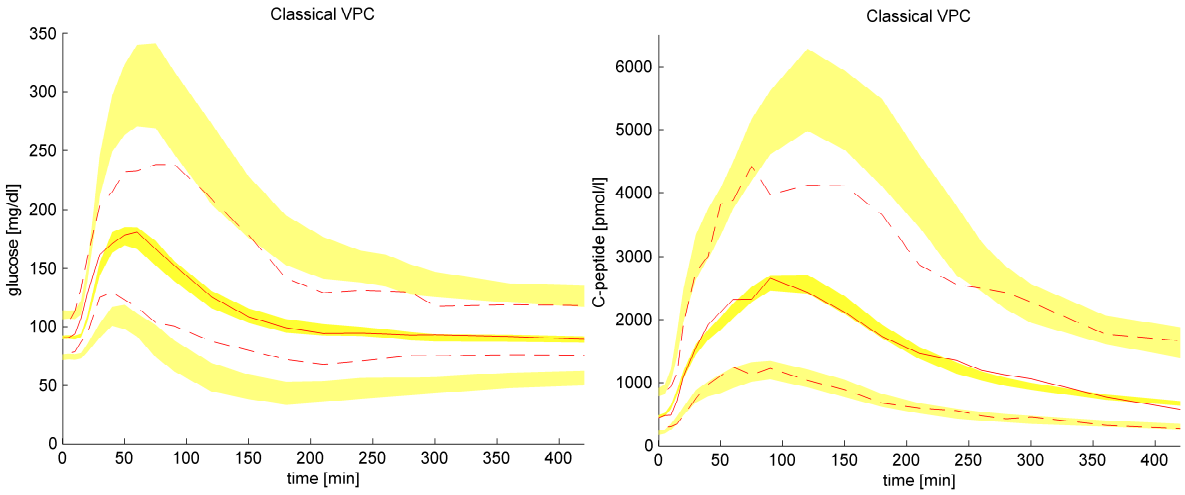

Figure 9.4: The classical VPC of the MTT glucose (on the left) and C-peptide (on the right) minimal model.

If we take into consideration in the step of simulation the MD or the NED (Fig. 9.5) the VPC performance is improved and consequently the conclusions that can be drawn are different from the ones relative to the classical VPC. The CI of the percentiles of the simulation better match with the percentiles of the observed data and there are no main differences in the plots using the NED or the MD correction. Finally in Fig. 9.6 we present the classical VPC and the VPC with MD on the simulated dataset obtained using the FF from the cluster analysis. Also with these models moving into a simulated context using a preliminary detection of the main FF kinetics through a cluster analysis helps to test the efficiency of the method despite an inevitable reduction of the variability population description under analysis.

PKPD example

In Fig. 9.7 we present the classical VPC of the PD of the Warfarin model together with the VPC both with NED and MD technique. The improvement due to the correction obtained using the MD or NED step is observable from the graphs. Note that the graphs are presented from hour 24 the time when the PCA is started to be measured. Moving into a more controlled environment, the simulated PCA data using the profiles of the PK identified by the cluster analysis, the same conclusions can be drawn by looking at Fig. 9.8. In particular if we take into consideration the MD step the CI of the percentiles follow the simulated data percentiles more precisely.

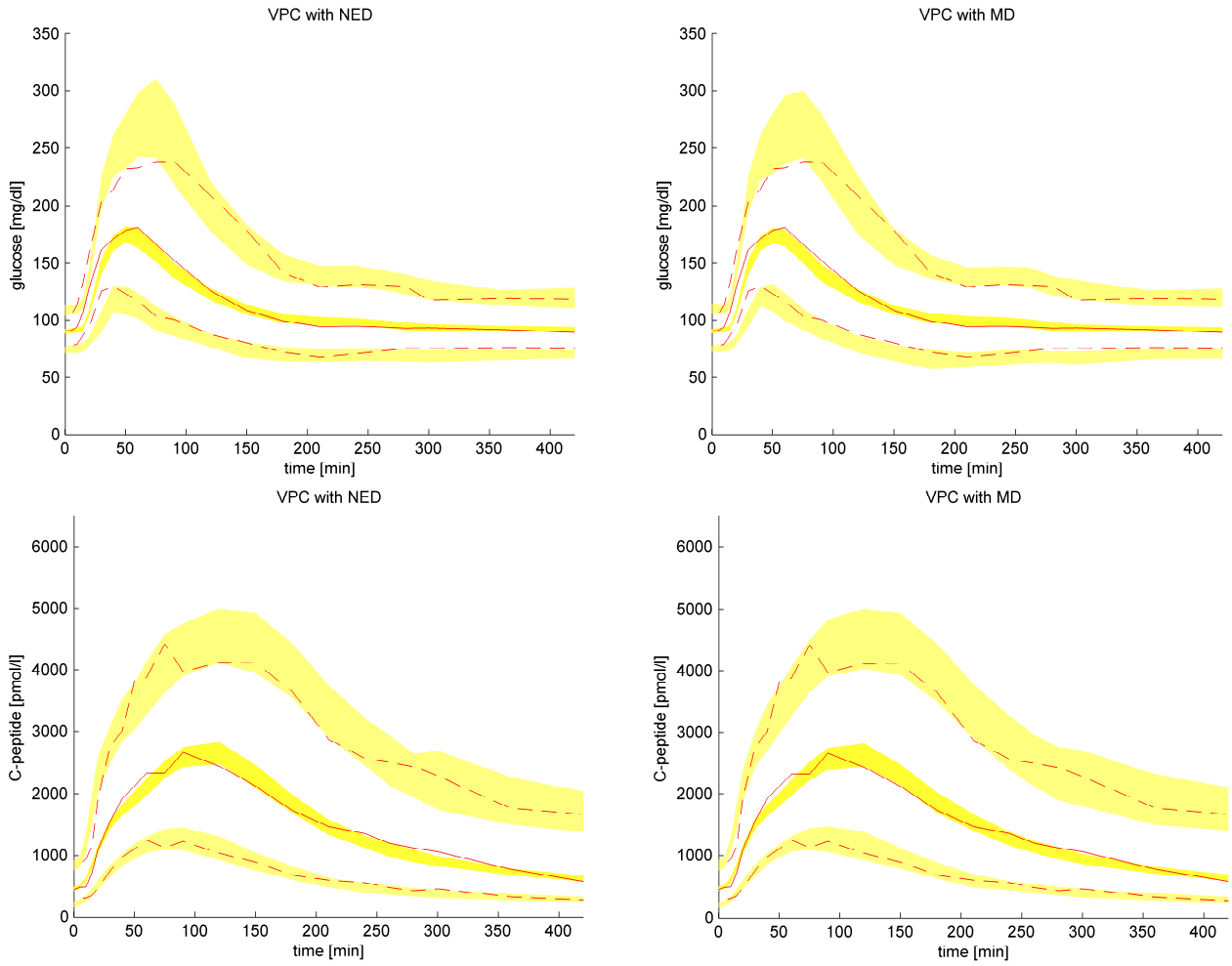

Figure 9.5: VPC with NED and MD of the MTT glucose (on the top) and C-peptide (on the bottom) minimal model.

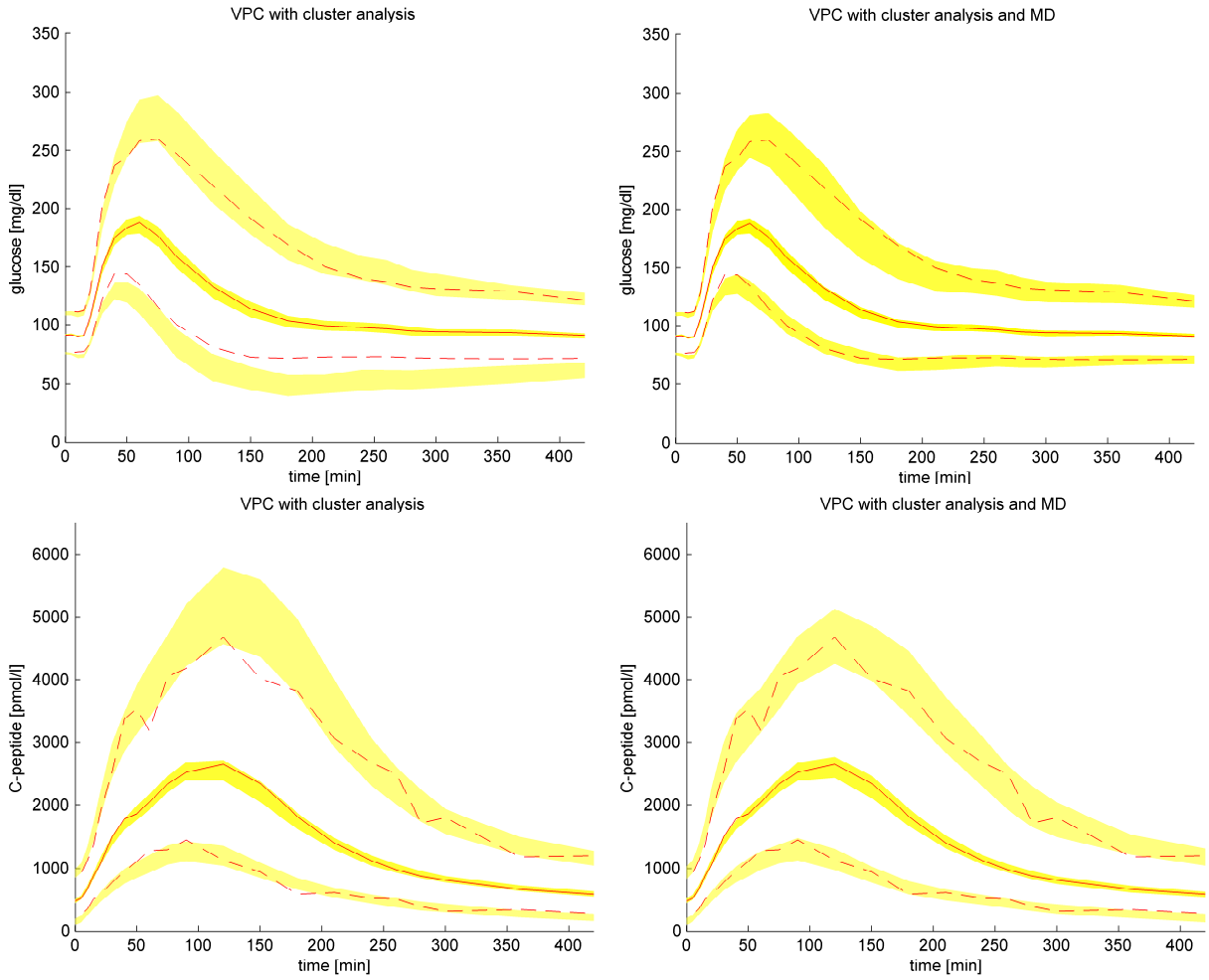

Figure 9.6: The classical VPC and with MD of the MTT glucose (on the top figure) and C-peptide (on the bottom figure) minimal model using simulated data obtained with FF resulted from a cluster analysis .

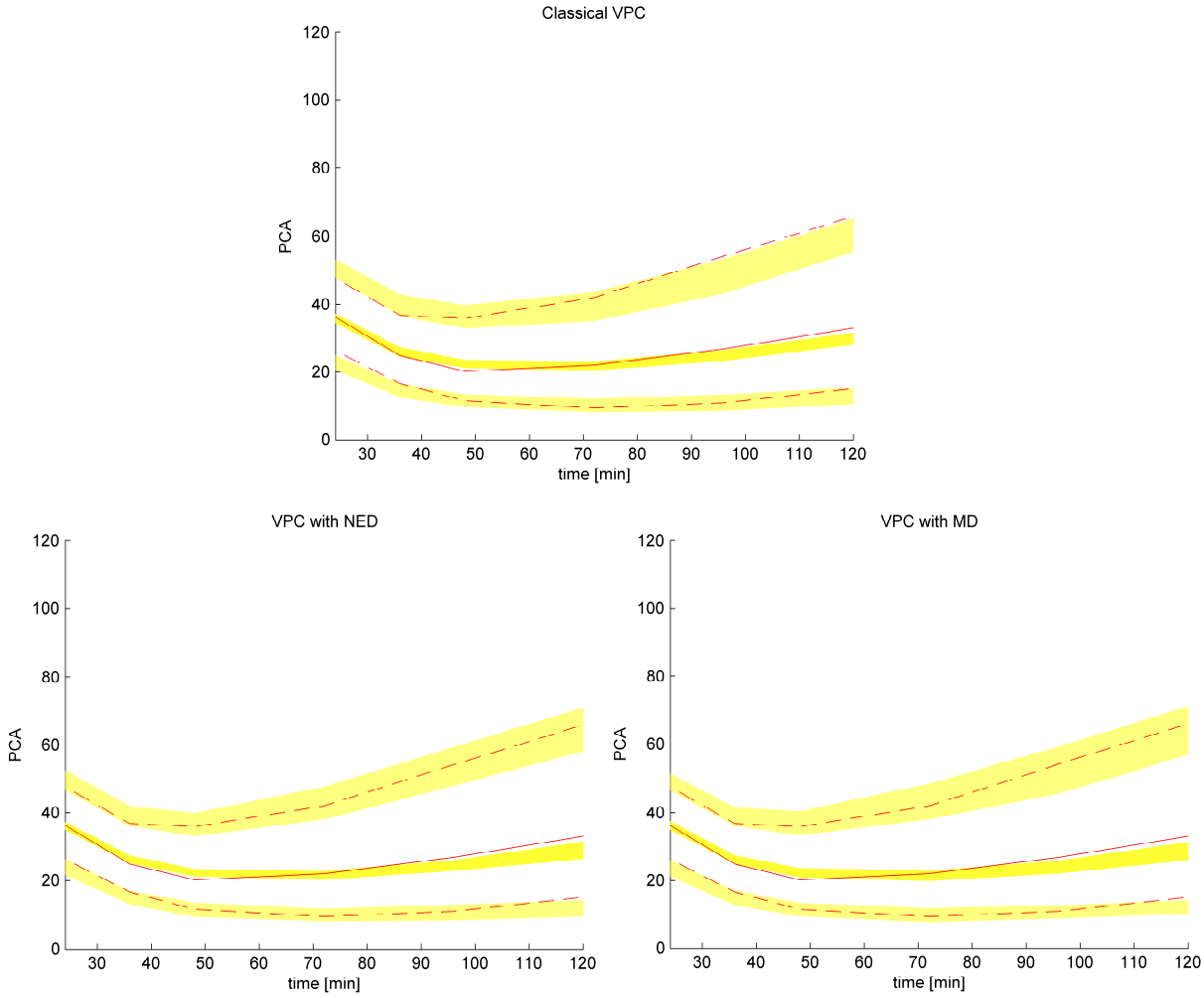

Figure 9.7: The classical VPC (on the top) and the VPC with NED (on the bottom left) and MD (on the bottom right) of the PD of the Warfarin model.

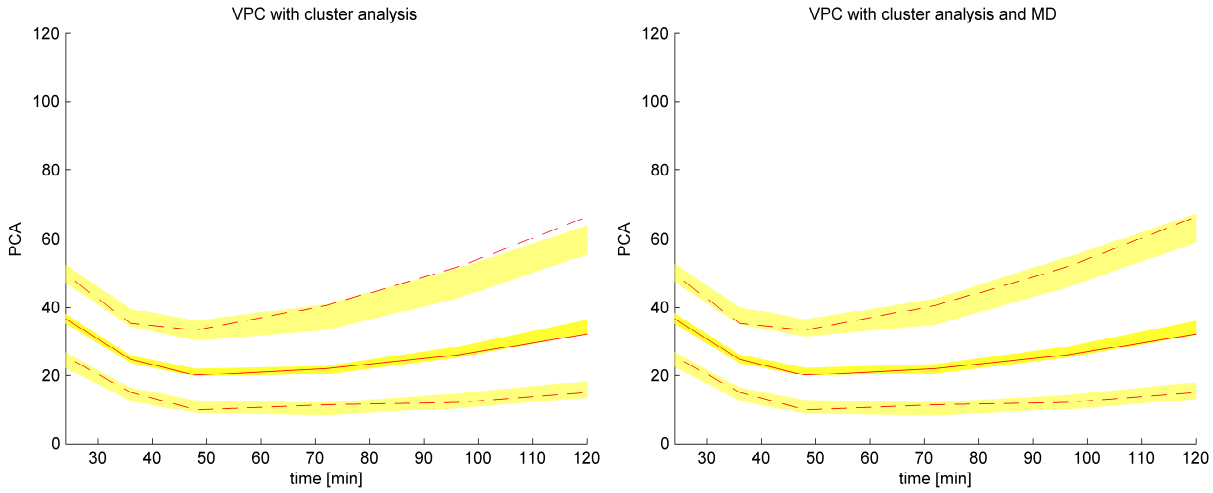

Figure 9.8: The classical VPC and the VPC with MD of the PD of the Warfarin model using simulated data obtained with FF resulted from a cluster analysis.

9.4 Discussion

During the model building process is fundamental to evaluate the model performance with appropriate tools. In the PKPD area the VPC is a commonly used diagnostic to test whether or not the model is able to reproduce the variability and the trend of the data. However this diagnostic tool presents some pitfalls in the simulation step when models with forcing functions (FF) are evaluated. In fact in this case there is a mismatch between each set of simulated parameters and the associated individual FF which can cause an incorrect profile simulation. This study aims to overcome this VPC limitation by taking into account in the simulation step a correlation term using the MD or NED that bounds the set of simulated parameters with the most appropriate FF. The classical VPC in the various examples presents mismatches between the CI of the percentiles and the percentiles of the observed data. This mismatch is more evident in the metabolic examples relative to the MTT that is by definition a less controlled experiment compared to the IVGTT since it includes the GI tract. The MTT produces very variable profiles and as a consequence is more probable a wrong association of the simulated parameters with the FF that it translates into an incorrect profile simulation. Moreover there is a difference between the classic VPC of the MTT c-peptide and the glucose model. This is due to the fact that the FF in the glucose minimal model are two independent signals whereas in the c-peptide minimal model the FF are the signal and its first derivative. The classical VPC relative to the IVGTT and to the Warfarin

present less mismatch in the CI of the percentiles with the observed percentiles because the profiles measured are less variable among the subjects. On the use of the MD or the NED step from the corresponding VPC graphs no main differences are present even if there should be an improvement in the VPC performance using the MD technique instead of the NED when the estimated parameters have a multivariate distribution with a full covariance matrix. For example the MTT c-peptide minimal model was implemented and estimated supposing that the parameters come from a multivariate distribution with a full covariance but no main advantages are evident from the graphs when using the MD technique instead of the NED. As far as the simulated dataset is concerned that was obtained using the FF identified by cluster analysis, the VPC with MD step on this more controlled dataset helps to reduce the error in the association but in case of big variability among the FF such as the MTT is not the best solution because the cluster analysis might do a strong approximation of the FF kinetics and as a consequence it reduces the estimated inter individual variability changing the characteristic of the population. This kind of approach was thought to be useful in typical PKPD experiments where the level of variability in the curves of the different subjects is smaller than the variability in the FF curves obtained from for example an MTT experiment.
In general this new VPC correction is appealing because it preserves the dynamics of the profiles in the time course keeping the characteristic of the easy visualization of the classical VPC unlike other methods proposed [66, 67, 68] where the dynamics are distorted. At the same time to apply this method the dataset under analysis has to be big in the number of subjects and rich in sampling enough to guarantee respectively a good characterization of the population and of the possible combination of the individual set of parameters with the FF and rich in order to have FFs well defined.

9.5 Conclusion

This work proposes a refinement of the simulated based diagnostic VPC which is relevant for a particular subset of models that present time varying known input (FF) like the minimal models or the PKPD models where the PK is the FF. Despite the simplicity of the method, the results show an evident improvement of the VPC that implies different conclusion on the goodness of the model. The method is able to preserve the time dynamic of the signal keeping the immediateness of diagnostic interpretation of the well-known VPC but it requires at the same time a rich sampling dataset and a big number of subjects.

Conclusions

In this thesis is carried on the investigation of the glucose-insulin system started by Denti et al by exploiting the potentials of the NLMEM technique. This technique is particularly widespread in the epidemiological studies and pharmacokinetic and pharmacodynamic (PKPD) experiments as it allows the parameter estimation in heavily discarded and variable datasets and the quantification of the sources of variability of the system. These two aspects mean a cost reduction of the trials, less invasive experiments and more flexibility for the study designer thanks to the technique powerful statistical tools. Despite all these advantages in the metabolic field the population approach is not yet well known and used. This thesis aims to investigate the glucose-insulin system applying the NLMEM technique.

In particular the glucose-insulin system was studied referring to the minimal models that were developed so far using the traditional individual weighted linear least square (WLS). These models were revised by adding some new modeling parts and by avoiding Bayesian a priori information thanks to the fact that the NLMEM approach can handle data sparseness or individual lack of information resorting from the entire population. Moreover the models performance on discarded dataset was investigated paving the way to other studies that aim to narrow down the protocol to deal with the typical epidemiological study conditions. Note that all these improvements made on the minimal models structure would not be feasible using the traditional individual approach. To sum

up our contribution to the metabolic field with this thesis is:

- the minimal models revision by exploiting the NLMEM method that allows further studies to introduce the covariate information and to reduce the experiment sampling scheme;
- the covariate information integration in the C-peptide minimal model after an intravenous glucose load that allows a personalized individual parameter estimation;
- the implementation of an integrated glucose insulin model after an intravenous glucose load that allows to have a complete description of the system kinetic without using forcing functions and a complete characterization of the population distribution;
- the development of an extension of the Visual Predictive Check method to evaluate the performance of models with forcing function.

Acknowledgments

I would like to thank Prof. Alessandra Bertoldo for all the fruitful discussions in these three years.
I would like to thank Dr. Paolo Denti for giving me the possibility of joining the pharmacometrics group at the University of Cape Town. I would like to thank him also for all the useful discussions and for the advice on the NONMEM implementation of the population models.

Bibliography

[1] International Diabetes Federation (IDF). http://www.idf.org/diabetesatlas/5e/Update2012.

[2] P. Denti, A. Bertoldo, P. Vicini, and C. Cobelli. Nonlinear mixed effects to improve glucose minimal model parameter estimation: a simulation study in intensive and sparse sampling. *Biomedical Engineering, IEEE Transactions on*, 56(9):2156–2166, 2009.

[3] P. Denti, A. Bertoldo, P. Vicini, and C. Cobelli. Ivgtt glucose minimal model covariate selection by nonlinear mixed-effects approach. *American Journal of Physiology-Endocrinology And Metabolism*, 298(5):E950–E960, 2010.

[4] P. Denti. Nonlinear mixed-effects modelling of glucose-insulin metabolism. 2009.

[5] R.C. Bonadonna. *Il diabete mellito. Principi e pratica*. Verduci Editore, 1997.

[6] C. Rugarli. *Diabete mellito e ipoglicemiePatogenesi*, chapter 64. Masson Editore, 2010.

[7] World Health Organization (WHO). http://www.who.int/diabetes/en/.

[8] American Diabetes association (ADA). http://www.diabetes.org/diabetes-basics/?loc=GlobalNavDB.

[9] W.S. Cutfield, C.A. Jefferies, W.E. Jackson, E.M. Robinson, and P.L. Hofman. Evaluation of homa and quicki as measures of insulin sensitivity in prepubertal children. *Pediatric diabetes*, 4(3):119–125, 2003.

[10] R.A. DeFronzo, J.D. Tobin, and R. Andres. Glucose clamp technique: a method for quantifying insulin secretion and resistance. *American Journal of Physiology-Endocrinology And Metabolism*, 237(3):E214, 1979.

[11] C. Cobelli and A. Caumo. Using what is accessible to measure that which is not: necessity of model of system. *Metabolism*, 47(8):1009–1035, 1998.

[12] C. Cobelli, C. Dalla Man, G. Sparacino, L. Magni, G. De Nicolao, and B.P. Kovatchev. Diabetes: models, signals, and control. *Biomedical Engineering, IEEE Reviews in*, 2:54–96, 2009.

[13] G. Sparacino, C. Tombolato, and C. Cobelli. Maximum-likelihood versus maximum a posteriori parameter estimation of physiological system models: the c-peptide impulse response case study. *Biomedical Engineering, IEEE Transactions on*, 47(6):801–811, 2000.

[14] G. Pillonetto, G. Sparacino, and C. Cobelli. Numerical non-identifiability regions of the minimal model of glucose kinetics: superiority of bayesian estimation. *Mathematical biosciences*, 184(1):53–67, 2003.

[15] P. Magni, G. Sparacino, R. Bellazzi, G.M. Toffolo, and C. Cobelli. Insulin minimal model indexes and secretion: proper handling of uncertainty by a bayesian approach. *Annals of biomedical engineering*, 32(7):1027–1037, 2004.

[16] P. Magni, G. Sparacino, R. Bellazzi, and C. Cobelli. Reduced sampling schedule for the glucose minimal model: importance of bayesian estimation. *American Journal of Physiology-Endocrinology And Metabolism*, 290(1):E177–E184, 2006.

[17] R.N. Bergman, Y.Z. Ider, C.R. Bowden, and C. Cobelli. Quantitative estimation of insulin sensitivity. *American Journal of Physiology-Endocrinology And Metabolism*, 236(6):E667, 1979.

[18] C. Cobelli, A. Caumo, and M. Omenetto. Minimal model sgoverestimation and siunderestimation: improved accuracy by a bayesian two-compartment model. *American Journal of Physiology-Endocrinology And Metabolism*, 277(3):E481–E488, 1999.

[19] G. Toffolo, F. De Grandi, and C. Cobelli. Estimation of β-cell sensitivity from intravenous glucose tolerance test c-peptide data: knowledge of the kinetics avoids errors in modeling the secretion. *Diabetes*, 44(7):845–854, 1995.

[20] E. Van Cauter, F. Mestrez, J. Sturis, and K.S. Polonsky. Estimation of insulin secretion rates from c-peptide levels: comparison of individual and standard kinetic parameters for c-peptide clearance. *Diabetes*, 41(3):368–377, 1992.

[21] G. Toffolo, M. Campioni, R. Basu, R.A. Rizza, and C. Cobelli. A minimal model of insulin secretion and kinetics to assess hepatic insulin extraction. *American Journal of Physiology-Endocrinology And Metabolism*, 290(1):E169–E176, 2006.

[22] C. Della Man, A. Caumo, and C. Cobelli. The oral glucose minimal model: estimation of insulin sensitivity from a meal test. *Biomedical Engineering, IEEE Transactions on*, 49(5):419–429, 2002.

[23] C. Dalla Man, A. Caumo, R. Basu, R. Rizza, G. Toffolo, and C. Cobelli. Minimal model estimation of glucose absorption and insulin sensitivity from oral test: validation with a tracer method. *American Journal of Physiology-Endocrinology And Metabolism*, 287(4):E637–E643, 2004.

[24] E. Breda, M.K. Cavaghan, G. Toffolo, K.S. Polonsky, and C. Cobelli. Oral glucose tolerance test minimal model indexes of β-cell function and insulin sensitivity. *Diabetes*, 50(1):150–158, 2001.

[25] G. Toffolo, E. Breda, M.K. Cavaghan, D.A. Ehrmann, K.S. Polonsky, and C. Cobelli. Quantitative indexes of β-cell function during graded up&down glucose infusion from c-peptide minimal models. *American Journal of Physiology-Endocrinology And Metabolism*, 280(1):E2–E10, 2001.

[26] M. Davidian and D. M. Giltinan. *Nonlinear models for repeated measurement data*. Boca Raton, Fla.: Chapman Hall/CRC, 1998.

[27] J.L. Steimer, A. Mallet, J.L. Golmard, and J.F. Boisvieux. Alternative approaches to estimation of population pharmacokinetic parameters: comparison with the nonlinear mixed-effect model. *Drug Metabolism Reviews*, 15(1-2):265–292, 1984.

[28] R.J. Bauer, S. Guzy, and C. Ng. A survey of population analysis methods and software for complex pharmacokinetic and pharmacodynamic models with examples. *The AAPS journal*, 9(1):60–83, 2007.

[29] SL Beal and LB. Sheiner. *NONMEM Users Guide*. Ellicott City: GloboMax ICON Development Solutions Press, 1989-2012.

[30] R. Bauer and S. Guzy. Monte carlo parametric expectation maximization (mc-pem) method for analyzing population pharmacokinetic/pharmacodynamic data. *Advanced Methods of Pharmacokinetic and Pharmacodynamic Systems Analysis Volume 3*, pages 135–163, 2004.

[31] E. Kuhn and M. Lavielle. Maximum likelihood estimation in nonlinear mixed effects models. *Computational Statistics & Data Analysis*, 49(4):1020–1038, 2005.

[32] D.J. Lunn, N. Best, A. Thomas, J. Wakefield, and D. Spiegelhalter. Bayesian analysis of population pk/pd models: general concepts and software. *Journal of pharmacokinetics and pharmacodynamics*, 29(3):271–307, 2002.

[33] P. Vicini and C. Cobelli. The iterative two-stage population approach to ivgtt minimal modeling: improved precision with reduced sampling. *American Journal of Physiology-Endocrinology and Metabolism*, 280(1):E179–E186, 2001.

[34] O.F. Agbaje, S.D. Luzio, A.I.S. Albarrak, D.J. Lunn, D.R. Owens, and R. Hovorka. Bayesian hierarchical approach to estimate insulin sensitivity by minimal model. *Clinical Science*, 105(5):551–560, 2003.

[35] the RFPK team Univeristy of Washington. *System for population kinetics (SPK)*. http://spk.rfpk.washington.edu.

[36] P.H.R. Barrett, B.M. Bell, C. Cobelli, H. Golde, A. Schumitzky, P. Vicini, and D.M. Foster. Saam ii: simulation, analysis, and modeling software for tracer and pharmacokinetic studies. *Metabolism*, 47(4):484–492, 1998.

[37] R.M. Savic and M.O. Karlsson. Importance of shrinkage in empirical bayes estimates for diagnostics: problems and solutions. *The AAPS journal*, 11(3):558–569, 2009.

[38] A. Caumo, P. Vicini, J.J. Zachwieja, A. Avogaro, K. Yarasheski, D.M. Bier, and C. Cobelli. Undermodeling affects minimal model indexes: insights from a two-compartment model. *American Journal of Physiology-Endocrinology And Metabolism*, 276(6):E1171–E1193, 1999.

[39] A. Caumo, P. Vicini, and C. Cobelli. Is the minimal model too minimal? *Diabetologia*, 39(8):997–1000, 1996.

[40] C. Cobelli, F. Bettini, A. Caumo, and M.J. Quon. Overestimation of minimal model glucose effectiveness in presence of insulin response is due to undermodeling. *American Journal of Physiology-Endocrinology And Metabolism*, 275(6):E1031–E1036, 1998.

[41] R.M. Savic, D.M. Jonker, T. Kerbusch, and M.O. Karlsson. Implementation of a transit compartment model for describing drug absorption in pharmacokinetic studies. *Journal of pharmacokinetics and pharmacodynamics*, 34(5):711–726, 2007.

[42] BJ Anderson and NHG Holford. Mechanism-based concepts of size and maturity in pharmacokinetics. *Annu. Rev. Pharmacol. Toxicol.*, 48:303–332, 2008.

[43] N. Holford. The visual predictive check: superiority to standard diagnostic (rorschach) plots, inpopulation approach group in europe, page 14. 2005. www.pagemeeting.org/?abstract=738.

[44] A. Largajolli, A. Bertoldo, and C. Cobelli. Visual predictive check (vpc) in models with forcing functions, in population approach group in europe, page 21. 2012. In *Abstr.* www.pagemeeting.org/?abstract=2556.

[45] G. Toffolo, W.T. Cefalu, C. Cobelli, et al. Beta-cell function during insulin-modified intravenous glucose tolerance test successfully assessed by the c-peptide minimal model. *Metabolism: clinical and experimental*, 48(9):1162, 1999.

[46] R. Basu, E. Breda, A.L. Oberg, C.C. Powell, C. Dalla Man, A. Basu, J.L. Vittone, G.G. Klee, P. Arora, M.D. Jensen, et al. Mechanisms of the age-associated deterioration in glucose tolerance contribution of alterations in insulin secretion, action, and clearance. *Diabetes*, 52(7):1738–1748, 2003.

[47] M.D. Jensen, J.A. Kanaley, J.E. Reed, and P.F. Sheedy. Measurement of abdominal and visceral fat with computed tomography and dual-energy x-ray absorptiometry. *The American journal of clinical nutrition*, 61(2):274–278, 1995.

[48] J.W. Mandema, D. Verotta, and L.B. Sheiner. Building population pharmacokineticpharmacodynamic models. i. models for covariate effects. *Journal of Pharmacokinetics and Pharmacodynamics*, 20(5):511–528, 1992.

[49] R Development Core Team. *R: A Language and Environment for Statistical Computing.* http://www.r-project.org/.

[50] E.N. Jonsson and M.O. Karlsson. Xposeâan s-plus based population pharmacokinetic/pharmacodynamic model building aid for nonmem. *Computer methods and programs in biomedicine*, 58(1):51–64, 1998.

[51] O. Schabenberger. Mixed model influence diagnostics. In *SUGI*, volume 29, pages 189–29, 2005.

[52] R. Basu, C. Dalla Man, M. Campioni, A. Basu, G. Klee, G. Toffolo, C. Cobelli, and R.A. Rizza. Effects of age and sex on postprandial glucose metabolism differences in glucose turnover, insulin secretion, insulin action, and hepatic insulin extraction. *Diabetes*, 55(7):2001–2014, 2006.

[53] MO Karlsson and RM Savic. Diagnosing model diagnostics. *Clinical Pharmacology & Therapeutics*, 82(1):17–20, 2007.

[54] S. Wanant and M.J. Quon. Insulin receptor binding kinetics: modeling and simulation studies. *Journal of theoretical Biology*, 205(3):355–364, 2000.

[55] C. Cobelli, G.M. Toffolo, C. Dalla Man, M. Campioni, P. Denti, A. Caumo, P. Butler, and R. Rizza. Assessment of β-cell function in humans, simultaneously with insulin sensitivity and hepatic extraction, from intravenous and oral glucose tests. *American Journal of Physiology-Endocrinology And Metabolism*, 293(1):E1–E15, 2007.

[56] CD Man, R.A. Rizza, and C. Cobelli. Meal simulation model of the glucose-insulin system. *Biomedical Engineering, IEEE Transactions on*, 54(10):1740–1749, 2007.

[57] BP Kovatchev, MD Breton, C. Dalla Man, and C. Cobelli. In silico model and computer simulation environment approximating the human glucose/insulin utilization. *Food and Drug Administration Master File MAF*, 1521, 2008.

[58] B.P. Kovatchev, M. Breton, C. Dalla Man, and C. Cobelli. Biosimulation modeling for diabetes: In silico preclinical trials: A proof of concept in closed-loop control of type 1 diabetes. *Journal of diabetes science and technology (Online)*, 3(1):44, 2009.

[59] N.G. Nerella, L.H. Block, and P.K. Noonan. The impact of lag time on the estimation of pharmacokinetic parameters. i. one-compartment open model. *Pharmaceutical research*, 10(7):1031–1036, 1993.

[60] R. Basu, B. Di Camillo, G. Toffolo, A. Basu, P. Shah, A. Vella, R. Rizza, and C. Cobelli. Use of a novel triple-tracer approach to assess postprandial glucose metabolism. *American Journal of Physiology-Endocrinology and Metabolism*, 284(1):E55–E69, 2003.

[61] C. Dalla Man, M. Campioni, K.S. Polonsky, R. Basu, R.A. Rizza, G. Toffolo, and C. Cobelli. Two-hour seven-sample oral glucose tolerance test and meal protocol minimal model assessment of β-cell responsivity and insulin sensitivity in nondiabetic individuals. *Diabetes*, 54(11):3265–3273, 2005.

[62] G. Bock, C. Dalla Man, M. Campioni, E. Chittilapilly, R. Basu, G. Toffolo, C. Cobelli, and R. Rizza. Pathogenesis of pre-diabetes mechanisms of fasting and postprandial hyperglycemia in people with impaired fasting glucose and/or impaired glucose tolerance. *Diabetes*, 55(12):3536–3549, 2006.

[63] A. Basu, C. Dalla Man, R. Basu, G. Toffolo, C. Cobelli, and R.A. Rizza. Effects of type 2 diabetes on insulin secretion, insulin action, glucose effectiveness, and postprandial glucose metabolism. *Diabetes Care*, 32(5):866–872, 2009.

[64] C. Dalla Man, G. Bock, P.D. Giesler, D.B. Serra, M.L. Saylan, J.E. Foley, M. Camilleri, G. Toffolo, C. Cobelli, R.A. Rizza, et al. Dipeptidyl peptidase-4 inhibition by vildagliptin and the effect on insulin secretion and action in response to meal ingestion in type 2 diabetes. *Diabetes Care*, 32(1):14–18, 2009.

[65] MO Karlsson and NHG Holford. A tutorial on visual predictive checks., inpopulation approach group in europe, page 17. 2008. In *Abstr.* www.pagemeeting.org/?abstract=1434.

[66] T.M. Post, J.I. Freijer, B.A. Ploeger, and M. Danhof. Extensions to the visual predictive check to facilitate model performance evaluation. *Journal of pharmacokinetics and pharmacodynamics*, 35(2):185–202, 2008.

[67] D.D. Wang and S. Zhang. Standardized visual predictive check versus visual predictive check for model evaluation. *The Journal of Clinical Pharmacology*, 52(1):39–54, 2012.

[68] M. Bergstrand, A.C. Hooker, J.E. Wallin, and M.O. Karlsson. Prediction-corrected visual predictive checks for diagnosing nonlinear mixed-effects models. *The AAPS Journal*, 13(2):143–151, 2011.

[69] NH Holford et al. Clinical pharmacokinetics and pharmacodynamics of warfarin. understanding the dose-effect relationship. *Clinical pharmacokinetics*, 11(6):483, 1986.

[70] NH Holford. Rational warfarin dosing: a pharmacokinetic-pharmacodynamic analysis. *Clin Pharmacol Ther*, 39:199, 1986.

[71] Holford N. Pkpd workshop: An overview on how to use nonmem for pkpd analyses, in population approach group in europe, page 14. 2005. In *Abstr.* www.pagemeeting.org/?abstract=838.

[72] D.E. Mager, E. Wyska, and W.J. Jusko. Diversity of mechanism-based pharmacodynamic models. *Drug Metabolism and Disposition*, 31(5):510–518, 2003.

[73] M.U. Guide. The mathworks. *Inc., Natick, MA*, 5, 1998.